A STUDY ON THE EFFECT OF PIPE - SOIL RELATIVE STIFFNESS ON THE BEHAVIOUR OF BURIED FLEXIBLE PIPES

A THESIS SUBMITTED TO
THE GRADUATE SCHOOL OF NATURAL AND APPLIED SCIENCES
OF
MIDDLE EAST TECHNICAL UNIVERSITY

BY

MEHMET BİRCAN

IN PARTIAL FULFILLMENT OF THE REQUIREMENTS
FOR
THE DEGREE OF MASTER OF SCIENCE
IN
CIVIL ENGINEERING

JANUARY 2010

Approval of the thesis:

A STUDY ON THE EFFECT OF PIPE - SOIL RELATIVE STIFFNESS ON THE BEHAVIOUR OF BURIED FLEXIBLE PIPES

Submitted by **MEHMET BİRCAN** in partial fulfilment of the requirements for the degree of **Master of Science in Civil Engineering Department, Middle East Technical University** by,

Prof. Dr. Canan Özgen _____
Dean, Graduate School of **Natural and Applied Sciences**

Prof. Dr. Güney Özcebe _____
Head of Department, **Civil Engineering**

Prof. Dr. M. Yener Özkan
Supervisor, **Civil Engineering Dept., METU** _____

Examining Committee Members:

Prof. Dr. Orhan Erol _____
Civil Engineering Dept., METU

Prof. Dr. M. Yener Özkan _____
Civil Engineering Dept., METU

Prof. Dr. Erdal Çokça _____
Civil Engineering Dept., METU

Dr. Oğuz Çalışan _____
Company Manager, Çalışan Geoteknik
Hizmetler Ltd. Şti.

Gülru Yıldız, M.Sc. _____
Civil Engineer, Ada Mühendislik

Date: *29.01.2010*

I hereby declare that all information in this document has been obtained and presented in accordance with academic rules and ethical conduct. I also declare that, as required by these rules and conduct, I have fully cited and referenced all material and results that are not original to this work.

Name, Last name : Mehmet Bircan

Signature :

ABSTRACT

A STUDY ON THE EFFECT OF PIPE - SOIL RELATIVE STIFFNESS ON THE BEHAVIOUR OF BURIED FLEXIBLE PIPES

Bircan, Mehmet

M.Sc., Department of Civil Engineering

Supervisor: Prof. Dr. M. Yener Özkan

January 2010, 159 pages

In this study, the effect of pipe-soil relative stiffness on the behaviour of buried flexible pipes was investigated considering the pipe size, material type, stiffness, pipe-soil and natural soil-backfill interfaces and geometry of the trench using the finite element method. For this purpose, a parametric study was conducted to examine the effect of different variables on the resulting earth loads and deformations imposed on the buried pipes. Various types of trench pipe-soil cases were analysed for a certain natural ground and backfill material by the PLAXIS finite element code which allows simulating non-linear soil behaviour, the stages of construction as well as the pipe-soil interaction aspects of the problem. Loads and deformations obtained by the finite element method were compared with those calculated by the conventional approaches for different pipe-soil stiffness ratios. The finite element results obtained for the deformation of typically flexible Polyethylene pipes were then used to back-calculate the range of modulus of soil reaction, E', values for various pipe-soil relative stiffness and they were compared with the suggested value proposed by Howard (1977).

Keywords: Buried Flexible Pipes, Pipe-Soil Relative Stiffness, Modulus of Soil Reaction, Finite Element Method.

ÖZ

BORU-ZEMİN GÖRECELİ RİJİTLİK ORANININ GÖMÜLÜ ESNEK BORULARIN DAVRANIŞINDAKİ ETKİSİ ÜZERİNE BİR ÇALIŞMA

Bircan, Mehmet
Yüksek Lisans, İnşaat Mühendisliği Bölümü
Tez Yöneticisi: Prof. Dr. M. Yener Özkan

Ocak 2010, 159 sayfa

Bu çalışmada, boru-zemin göreceli rijitlik oranının gömülü esnek boruların davranışı üzerindeki etkisi boru ölçüleri, malzeme cinsi, rijitliği, boru-zemin ve doğal zemin-geri dolgu arayüz elemanları ile kanal geometrisi göz önüne alınarak sonlu elemanlar yöntemiyle araştırılmıştır. Bu amaçla, çeşitli değişkenlerin gömülü boruların maruz kaldığı toprak yükü ve deformasyonlar üzerindeki tesirini inceleyen parametrik bir çalışma yapılmıştır. Belirli bir doğal zemin ve geri dolgu malzemesi içinde, değişik tiplerde kanal boru-zemin durumları lineer olmayan zemin davranışı, inşaat yapım aşamaları ile problemin boru-zemin etkileşim yönünü de modellemeye izin veren PLAXIS sonlu eleman programı ile analiz edilmiştir. Sonlu eleman analizlerinden elde edilen yük ve deformasyonlar ile geleneksel yaklaşımlardan hesaplanan sonuçlar, değişik boru-zemin rijitlik oranları için karşılaştırılmıştır. Daha sonra, tipik esnek Polietilen borular için sonlu eleman yönteminden bulunan deformasyon sonuçları çeşitli boru-zemin göreceli rijitlik değerlerine karşılık gelen zemin reaksiyon modülü, E', değer aralığının geri hesaplanmasında kullanılmış ve Howard (1977) tarafından önerilen değerle karşılaştırılmıştır.

Anahtar Kelimeler: Gömülü Esnek Borular, Boru-Zemin Göreceli Rijitlik Oranı, Zemin Reaksiyon Modülü, Sonlu Eleman Yöntemi.

To My Family

ACKNOWLEDGEMENTS

The author wishes to express his deepest gratitude to his supervisor Prof. Dr. M. Yener Özkan for his guidance, advice, criticism, encouragements and insight throughout the researh.

TABLE OF CONTENTS

LIST OF FIGURES

FIGURES

LIST OF TABLES

TABLES

CHAPTER 1

INTRODUCTION

1.1 *General*

Underground conduits have served to improve people's living standards since the beginning of civilization. Remnants of such structures from ancient civilizations have been found in Europe, Asia, and even the western hemisphere, where some of the ancient inhabitants of South and Central America had water and sewer systems (Moser and Folkman, 2008). In fact, water, storm water and sewage conduits have been constructed below ground by way of installing brick and/or mud-lined structures. The function of the brick or masonry lining was to protect the conduits against collapse resulting from earth and other loadings. Historical examples of such typical infrastructure works were documented in ancient Babylon, Athens, and Rome (Bulson, 1985). Further to the development and evolution of new infrastructure materials into reliable, practical and economical alternatives, brick and mud-lined underground conduits were replaced with concrete, steel, cast and ductile iron, followed by more flexible polymer-based materials such as polyethylene. Together with the replacement of new materials, the requirement for rational design frameworks for the selection of acceptable sections and characteristics for an expanding range of applications was clear (Szechy, 1973).

Today, a vast majority of the modern urban infrastructure systems are buried below the ground. Water mains, sewer lines, drainage lines, gas lines, telephone and electrical conduits and many other networks are regularly laid through underground conduits running below roads and trafficked areas.

Considering the wide usage, significance and sensitivity of such infrastructure systems, behaviour of buried conduits under different circumstances should be known and they need to be properly designed and installed to resist the imposed stresses, loads and deformations. For this purpose, considerable research efforts have been carried out by many engineers and organizations for the determination of resulting loads and deformations on buried conduits. It is now possible to use engineering science to design these underground conduits with a degree of precision comparable with that obtained in designing buildings and bridges (Moser and Folkman, 2008).

1.2 *Problem Statement*

The structural integrity of buried flexible pipes mainly comes from the lateral support of the soil. Since this lateral support is so critical, a design parameter indicating the strength of the soil is essential. This design parameter developed by Dr. Spangler and Watkins at the Iowa State College is the soil modulus of elasticity, E'. The available methods for the design of buried flexible pipes require checking for different performance limits which are directly related to the stress, strain, and deflection or buckling. Many of these design checks involve the use of modulus of soil reaction, E'. The most widely used E' values comes from the empirical data used by Howard (1977). However, when the possible E' values are examined and back-calculated based on the data from actual pipeline installations on site, a significant degree of error is reached for the proposed E' values. This fact was pointed out by the study of Jeyapalan and Watkins (2004) and the degree of error was stated as unacceptable. Therefore the proposed E' values may not accurately correlate to the project site where the pipe will be buried.

In the paper of Jeyapalan and Watkins (2004), it is also stated that the E' is not a fundamental geotechnical engineering property of the soil. This property can not be measured either in the laboratory or in the field. This is an empirical soil-pipe system parameter, which could be obtained only from back-calculating by knowing the values of other parameters in the modified Iowa

equation. Further to many other variables that should be taken into consideration, the pipe-soil relative stiffness has a significant effect on the value one uses for E' in design. As a matter of fact, behaviour of buried flexible pipes is a function of pipe-soil system and is certainly affected by the relative stiffness parameter. In the work presented in this thesis, the focus is on the effect of pipe-soil relative stiffness on loads and deformations imposed on underground conduits for trench-type installations and the resulting back-calculated E' values.

1.3 *Objectives of the Thesis*

The objectives of this thesis are (1) to model and analyse different types of buried pipe systems considering the effect of pipe size, material, stiffness, interface elements and trench geometry using finite element method, and (2) to investigate the effect of pipe-soil relative stiffness on the behaviour of buried flexible pipes in relation to its impact on the resulting deformations and earth loads on pipes, and (3) to back-calculate the range of modulus of soil reaction, E' values resulting from the FEA of typically flexible polyethylene pipes in order to present the impact of pipe-soil relative stiffness parameter accordingly.

The finite element analyses were carried out for a number of trench pipe-soil cases taking into account the soil-structure interaction aspects of the problem and the stages of construction.

1.4 *Scope of the Thesis*

First, a comprehensive literature survey was done to review some familiar analytical methods available for underground flexible pipe systems. The available methods for the analysis and design of buried pipes are generally based on empirical and/or simplified theoretical solutions which tend to ignore a number of important parameters related to the soil-structure interaction aspects of the problem and the stages of construction. In the study presented in this thesis, the effect of pipe-soil relative stiffness on the behaviour of buried flexible pipes was studied considering the effect of pipe size, material, stiffness and interfaces

and geometry of the trench installation using the finite element method which allowed simulating the stages of construction as well. For this purpose, a parametric study was conducted to investigate the effect of the different variables on the resulting loads and deformations on the pipes in the same natural ground and backfill conditions. In total, 45 trench-pipe cases were investigated. The finite element analyses were performed with the PLAXIS finite element code and the modelling of soil materials was performed using the Hardening-Soil constitutive model. The finite element results for the deformation of flexible pipes (Polyethylene) were then used to back-calculate the E' values for differing pipe-soil relative stiffness. The pipe-soil stiffness ratio ($S_r = PS/E_{50}$) parameter which was defined for the purpose of this study was used in the comparison and discussion of results.

1.5 *Outline of the Thesis*

In Chapter 2, a comprehensive review of literature is presented for the available analytical methods used to estimate the loads and deformations imposed on the buried flexible pipes. Characteristics of buried pipe installations, modelling the behaviour of flexible pipes as well as their performance limits are discussed. In addition, special emphasis is put on the modulus of soil reaction, E' parameter and a detailed review of this design parameter is presented.

Chapter 3 is a presentation of the features and capabilities of the finite element code, PLAXIS 2D – Version 8 which is utilized in this thesis.

Chapter 4 gives detailed information on the Hardening-Soil constitutive model which is used to simulate the soil behaviour in all trench pipe-soil cases modelled and analysed with the PLAXIS finite element code throughout this study.

Chapter 5 describes the methodology and analysis approach for the two dimensional finite element analyses of a number of trench pipe-soil cases which are carried out using the finite element code PLAXIS 2D – Version 8. The input parameters, details of calculation process and a summary of

graphical output presentation are given.

Chapter 6 presents and discusses the numerical results of analyses in order to find out the effect of pipe-soil relative stiffness on the loads and deformations developed on the buried pipes. Additionally, some of the conventional methods for estimating the loads and deformations are evaluated and the results of these methods are compared to those of FEA. The finite element results for the deformation of typically flexible polyethylene pipes are then used to back-calculate the range of modulus of soil reaction, E' values against the proposed value of Howard. Hence, the effect of relative stiffness parameter on the values of E' is commented as well.

In Chapter 7, summary and conclusions are presented.

CHAPTER 2

LITERATURE REVIEW

In the early 1900s, Anson Marston developed a method of calculating the earth load to which a buried conduit is subjected in service. This method, the Marston load theory, serves to predict the supporting strength of pipe under various installation conditions. M. G. Spangler, working with Marston, developed a theory for flexible pipe design. Their research led to the well-known Marston-Spangler theory which is still the basis for most current buried pipe design. In addition, much testing and research have produced quantities of empirical data which also can be used in the design process. Digital computers, combined with finite element techniques and sophisticated soil models, have given the engineering profession design tools which have produced even more precise designs (Moser and Folkman, 2008).

2.1 *General Theories and Discussions on Buried Pipes*

2.1.1 Classification of Underground Conduits

Marston has classified the underground conduits in two major classes for load computation purposes. These classes are ditch conduit and projecting conduit and are based on the construction methods that influence the distribution of the load on the pipe.

Ditch conduit: A ditch conduit is defined as a pipe installed in a relatively narrow trench in undisturbed soil and then covered with earth backfill.

Projecting conduit: A projecting conduit is defined as a pipe installed above the

natural ground surface or in a relatively narrow and shallow trench, and then covered with an embankment fill. The projecting conduit class is further divided into two subclasses as positive projecting conduit and negative projecting conduit: *Positive projecting conduit:* This subclass of the projecting conduit is installed instead in a shallow bedding with its top projecting above the natural ground surface.

Negative projecting conduit: This subclass of the projecting conduit is installed in relatively narrow and shallow trench with its top remaining below the natural ground surface.

Imperfect ditch or induced trench conduit: This is a special case of the negative projecting conduit. In fact, it is an artificially constructed negative projecting conduit. The conduit is first installed as a positive projecting conduit. Then the soil backfill at the sides and over the conduit is compacted up to some specified elevation above its crown. Next, a trench of the same width as the outside horizontal dimension of the pipe is excavated down to the structure and refilled with very loose, compressible material. Finally, the embankment is completed to its final height.

Figure 2.1 below illustrates the general types of installation.

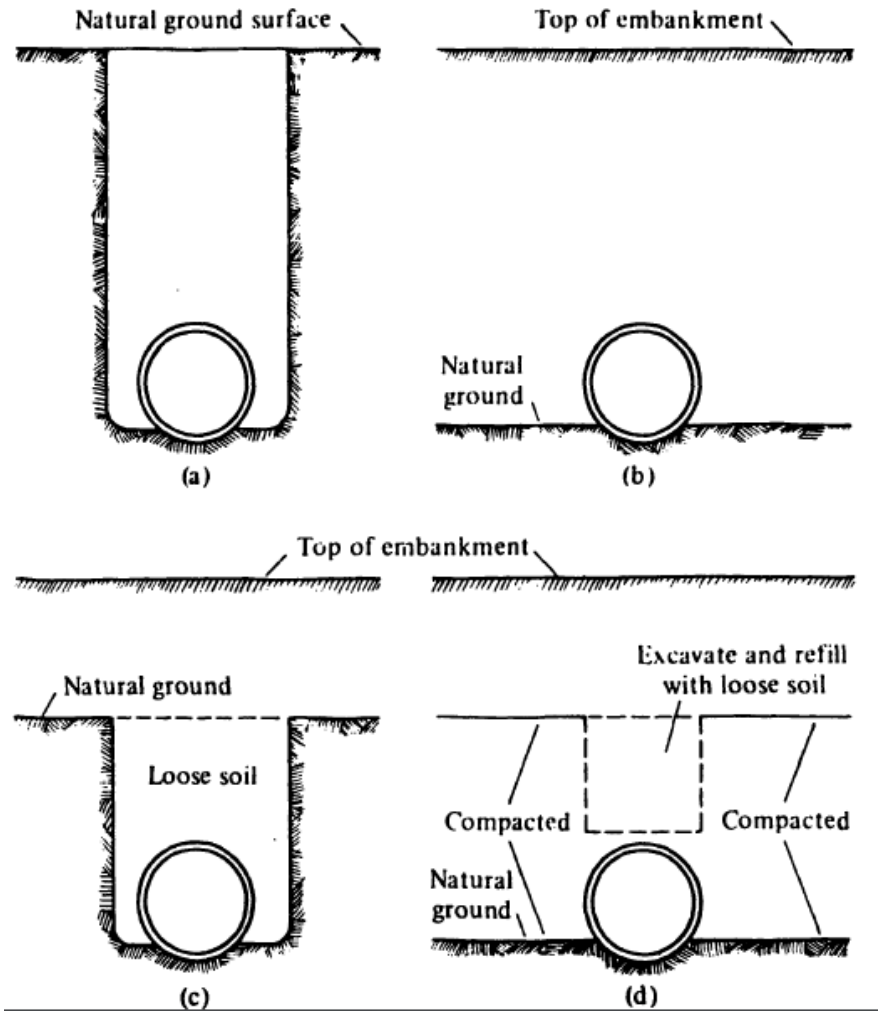

Figure 2.1 a) Trench b)Positive projecting c) Negative projecting d) Imperfect ditch (Spangler, Handy, 1982)

2.1.2 Loads on Pipes Buried In Trenches

2.1.2.1 Earth Loads on Ditch Conduits

The Marston load theory is based on the concept of a prism of soil in the trench that imposes a load on the pipe, as shown in Figure 2.3. A trench (ditch) conduit as defined by Marston was a relatively narrow ditch dug in undisturbed soil. In fact, the load on a buried pipe is not exactly equal to the weight of the overlying soil prism which is given to be the pipe outside diameter times the height of backfill above the pipe times the unit weight of the backfill material. The load acting on a pipe depends on the movement of the soil prism relative to the soil on the sides which is explained with the phenomenon of arching.

Arching can be best described as a transfer of forces between a yielding (moving) mass of geomaterial and adjoining stationary members. A redistribution of stresses in the soil body takes place and the shearing resistance tends to keep the yielding mass in its original position resulting in a change of the pressure on both of the yielding part's support and the adjoining part of soil (Terzaghi, 1943). In case the yielding part moves downward, the shear resistance will act upward and reduce the stress at the base of the yielding mass (Figure 2.2). Contrarily, if the yielding part moves upward, the shear resistance will act downward to hinder its movement and cause increase of stress at the support of the yielding part.

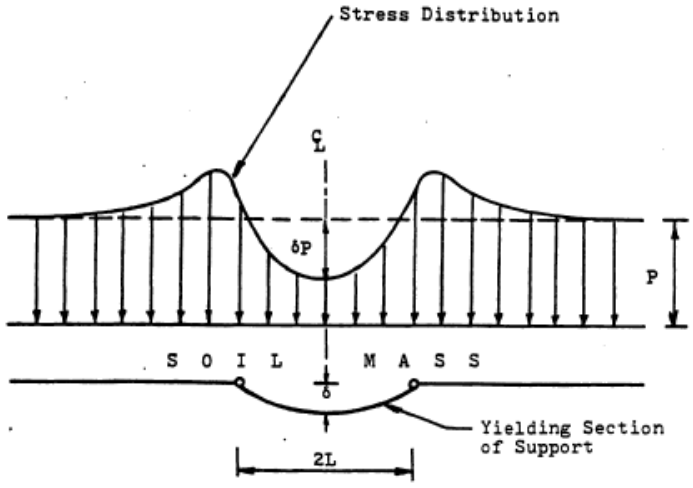

Figure 2.2 Stress Distribution in the Soil above a Yielding Base (Bjerrum et. al., 1972; Revised by Evans, 1984)

In the case of ditch conduit, the backfill material and the pipe tend to settle downward relative to the sides of the trench. Therefore, the shearing forces which act upward along the sides of the trench reduce the vertical load on the pipe due to the effect of arching.

There have been many experimental studies to examine stress distribution and arching, the most famous being conducted by Terzaghi using a deflecting trapdoor in the base of a soil bin. In the analyses of Janssen, based on the trapdoor experiments, he assumed that the surfaces of sliding (shearing planes) that occur when the door is deflected downward are vertical (Bulson, 1985). He also assumed that the vertical pressure on the yielding element is equal to the difference

between the pressure due to the weight of the soil above the element and the frictional resistance along the sides of the element.

Marston load theory recognizes that the amount of load taken by a pipe is affected by the relative movement between the backfill and the natural soil, as settlement of both the backfill and pipe occurs (Moser and Folkman, 2008).

Marston proposed that the weight of the backfill was partly resisted by frictional shear forces at the walls of the trench which developed with time. He also conservatively assumed that the cohesion of the soil is negligible when developing the equilibrium of vertical forces to derive his solution and the formula for vertical load on top of the conduit was developed as follows:

$$V = \frac{\gamma B_d^2}{2K\mu'}\left(1 - e^{-2K\mu'(h/B_d)}\right) \tag{2.1}$$

V : Vertical load on any horizontal plane in the backfill (N/m)

γ : Unit weight of the backfill material (N/m^3)

B_d : Horizontal width of the ditch at the crown (m)

K : Ratio of active lateral unit pressure to vertical unit pressure (Rankine's ratio)

h : Distance from the ground surface to any horizontal plane in backfill (m)

φ : Friction angle of the fill material (^{o})

μ : Coefficient of internal friction of backfill (tan φ)

φ' : Friction angle between the fill material and the sides of the ditch (^{o})

μ' : Coefficient of friction between backfill and sides of ditch (tan φ')

Rankine's ratio is expressed with the formula:

$$K = \frac{\sqrt{\mu^2+1}-\mu}{\sqrt{\mu^2+1}+\mu} = \frac{1-\sin\varphi}{1+\sin\varphi} = \tan^2(45-\frac{\varphi}{2})$$

In a further study for the value of K, Christensen (1967) proposed the following formula:

$$K = \left(1 + 2\tan^2\varphi\right)^{-1} = \frac{1-\sin^2\varphi}{1+\sin^2\varphi}$$

It was proposed by Wetzorke that the value of K should be 0.5 for loose fill and 1.0 for dense fill (Bulson, 1985).

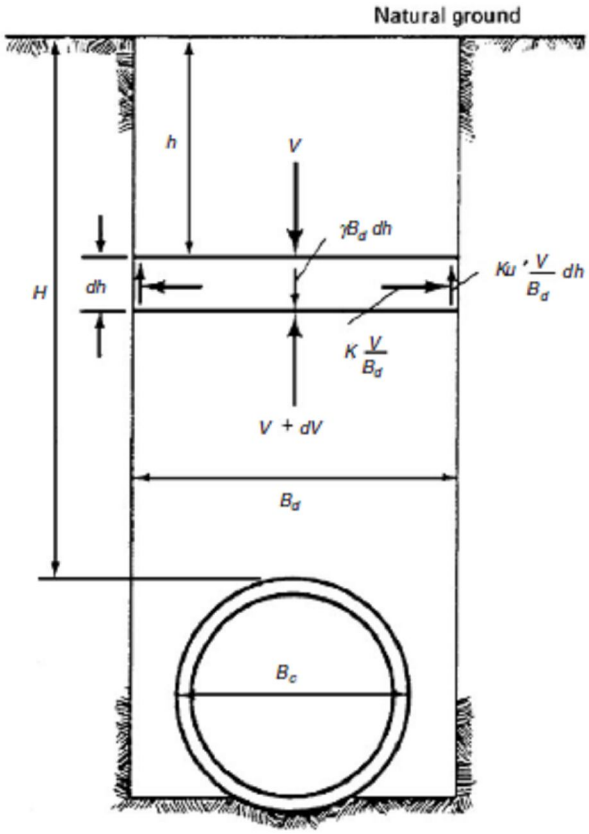

Figure 2.3 Basis for Marston's theory of loads on buried pipe

To what extent this vertical load *V* is imposed on the conduit is dependent upon the relative stiffness of the pipe and soil. For very rigid pipe, the sidefills may be very compressible in relation to the pipe and the side fills may move downward relative to the soil prism causing the pipe to carry the entire load *V*. For flexible pipe, the imposed load will be substantially less than *V* since the pipe will be less rigid than the sidefill soil and the soil prism may move downward relative to the side fills, because of the deflection of the pipe.

Hence, the maximum load acting on a rigid conduit (with relatively compressible side fills) in a ditch was defined by Marston with the following formula:

$$W_d = C_d \gamma B_d^{\,2} \qquad C_d = \left(\frac{1 - e^{-2K\mu'(h/B_d)}}{2K\mu'} \right) \tag{2.2}$$

The load coefficient, C_d is an exponential function of the coefficient of friction ($\mu' = \tan \varphi'$) between backfill and sides of ditch and the coefficient of lateral earth pressure, K, as well as the depth of soil cover, H and the width of the trench, B_d (see Figure 2.4). The values of K, μ, μ' were determined experimentally by Marston and were found to vary with the types of soil and backfill. Typical values are given in below Table 2.1.

The coefficient of friction μ was observed to vary from 0.3 to 0.5, which corresponds to values of the angle of friction between the backfill and the natural soil, φ ranging from 17 to 27°. The lateral earth pressure coefficient, K, was found to present little variation with observed values ranging from only 0.33 to 0.37. If K is taken to be equivalent to K_o, the lateral earth pressure coefficient at rest, and assuming that Jaky's expression for K_o applies, then these prescribed values would be typical for a cohesionless material with a friction angle of approximately 40°.

Table 2.1 Approximate Values of Soil Unit Weight, Ratio of Lateral to Vertical Earth Pressure, and Coefficient of Friction against Sides of Trench

Soil type	Unit weight, lb/ft^3	Rankine's ratio K	Coefficient of friction μ
Partially compacted damp top soil	90	0.33	0.50
Saturated top soil	110	0.37	0.40
Partially compacted damp clay	100	0.33	0.40
Saturated clay	120	0.37	0.30
Dry sand	100	0.33	0.50
Wet sand	120	0.33	0.50

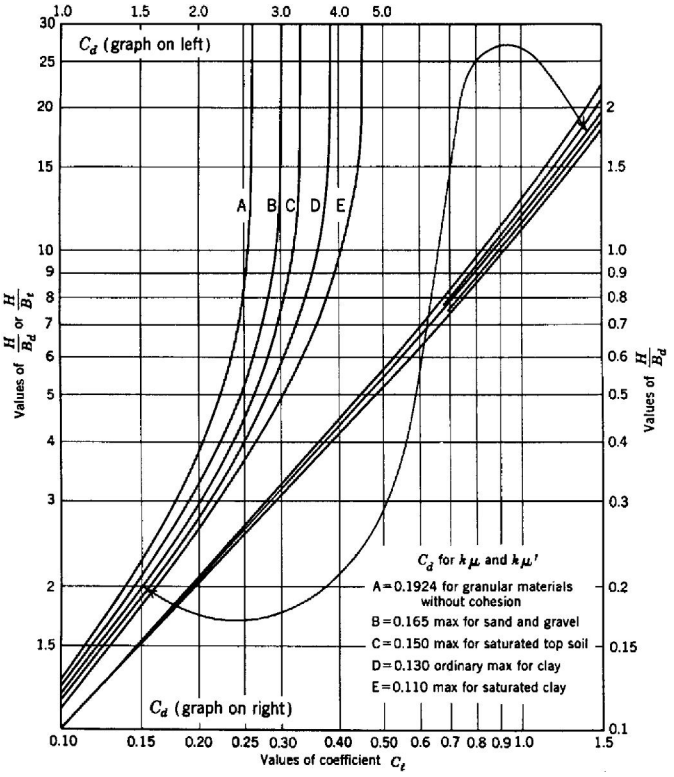

Figure 2.4 Computational diagram for earth loads on trench conduits completely buried in trenches.

Establishing that the soil parameters, μ and K do not vary significantly, it can be stated that the load coefficient, C_d is mainly a function of the relative depth of cover above the pipe. The coefficient for a rigid pipe, C_d, is approximately 0.85 at H/B_d equal to 1 and increases to 1.5 for an H/B_d ratio of 2. This implies that the proportion of prism load ($\gamma B_d H$) transferred to the pipe decreases from 85% to 75% as the cover height increases from one times the trench width to twice the trench width. The load on the pipe is more dependent on soil type for greater cover heights. If the cover height is greater than $10B_d$, C_d is almost constant.

In case the relative stiffness of the pipe to the soil at the side fill is reasonably estimated, the load on a flexible pipe can be approximated. If it can be assumed that the soil at the side fill has the same degree of stiffness as the pipe itself, then the load can be proportioned on the basis of area, i.e.

$$W_c = \frac{W_d}{B_d} \times B_c \qquad\qquad W_c = C_d \times \gamma \times B_d \times B_c \qquad (2.3)$$

W_c : Load on flexible pipe

B_c : Outside diameter of the conduit

2.1.2.2 Earth Loads on Ditch Conduits with Sloping Sides

Due to the danger of trench cave-ins, many trenches are now cut with sloping sides if the ditches are not too deep and space is available. The width of the ditch (B_d) given in the above formulas is the width of a normal trench with vertical sides. In case the ditch conduits are placed in trenches with sloping sides, the width of the ditch (B_d) must be taken as the width of the trench at the crown of the pipe (Schlick, 1932).

2.1.3 Loads on Pipes Buried In Embankments

2.1.3.1 Earth Loads on Positive Projecting Conduits

An embankment is where the top of the pipe is above the natural ground. As given in the classification of underground conduits, this type of installation is defined as a positive projecting conduit. The shear planes at which the shear forces act in a positive projecting conduit are assumed to be the vertical planes extending upward from the sides of the conduit. Figures 2.5 and 2.6 show two cases of positive projecting conduits as proposed by Marston. In the first case, the ground at the sides of the pipe settles more than the top of the pipe. In the other case, the top of the pipe settles more than the soil at the sides of the pipe.

The term pB_c, is the distance from the pipe's crown to the ground surface where p is the projection ratio and B_c is the outside diameter of the conduit.

The flexibility of the pipe has a significant effect on the vertical load applied on the pipe. The magnitudes and directions of the relative movements between the soil prism ABCD (interior prism) (Figures 2.5 and 2.6) and the side fills (exterior prisms) are affected by the settlements of certain elements of the conduit, the settlement of natural ground and the settlement of the side fills. Marston combined these settlements into an abstract ratio, called the settlement ratio which is defined in equation 2.4. The values of settlement ratio for design purposes are presented in

Table 2.2.

$$r_{sd} = \frac{(S_m + S_g) - (S_f + d_c)}{S_m} \tag{2.4}$$

r_{sd} : Settlement ratio

S_m : Settlement of the side fill of height pB_c

S_g : Settlement of the natural ground surface at sides of pipe

S_f : Settlement of foundation underneath pipe

d_c : Pipe's deflection

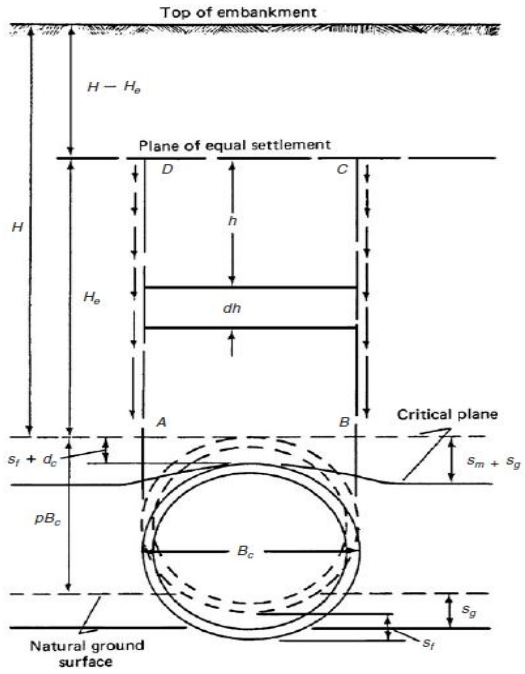

Figure 2.5 Positive projecting conduit - Projection conditions

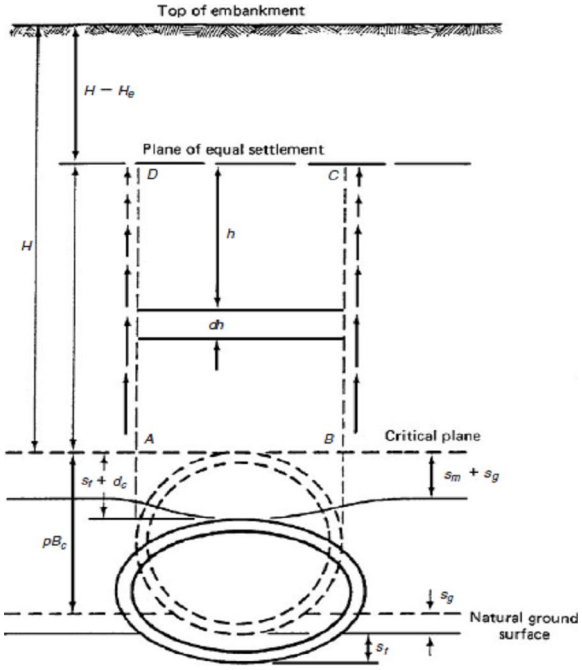

Figure 2.6 Positive projecting conduit – ditch condition

Marston also defined a critical plane which is the horizontal plane passing through the pipe crown as shown in Figure 2.6. During and after construction of the embankment, this plane settles downward. If the critical plane settles more than the crown of the pipe, then the settlement ratio, r_{sd} is positive; the shearing forces on the soil prism are directed downward and the vertical load on the pipe is greater than the weight of the soil prism. This is called 'projection condition'. On the other hand, if the critical plane settles less than the crown, then the settlement ratio, r_{sd} is negative;

the shearing forces on the soil prism are directed upward and the vertical load on the pipe is reduced. This case is called the 'ditch condition'. If the settlement ratio, r_{sd} is zero, then the load on the pipe exactly equals the weight of the soil prism.

Table 2.2 Design values of settlement ratio (Spangler and Handy, 1982)

Conditions	Settlement ratio
Rigid culvert on foundation of rock or unyielding soil	+1.0
Rigid culvert on foundation of ordinary soil	+0.5 to +0.8
Rigid culvert on foundation of material that yields with respect to adjacent natural ground	0 to +0.5
Flexible culvert with poorly compacted side fills	-0.4 to 0
Flexible culvert with well-compacted side fills	-0.2 to +0.8

In the case of projecting conduit, the vertical shear planes may not extend up to the top of the embankment (Fig. 2.6). The horizontal plane where the vertical shear planes extend is called the plane of equal settlement and the shearing forces are zero at this plane. Above this plane, the soil prism above the conduit settles at the same rate as the side fills (Spangler and Handy, 1982). In case the plane of equal settlement is located within the embankment, i.e. the height of the plane of equal settlement above the crown, H_e is less than the total height of the embankment H, then this is called the incomplete projection or incomplete ditch condition. If the shear forces extend all the way to the top of the embankment, i.e. H_e is greater than or equal to H, then this is called the complete projection or complete ditch condition.

Using the above discussed parameters, Marston derived formulas for the vertical load on positive projecting (embankment) conduits. For the complete ditch or projection condition the formula is:

$$W_c = C_c \gamma B_c^{\,2} \qquad C_c = \frac{e^{\pm 2K\mu(H/B_c)} - 1}{\pm 2K\mu} \tag{2.5}$$

C_c : Load coefficient for positive projecting conduit. Figure 2.7 is a typical diagram of C_c for the various values of H/B_c and $r_{sd}p$.

The load coefficient for the incomplete ditch projection condition is:

$$C_c = \frac{e^{\pm 2K\mu(H_e/B_c)} - 1}{\pm 2K\mu} + \left(\frac{H}{B_c} - \frac{H_e}{B_c}\right) e^{\pm 2K\mu(H_e/B_c)} \tag{2.6}$$

The plus signs are used for the complete projection condition and the minus signs are used for the complete ditch condition.

The formula developed by Marston for the value of H_e is:

$$\left[\frac{1}{2K\mu} \pm \left(\frac{H}{B_c} - \frac{H_c}{B_c}\right) \pm \frac{r_{sd}\,p}{3}\right] \frac{e^{\pm 2K\mu(H_e/B_c)} - 1}{\pm 2K\mu} \pm \frac{1}{2}\left(\frac{H_e}{B_c}\right)^2$$
$$\pm \frac{r_{sd}\,p}{3}\left(\frac{H}{B_c} - \frac{H_e}{B_c}\right) e^{\pm 2K\mu(H_e/B_c)} - \frac{1}{2K\mu}\frac{H_e}{B_c} \pm \frac{H}{B_c}\frac{H_e}{B_c} = r_{sd}\,p\frac{H}{B_c} \tag{2.7}$$

Since the only unknown parameter in this equation is H_e, the equation can be solved by trial and error. Again, the plus signs are used for the incomplete projection condition and the minus signs are used for the incomplete ditch condition. Another method was proposed by Wastlund and Eggwertz for the evaluation of H_e (Bulson, 1985).

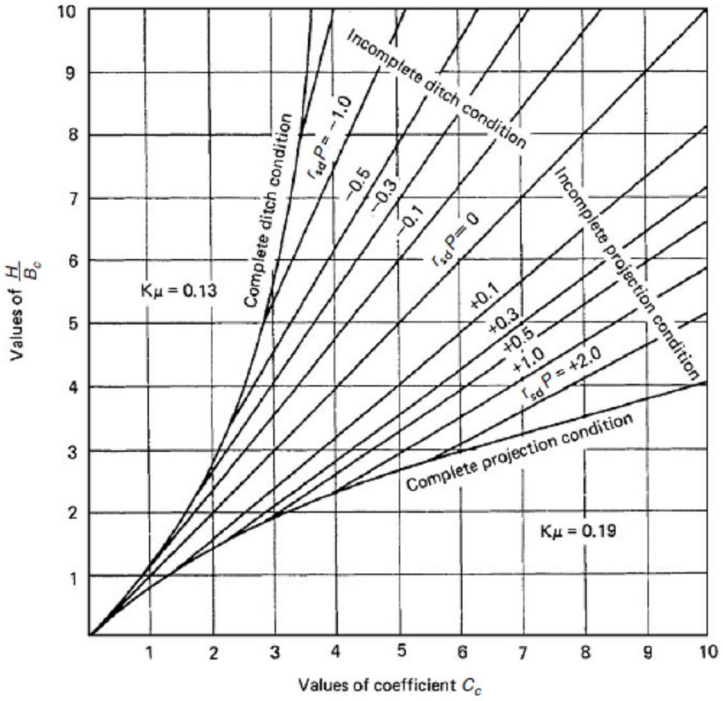

Figure 2.7 Diagram for coefficient Cc for positive projecting conduits (Spangler and Handy, 1982)

2.1.3.2 Earth Loads on Imperfect Ditch (Induced Trench) Conduits

The imperfect ditch or induced trench method of construction was suggested by Marston in order to reduce the load on the conduit under the projection condition. In the case of imperfect ditch conduit, demonstrated in Figure 2.8, it is aimed to insure that the soil prism above the pipe (interior prism) will settle more than the side fills (exterior prisms), hence generating friction forces which are directed upward on the sides of the soil prism. The settlement ratio is given by the following formula:

$$r_{sd} = \frac{S_g - (S_d + S_f + d_c)}{S_d} \tag{2.8}$$

S_d : Settlement of the fill in ditch within height $p'B_c$

A different projection ratio, which is designated by p' is referred in the imperfect ditch condition. The projection ratio p' is defined as the depth of the trench divided by its width. Moreover, the critical plane is now established to be the horizontal plane at the level of the compacted backfill surface in the trench backfill material.

The settlement ratio, r_{sd} is always negative in imperfect ditch conduit case, which implies that the direction of shear forces at the sides of the interior prism is always upward. In other words, the arching effect will always transmit the load on the conduit to the side fill.

The vertical load on imperfect ditch conduits is calculated from the formula:

$$W_c = C_n \gamma B_c^2 \tag{2.9}$$

C_n : Load coefficient for imperfect ditch conduit.

Spangler and Handy (1982) provided several sets of C_n computation diagrams with different parameter values. A typical C_n diagram for imperfect ditch conduit and negative projecting conduit when $p'=0.5$ is presented in Figure 2.9.

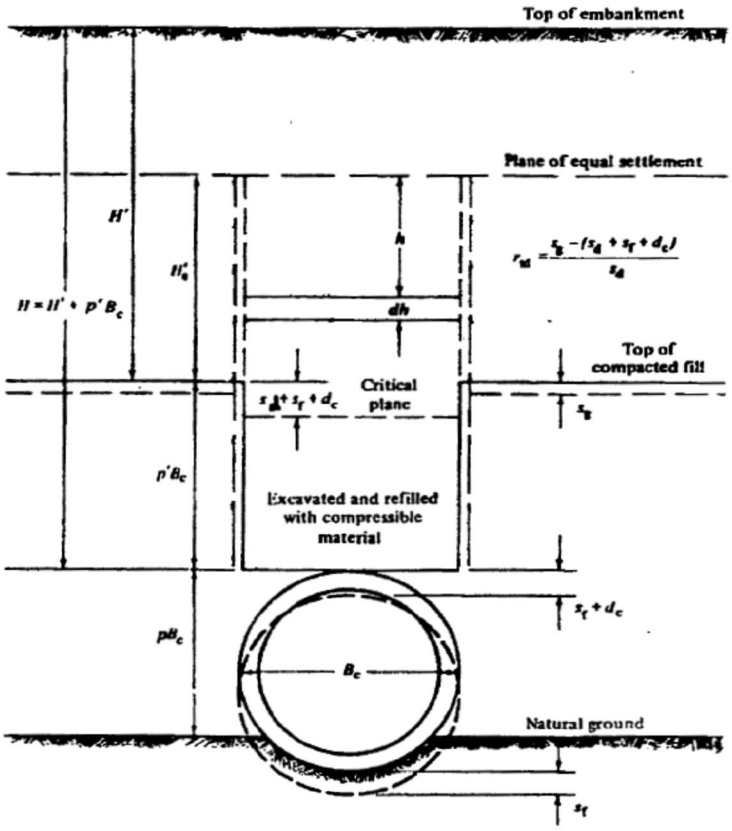

Figure 2.8 Imperfect ditch conduit conditions

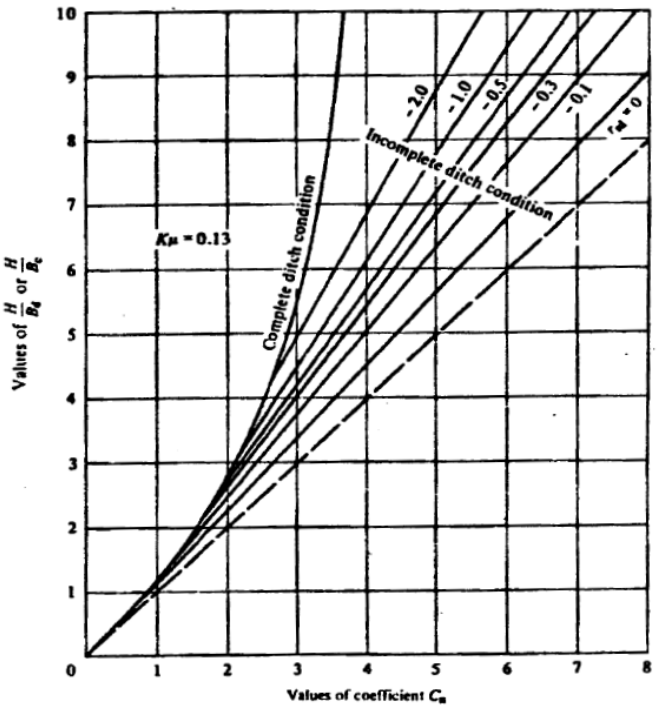

Figure 2.9 Diagram for coefficient Cn for imperfect ditch conduits (Spangler and Handy, 1982)

2.1.3.3 Earth Loads on Negative Projecting Conduits

The analysis of loads on negative projecting conduits follows the same procedures as for the imperfect ditch conduits, but uses B_d (width of shallow ditch in which the pipes is installed) as the width factor instead of the width of the imperfect ditch, B_c.

2.1.3.4 Earth Loads on Conduits in Wide Trenches

Schlick (1932) found that Marston's equation, Eq. (2.2), for W_d was valid and applicable until the point where the ditch conduit load W_d was equal to the projection conduit load W_c. Therefore, for an increasing trench width, the load is calculated according to Eq. (2.2) until the ditch load is equal to the embankment load and then it is calculated according to Eq. (2.5). The trench width at which this occurs is called the transition width. Figure 2.10 is a plot of the values of H/B_c and $r_{sd}p$ that give Bd/Bc values that represent the transition width. It is generally suggested that an $r_{sd}p$ value of 0.5 be used to determine the transition width (Moser and Folkman, 2008).

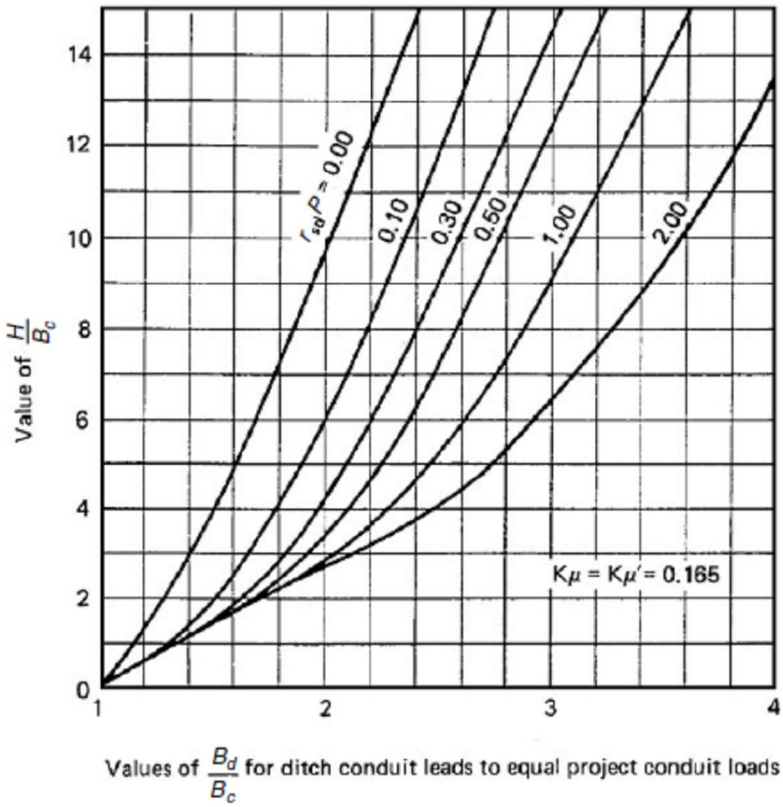

Figure 2.10 Curves for transition-width ratio (Spangler and Handy, 1982)

2.1.4 Further Theories for the Earth Loads on Pipes

Although Marston's theory is a very useful tool, it has got limitations as it does not properly account for pipe-soil interaction or arching within the backfill for non-rigid pipes. It is also not readily amenable to variations in the properties of the backfill or natural ground over the depth of the trench. The main limitations of Marston load theory, as stated by Sladen and Oswell (1988), are;

- the simplifying assumptions concerning the geometry of the failure prism,
- the uniformity of vertical stresses within the prism,
- the lack of consideration of the stiffness of the backfill soil.

Kellogg (1993) extended Marston's theory to cover sloping trenches.

Molin (1981) established that the vertical soil pressure, w, over a pipe buried in an infinitely wide trench (e.g. under embankment fill) increased with the pipe stiffness and proposed that the average pressure at the top of pipe could be given with the formula;

$$C = \frac{36S_r(20S_r + 1)}{(12S_r + 1)(36S_r + 1)} \qquad w = Cq_0 \tag{2.10}$$

q_o : pressure at crown level without a pipe

C : load factor (minimum 1)

S_r : Stiffness ratio=$\delta S/E'$

S : Stiffness of pipe=EI/D^3

E' : Horizontal modulus of soil reaction as defined by the Iowa formula (see section 2.3)

Equation 2.10 for load factor, C is a design approximation of the theoretical cases which correspond to full slip between the pipe and the soil and no slip. Maximum C values and hence the pressures above pipes are developed in full slip case (Crabb and Carder, 1985). The minimum value of 1 for C requires pipe stiffness values exceeding common flexible pipes. Therefore, Molin's expressions have little effect on flexible pipes.

In the German pipe design method (ATV Code, 1984), pipe loads for all pipe types can be calculated considering the effects of pipe stiffness and the variation of soil modulus around the pipe. The method is semi-empirical although it is basically similar to Marston theory.

In their study for the comparison of German to Marston Design Method, Jeyapalan and Hamida (1988) showed that Marston loads are always greater. While the German method was assumed to result correct loads, Jeyapalan and Hamida concluded that even for relatively stiff, vitrified clay pipes, Marston theory is mainly conservative for 'small pipes backfilled with well-compacted granular material'. Loads may be overestimated by 100%. According to the German design method, the load at the pipe crown is:

$$W_{GDM} = C_d L \gamma B D \tag{2.11}$$

C_d : Marston load coefficient

L : load redistribution coefficient

The load redistribution coefficient, L, depends on soil modulus around the pipe, the ratio of pipe stiffness to side fill stiffness and the geometry of the buried pipe installation.

2.1.5 Live Loads (Wheel Loading)

When the pipes are buried at shallow depths, they will be subjected to the loads exerted by traffic. Wheel loads from trucks, airplanes or trains cause concentrated loads on buried pipes. Simple load distributions have been applied in the past for the purpose of pipe design, based on the assumption of elastic backfill behaviour. Certain standards allow load spreading of concentrated road vehicle loads depending on the cover height. The surface patch plan dimensions increase at the pipe crown, thereby reduces the applied vertical stress. The French mathematician Boussinesq also calculated the distribution of stresses in a semi-infinite elastic medium due to a point load applied at its surface. This solution assumes an elastic, homogeneous, isotropic medium, which is not the case for a real soil. However, as shown by the

experiments, the classical Boussinesq solution gives reasonably good results for soil when it is properly applied (Moser and Folkman, 2008). Numerical analyses can be used to more accurately assess the influence of wheel loading.

2.1.6 Characteristics of Buried Pipe Installations

Buried pipe installations have a characteristic nature which leads to the formation of soil zones of different strengths and stiffnesses within an initially homogeneous backfill material. The application of compaction is restricted by the geometry of the trench and the sensitivity of the installed flexible pipe to compaction of material around it. Typical zones and the terminology used to describe these zones are given in Figure 2.11.

The zones lead to the definition of the structural zone for a pipe and its backfill. The structural backfill extends from the base of the bedding to a maximum of 300 mm above the pipe. In this zone, granular material is strongly preferred for easier compaction, high earth pressure response and stability when saturated and confined. Some other materials have been accepted for use for economic reasons in case loads are low to moderate (Molin, 1981, Janson and Molin, 1981). Vertical soil support is provided by the bedding.

The lateral support zone is unlikely to be uniform. Many researchers pointed the difficulty in compacting underneath the pipe in the haunch zone and suggested using crushed rock backfills which need little compaction (e.g. Webb, McGrath and Selig, 1996, Rogers, Fleming, Loeppky and Faragher, 1995, and Rogers, Fleming and Talby, 1996) and cementitious slurries.

The natural soil forming the trench walls has an influence on the lateral soil support. This has been addressed by Leonhardt (1973) and will be further explained in Section 2.3.2.

The selection of final backfill material depends on the economics of the construction which will be influenced mainly by the trench geometry and the suitability of the excavated material. Therefore it may or may not be the same as the pipe embedment zone material (it is not the same in this study).

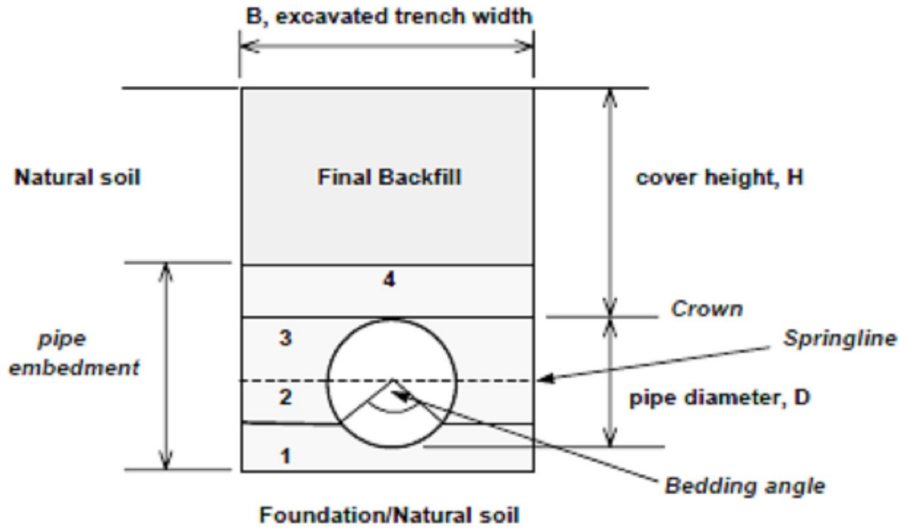

Zone	Description	Level of Compaction
1	Bedding	Well compacted and usually shaped to receive the pipe to distribute the load support.
2	Haunching	Poorly compacted, particularly in a narrow trench. Rodded or tamped at best.
3 and 4	"Initial Backfill"	Moderately compacted.
3	Springline to crown	Moderately compacted by rodding or tamping.
4	Approx 150 to 300 mm above the pipe	Moderately compacted by rodding or tamping or a few passes of a vibrating plate.

Figure 2.11 The zones within a backfill

2.1.7 Primary Model of the Behaviour

The primary model for the design of flexible pipes is the 'thin elastic ring' (Prevost and Kienow, 1994). The stress tables in structural engineering textbooks present solutions for the maximum moments and ring deflection under different loading conditions.

Figure 2.12 below presents a typical stress distribution that is assumed in the soil

surrounding a buried pipe.

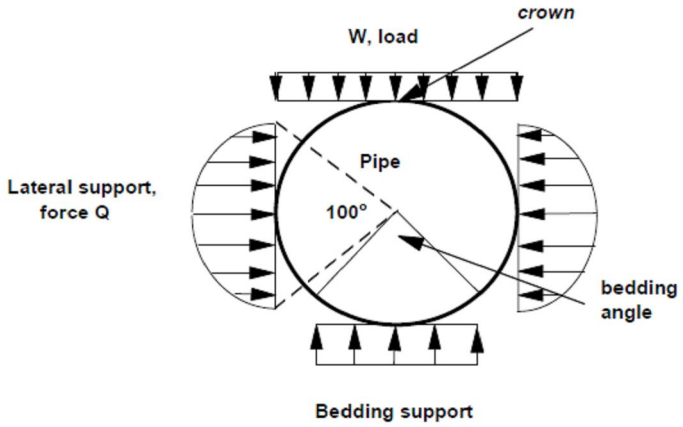

Figure 2.12 Generally assumed pipe pressure distributions

The above assumption for stress distribution is an effort to incorporate the effects of soil-structure interaction. In case the pipe is buried at shallow depths, the pipe is loaded at its crown by the weight of backfill material and live loading due to traffic. A uniform vertical pressure is assumed at the pipe crown. Part of this vertical pressure at pipe crown is resisted by the soil reaction from the foundation or bedding of the pipe. In a flexible pipe system, further support is provided by lateral sidefill pressure which develops as the pipe deflects under the vertical load (see Figure 2.13 below)

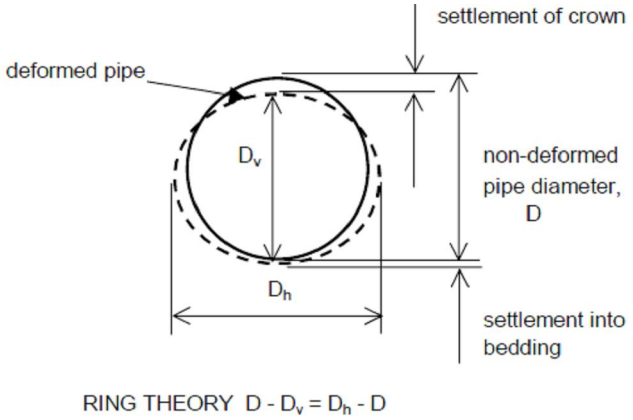

Figure 2.13 Pipe deformation

Lateral earth pressures may reach to passive pressure levels if the pipe deflects considerably. As an arbitrary assumption, the distribution of the side reaction is generally assumed to be parabolic.

The degree of reaction from the lateral earth pressure depends also on the nature and degree of compaction of the backfill, as well as the stiffness of the side walls of a trench (in case the pipe is installed in a trench rather than in an embankment fill). Therefore, the performance of a flexible pipe is significantly affected by the backfill and its construction. The designers unfortunately paid too much attention on the structural properties of the pipe in the past. The importance of sidefill compaction was demonstrated by Crabb and Carder (1985) in their experiments. Rogers et al. (1995) stated that soil stiffness rather than the stiffness of the pipe dominates the design of profile wall drainage pipe. This statement was supported by McGrath, Chambers and Sharff (1990) who designated the design problem as 'pipe-soil interaction' rather than 'soil-structure interaction'.

As per the 'ring behaviour', the decrease in vertical diameter is compensated by an increase of the same magnitude in the horizontal diameter, such that the deformed shape is elliptical. Knowing the pressure distribution around the pipe, moments, stresses and deformations may be evaluated assuming 'ring behaviour' is applicable. After Prevost and Kienow (1994), the maximum moment, M in the pipe is generally given by the expression:

$$M = mWR \tag{2.12}$$

m : moment coefficient based on ring theory

W : transverse uniform load on ring's section at crown level

R : ring radius

Marston's theory can be used to derive the transverse uniform load, however the resultant load above the pipe may not be uniform and the incorporation of the external live load effect in the load term, W, was considered to be uncertain by the authors.

The pipe deflection may be expressed as follows:

$$\Delta_i = \frac{Wd_r}{S} \tag{2.13}$$

Δ_i : Pipe deflection in direction, i

W : total transverse load on ring at crown level

d_r : deflection coefficient in the direction being considered

S : stiffness of pipe, EI/D^3

The deflection coefficient, d_r varies with the direction being considered and the pressure on the pipe, e.g. for a uniform pressure of w on the pipe, the deflection in the x direction, Δx is given by;

$$\frac{\Delta_x}{D} = \frac{wd_x}{S} \tag{2.14}$$

The pipe initially tends to deform as an ellipse as shown in Figure 2.13. Therefore it has been a common assumption that the lateral diametric increase of the pipe is equal to the vertical diametric reduction. Since the horizontal modulus of soil reaction, E' (in Iowa formula), is defined as the force per unit length along the pipe to cause a unit displacement, then the side thrust on the pipe may be expressed in terms of the lateral deformation. Subsequently, lateral deflections may be determined separately for the vertical and lateral load components using the ring equations available in structural texts, and the total lateral deflection is estimated by algebraic summation. This process leads to the Spangler or Iowa equation.

2.1.8 Iowa Deflection Formula

M. G. Spangler, a student of Anson Marston, observed that the Marston theory for calculating loads on buried pipe was not adequate for flexible pipe design. A conduit that will deflect at least 2% without any sign of failure or cracks in normal loading conditions may be defined as a flexible pipe (Uni-Bell, 1993). In fact, the ability of a flexible pipe to support vertical soil loads is derived from its flexibility. As explained in the previous sections, the capability of the pipe to deflect under load causes developing of passive soil support at the sides of the pipe. At the same time, the ring deflection relieves the pipe of the major portion of the vertical soil load which is picked up by the surrounding soil in an arching action over the pipe. These considerations together with the idea that the ring deflection may form a basis for flexible pipe design, leaded M. G. Spangler to study flexible pipe behaviour.

2.1.8.1 Pipe Stiffness

The pipe stiffness, PS which relates to the resistance of a flexible pipe to applied loads can be determined by conducting parallel-plate loading tests in accordance with ASTM D2412, Standard Test Method for Determination of External Loading Characteristics of Plastic Pipe by Parallel-Plate Loading. The pipe stiffness (PS) as per ASTM D2412 is given as follows:

$$PS = \frac{F}{\Delta Y} = \frac{EI}{0.149r^3} \tag{2.15}$$

PS : Pipe stiffness

F : External load applied over a unit length of the pipe wall

ΔY : Vertical change in inside diameter of the pipe wall

EI : Stiffness factor

E : Modulus of elasticity

I : Moment of inertia

r : Mean radius of the pipe wall

For a solid pipe wall of unit length, the moment of inertia is:

$$I = \frac{t^3}{12} \tag{2.16}$$

t : Total wall thickness of the pipe

2.1.8.2 Spangler's Iowa Formula (1941)

In order to define the capability of a flexible pipe to resist ring deflection when not buried in the soil, Spangler first established the following relationships:

$$\Delta Y = \frac{0.149Fr^3}{EI} \tag{2.17}$$

$$\Delta X = \frac{0.136Fr^3}{EI} \tag{2.18}$$

$$\Delta X = 0.913\Delta Y \tag{2.19}$$

ΔX : Change in horizontal diameter

Afterwards, Spangler incorporated the effects of the surrounding soil on the pipe's deflection. This was accomplished by assuming that Marston's theory of loads applied and that this load would be uniformly distributed at the plane at the top of the pipe. He also assumed a uniform pressure over part of the bottom, depending upon the bedding angle. On the sides, he assumed the horizontal pressure h on each side would be proportional to the deflection of the pipe into the soil (distributed parabolically at middle 100^0). Based on Figure 2.14, he derived the Iowa formula through analysis as follows:

$$\Delta X = D_l \frac{KW_c r^3}{EI + 0.061er^4} \tag{2.20}$$

ΔX : Horizontal deflection

D_l : Deflection lag factor

K : Bedding constant (function of a bedding angle, Table 2.2)

W_c : Marston's load per unit length of pipe

r : Mean radius of the pipe

E : Modulus of elasticity of the pipe material

I : Moment of inertia of the pipe wall per unit length of pipe

e : Modulus of passive resistance of the side fill further modified by Watkins (2h/ Δ X)

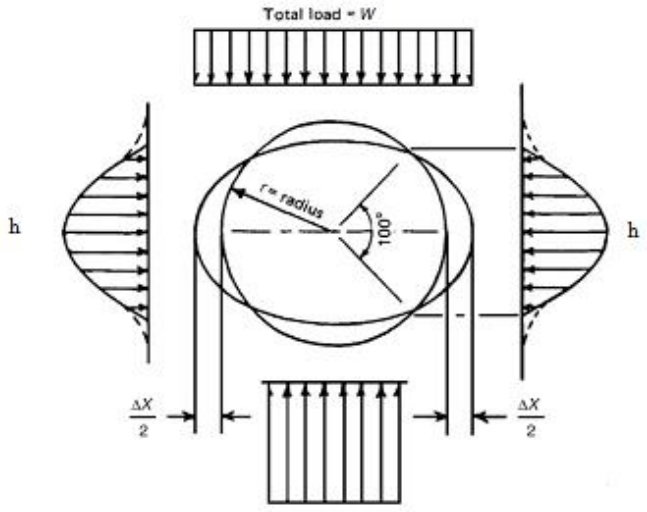

Figure 2.14 Basis of Spangler's derivation of the Iowa formula for deflection of buried pipes

The original Iowa formula predicts deflections of buried pipe if the three empirical constants: K, D_l and e are known. The bedding constant, K, is related to the angle of the vertical support of the pipe, ψ or the uniform soil reaction on the pipe, P due to the overburden pressure, W. Table 2.3 contains a list of bedding factors which were determined theoretically by Spangler (1941). Prevost and Kienow (1994) later suggested that the bedding support angle could be taken to be 90° with little danger of significant error in determining moments and deflections, giving rise to a value of K_s (modified bedding constant) of 0.012.

The deflection lag factor, D_l, considers the consolidation of the side fills with time. The deflection lag factor is unity for short term loading. For sustained loading, D_l increases with time due to consolidation effects arising from the lateral soil pressures developed beside the deflecting pipe (Howard, 1985). The experience of Spangler had shown that deflections could increase by as much as 30% over 40 years (Uni-Bell, 1993). For this reason, Spangler recommended the incorporation of a deflection lag factor of 1.5 as a conservative design practice.

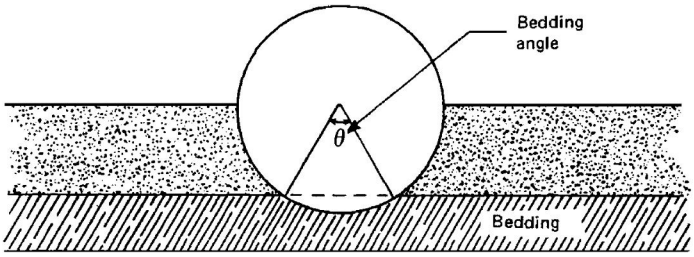

Figure 2.15 Bedding angle

Table 2.3 Values of Bedding Constant, K

Bedding angle, degree	K
0	0.110
30	0.108
45	0.105
60	0.102
90	0.096
120	0.090
180	0.083

2.1.9 Modified Iowa Deflection Formula

In 1958, Reynold K. Watkins was investigating the modulus of passive resistance, *e* through model studies and examined the Iowa formula dimensionally. Watkins found that *e* could not be a true property of the soil as its dimensions are not those of a true modulus. As a result, Watkins defined a new parameter named the modulus of soil reaction, *E'=er*. From the work of Watkins, the modified Iowa formula was written:

$$\Delta X = D_l \frac{KW_c r^3}{EI + 0.061E'r^3} \tag{2.21}$$

Further details and discussions on the modulus of soil reaction, E' parameter will be presented in section 2.3.

2.1.10 Modified Iowa Deflection Formula by Greenwood and Lang

The Marston-Spangler theory, developed for the prediction of deflections in flexible pipes, has been proven to be working further to the experiments of some well-known researchers like Spangler (1941), Watkins (1958) and Howard (1977). However, the modified Iowa deflection formula does not take into account the stages of construction and the pipe-soil interaction aspects of the problem in the calculation of the total deflection of a pipe.

It should be noted that the total deflection of a buried pipe is affected from many parameters. Listed below are the governing parameters as stipulated by Greenwood and Lang (1990):

- Pipe stiffness
- Soil stiffness (soil type, density, modulus and moisture content)
- Applied loads (vertical and lateral pressure loads due to overburden and applied surface loads)
- Trench configuration (trench geometry, native in situ soil condition and type of embedment)
- Haunch support
- Construction stages

- Non-elliptical deformation
- Initial ovalization (vertical elongation due to placement of embedment during construction)
- Time
- Temperature
- Variability (construction variability due to excavation, soil placement and compaction)

Spangler's Iowa formula is based on three major limiting assumptions: i) The vertical deflection is equivalent to the horizontal deflection; ii) The deformation of the pipe is elliptical; iii) The horizontal modulus of soil reaction is constant for the backfill material

The application of a horizontal modulus of soil reaction assumes that there is no soil support or soil stresses until deflections commence. However the placement of the pipe leads to in-situ soil stresses which increase the lateral resistance available. In Sweden, an alternative expression to the Iowa equation has been used, which allows for an initial lateral resistance due to the at rest earth pressures in the backfill (Molin, 1981).

The non-elliptical deformation and the initial deformation due to construction stages are not taken into account by Spangler's Iowa formula. Initial vertical deflections of the pipe are so significant that the earth load on pipe at the completion of the backfill may not cause the pipe to extend horizontally. The non-elliptical deformation is resulted from the non-uniform earth pressure around the pipe. Greenwood and Lang (1990) found out that the non-uniformity is a function of soil type, degree of compaction, split embedment and pipe stiffness.

Greenwood and Lang (1990) also proposed a modified Iowa formula, which is more complete than the original formula. Their modified Iowa formula included the work of Leonhardt (1972-1979) who developed a factor to consider the influence of the natural soil forming the trench walls on the lateral soil support. The effective sidefill stiffness is given by $\varsigma E'$, where ς is Leonhardt's correction factor on the modulus of soil reaction, E', as defined in the Iowa formula. A pipe-soil interaction

coefficient, C_l which is an empirical factor, is added to the soil resistance term to reflect the behaviour of flexible pipes in the field. The modified Iowa formula of Greenwood and Lang (1990) is presented below:

$$\Delta X = \frac{K(\gamma H)}{EI/r^3 + 0.061\varsigma C_l E'} - \delta_{vo} \tag{2.22}$$

ΔX : Horizontal deformation

K : Bedding factor (Table 2.4)

γ : Unit weight of the backfill

H : Height of the backfill above the pipe

E : Modulus of elasticity of pipe material

I : Moment of inertia of the pipe wall per unit length of pipe

r : Mean radius of the pipe

E' : Modulus of soil reaction in modified Iowa formula (Watkins)

δ_{vo} : Elongation due to compaction of the side fills

ς : Leonhardt's correction factor

$$\varsigma = \frac{1.662 + 0.639(B/D - 1)}{(B/D - 1) + \left[1.662 - 0.361(B/D - 1)\right]\frac{E'}{E_3}}$$

E_3 : Young's modulus of the natural soil forming the trench

B : The width of the trench

D : Pipe diameter

C_l : Pipe-soil interaction coefficient defined by Greenwood and Lang (1990)

$$C_l = a\left(\frac{EI}{1250.D^3}\right)^b$$

a,b : Parameters provided in below Table 2.5

Table 2.4 Bedding factor values, K (Greenwood and Lang, 1990)

Soil group	Range of fines %	Backfill standard Proctor density			
		>95	85-95	70-84	<70
Clean grave1	<5	0.083	0.083	0.083	0.083
	5-12	0.096	0.096	0.083	0.083
Dirty grave1	12-50	0.103	0.103	0.096	0.083
Clean sand	<5	0.103	0.103	0.096	0.083
	5-12	0.103	0.103	0.096	0.083
Dirty sand	12-50	0.103	0.103	0.096	0.083
		0.103	0.103	0.096	0.083
Inorganic clay and silt	>50	0.103	0.103	0.096	0.083

Table 2.5 a and b values for pipe soil interaction coefficient (Greenwood and Lang, 1990)

Backfill standard Proctor density	a	b
>95	1.240	0.180
85-95	0.938	0.245
70-84	0.643	0.353
<70	0.456	0.436

2.1.11 Watkins's soil-strain theory

A number of variations of Spangler and Watkins's modified Iowa formula have been proposed. All can be represented in simple terms as follows:

$$\text{Deflection} = \frac{\text{load}}{\text{Pipe stiffness} + (\text{constant})\,\text{soil stiffness}}$$

Watkins (1988) rearranged the Iowa equation to express the ratio of pipe deflection to vertical soil strain above the pipe, ε' (= w/E') and wrote the Iowa formula in terms of dimensionless ratios as follows:

$$\frac{\Delta y}{D\varepsilon} = \frac{PR_s}{E_s AR_s + B} \tag{2.23}$$

P : Vertical nominal pressure at top of pipe level

R_s : Stiffness ratio (This is the ratio of soil stiffness E_s to pipe-ring stiffness $S=EI/D^3$)

$$R_s = 12\frac{E_s D^3}{Et^3}$$

E_s : Slope of stress-strain curve for soil in one-dirnensiona1 consolidation test=P/ε

ε : Vertical soil strain

D : Outside diameter

A, B : Empirical constants including D_l and K of the Iowa formula

Δy : Change in vertical diameter

The equation can be rewritten as:

$$\frac{\Delta y}{D\varepsilon} = \frac{R_s}{AR_s + B} \tag{2.24}$$

Assuming the vertical and horizontal deflections at small strains are equal and that K is 0.1, the Iowa equation becomes;

$$\frac{\Delta y}{D\varepsilon} = \frac{R_s}{80 + 0.61R_s} \tag{2.25}$$

Watkins argued that the pipe deflection can not exceed the soil deformation, so the left hand side of the equation, should not exceed unity. However at values of ring stiffness ratios (R_s) greater than 200, this can occur. Figure 2.16 is a graph based on empirical data, which gives the ring deflection factor ($\Delta Y /D)/\varepsilon$) as a function of stiffness ratio. Watkins observed that usually the deflection factor approaches the unity because the stiffness ratio is usually greater than 300. As a result, the ring deflection becomes about as much as the side fills settlement. It is then possible to evaluate the pipe's deflection from the vertical soil main in the fill. Figure 2.17 presents vertical soil strain values as a function of soil compressibility and soil pressure.

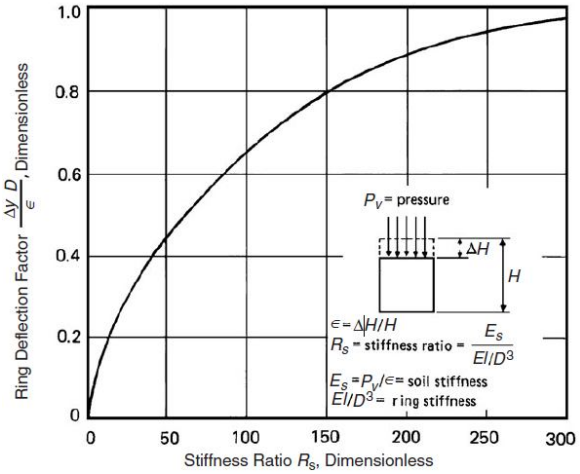

Figure 2.16 Ring deflection factor as a function of stiffness ratio (Moser and Folkman, 2008)

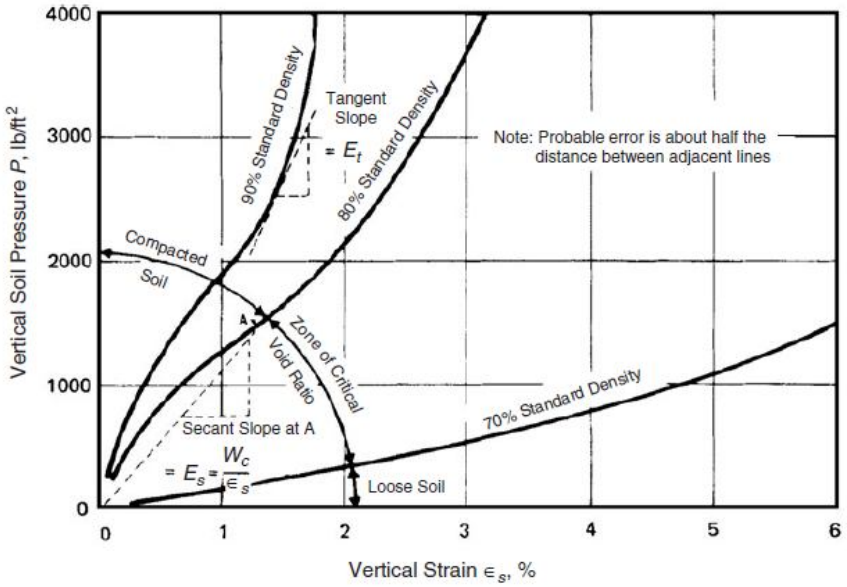

Figure 2.17 Plot of vertical stress-strain data for typical trench backfill (except clay) from actual tests (Moser and Folkman, 2008)

From extensive testing of flexible pipes, Watkins found an alternative and more satisfactory, empirical expression:

$$\frac{\Delta y}{D\varepsilon} = \frac{R_s}{30 + R_s} \tag{2.26}$$

Figure 2.18 provides a visual comparison of equations 2.25 and 2.26. The

comparison suggests that the Iowa equation overestimates deflections of more flexible pipes (higher R_s values) and may tend to slightly underestimate the deflections of less flexible pipes.

The elliptical pipe deformations assumption in the above equations is reasonable at relatively small deflection levels only. The deflection estimates from these equations generally become non-conservative as strains increase (Howard, 1985, Cameron, 1990 and Sargand, Masada and Hurd, 1996). Rogers (1987) found that elliptical deformations were associated only with poor sidefill or surround support.

The applicability of ring compression theory for flexible pipes buried in trenches was tested by Valsangkar and Britto (1978) through centrifuge tests. If ring theory is applicable then membrane compression stresses should govern and flexural stresses should be unimportant. It was concluded by their study that for pipes in narrow trenches, where the side cover is less than or equal to one diameter, the use of simple ring theory could not be justified. For this reason, the Iowa equation should not be used for ratios of trench width to pipe diameter (B/D) of 2 or less.

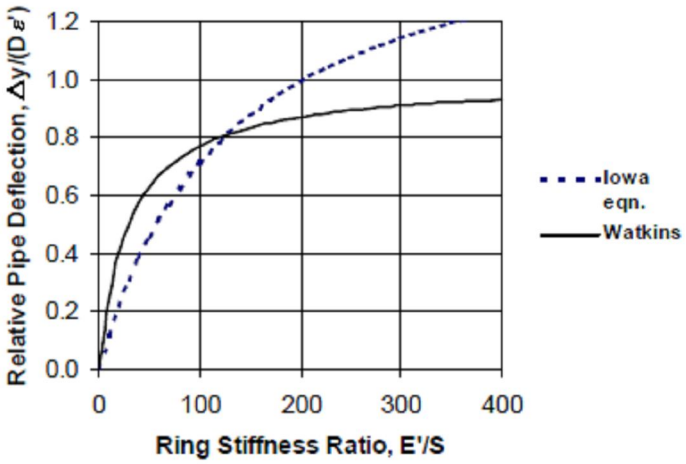

Figure 2.18 Comparison of Iowa equation and Watkins' (1988) empirical expression

2.1.12 Burns and Richard Elastic Solution

A theoretical solution was published by Burns and Richard (1964) for an elastic pipe buried in an infinite elastic medium and subjected to vertical and horizontal load. The Iowa formula is also a linear elastic theoretical solution; however it is

based on several field observations. Burns and Richard solution allows for a non-linear soil modulus correction and is based on the condition of full-bond or free-slip at the soil-pipe interface. It was assumed that no gap takes place at the pipe-soil interface for both cases. A summary of Burns and Richard solution is given below:

Extensional flexibility ratio: $UF = 2B\dfrac{M^* R}{EA} = (1+K)\dfrac{M^* R}{EA}$ (2.27)

Bending flexibility ratio: $VF = 2C\dfrac{M^* R^3}{6EI} = (1-K)\dfrac{M^* R^3}{6EI}$ (2.28)

$$M^* = \frac{E^*(1-\mu)}{(1+\mu)(1-2\mu)} \qquad K = \frac{\mu}{1-\mu}$$

$$B = \frac{1}{2}(1+K) = \frac{1}{2}\left(\frac{1}{1-\mu}\right) \qquad C = \frac{1}{2}(1-K) = \frac{1}{2}\left(\frac{1-2\mu}{1-\mu}\right)$$

In case of full bonding:

$$P_r = p\left\{B\left[1-a_0^*\right] - C\left[1-3a_2^* - 4b_2^*\right]\cos 2\theta\right\} \quad (2.29)$$

$$T_{r\theta} = p\left\{C\left[1+3a_2^* + 2b_2^*\right]\sin 2\theta\right\} \quad (2.30)$$

$$v = \frac{pR}{2M^*}\left\{\left[1-a_2^* + \left(\frac{2C}{B}\right)b_2^*\right]\sin 2\theta\right\} \quad (2.31)$$

$$w = \frac{pR}{2M^*}\left\{UF\left[1-a_0^*\right] - VF\left[1-a_2^* - 2b_2^*\right]\cos 2\theta\right\} \quad (2.32)$$

$$N = pR\left\{B\left[1-a_0^*\right] + C\left[1+a_2^*\right]\cos 2\theta\right\} \quad (2.33)$$

$$M = pR^2\left\{\frac{CUF}{6VF}\left[1-a_0^*\right] + \frac{C}{2}\left[1-a_2^* - 2b_2^*\right]\cos 2\theta\right\} \quad (2.34)$$

$$a_0^* = \frac{UF-1}{UF+(B/C)} \qquad a_2^* = \frac{C(1-UF)VF - (C/B)UF + 2B}{(1+B)VF + C(VF+1/B)UF + 2(1+C)}$$

$$b_2^* = \frac{(B+CUF)VF - 2B}{(1+B)VF + C(VF+1/B)UF + 2(1+C)}$$

In case of free slip:

$$P_r = p\left\{B\left[1-a_0^*\right] - C\left[1-3a_2^{**} - 4b_2^{**}\right]\cos 2\theta\right\} \quad (2.35)$$

$$v = \frac{pR}{6M^*}\left\{\left[VF + (C/2B)UF\right]\left[1+3a_2^* - 4b_2^{**}\right]\sin 2\theta\right\} \quad (2.36)$$

$$w = \frac{pR}{2M^*}\left\{UF\left[1-a_0^*\right] - \frac{2}{3}VF\left[1-a_2^{**} - 2b_2^{**}\right]\cos 2\theta\right\} \quad (2.37)$$

$$N = pR\left\{B\left[1-a_0^*\right]+\frac{C}{3}\left[1+a_2^{**}-4b_2^{**}\right]\cos 2\theta\right\} \tag{2.38}$$

$$M = pR^2\left\{\frac{CUF}{6VF}\left[1-a_0^*\right]+\frac{C}{3}\left[1-a_2^{**}-4b_2^{**}\right]\cos 2\theta\right\} \tag{2.39}$$

$$a_2^{**} = \frac{2VF-1+1/B}{2VF-1+3/B} \qquad b_2^{**} = \frac{2VF-1}{2VF-1+3/B}$$

R : Mean radius of the pipe

E : Young's modulus for material in cylinder wall

A : Area of the section of the pipe wall per unit length

I : Moment of inertia of the pipe

E^* : Young's modulus of the medium

μ : Poisson's ratio for medium

K : Rankine's ratio.

P_r : Radial stress

$T_{r\theta}$: Tangential stress

p : Applied vertical boundary pressure

r, θ, z : Cylindrical coordinates

v : Tangential displacement

w : Radial displacement in medium

N : Thrust in pipe wall

M : Bending moment in pipe wall

2.1.13 Other Methods and Approaches

Moore (1993) published the design considerations for plastic pipe enveloped in uniform soil. He suggested determining the vertical pressure above the pipe, p_v, in a deep embankment, simply by summation of the product of unit weights of layers above the crown by their thickness. In order to determine the same pressure for a pipe buried in a trench, the coefficient of friction between the trench wall and backfill, μ, was required to apply simple arching theory as below:

$$p_v = \gamma B\left[\frac{1-e^{-2K_0\mu H/B}}{2K_0\mu}\right] \tag{2.40}$$

H and B are the depth and width of the trench, respectively. The backfill material is assumed to be uniform in Equation 2.40.

The horizontal pressure, p_h, beside the pipe was based on the coefficient of earth pressure 'at rest', K_o, and vertical pressure, p_v. The soil pressures were determined on planes far enough from the pipe, which was suggested to be a minimum of one pipe diameter from the circumference (Hoeg 1968).

The vertical and horizontal pressures around the pipe were converted by Moore to isotropic and deviatoric stress components, defined as $p_m = (p_v + p_h)/2$ and $p_d = (p_v - p_h)/2$, respectively. These stress components are shown in Figure 2.19. Uniform circumferential hoop stress takes place under isotropic loading. This stress will cause circumferential shortening and may also lead to the development of significant flexural stresses. Adequate strength and stiffness should be provided in design to resist these stresses. The deviatoric stress set leads to elliptical deformation. This combination of deformations indicate that the vertical diametric strain should be greater the horizontal diametric strain if p_v is greater than p_h.

Based on elastic behaviour and thin ring theory, Moore presented equations for the stresses, thrusts and pipe deflections. The radial stress over the pipe for the isotropic loading is given as follows:

$$\sigma_0 = A_m p_m = \frac{2(1-v_s)E_p A}{E_p A + 2G_s r} \tag{2.41}$$

A_m : Arching coefficient

p_m : The mean stress, $(p_v + p_h)/2$

v_s : Poisson's ratio for the soil

E_p : The elastic modulus of the pipe

A : Cross sectional area of the pipe

G_s : Shear modulus of the soil

r : Radius of the pipe

In case the arching coefficient, A_m for the pipe-soil system is less than unity, the pipe is considered as flexible and positive arching take place.

Hoeg (1968) proposed an elastic solution to analyse the magnitude and distribution of static stresses around horizontal cylinders. The solution was based on plane strain condition. The soil was assumed to behave like a linearly elastic, isotropic and homogeneous material. The pipe is assumed to be elastic as well.

Two stiffness ratios are used in the mathematical solution: The compressibility ratio, C, which is the ratio of compressibility of the structural cylinder to that of a solid soil cylinder, and the flexibility ratio, F, which relates the flexibility of the structural cylinder to the compressibility of the solid soil cylinder.

$$C = \left(\frac{1}{2(1-v_s)}\right)\left(\frac{M_s(1-v_p^2)}{E_p}\right)\left(\frac{D}{t}\right) \tag{2.42}$$

$$F = \left(\frac{(1-2v_s)}{4(1-v_s)}\right)\left(\frac{M_s(1-v_p^2)}{E_p}\right)\left(\frac{D}{t}\right)^3 \tag{2.43}$$

M_s : The constrained or 1-D modulus of the soil

v_p : Poisson's ratio of the pipe material

E_p : Young's modulus of the pipe material

D : The average pipe diameter

t : The pipe thickness

Hoeg's (1968) expression for the arching coefficient for points on the pipe circumference is given as follows:

$$A_m = (1-a_1) = \left[1 - \frac{(1-2v_s)(C-1)}{(1-2v_s)C+1}\right] \tag{2.44}$$

The deviatoric stress component around the pipe, p_d, causes further radial stress in the pipe, $\sigma_{rd\theta}$, and shear stress, $\tau_{d\theta}$. Both pipe stresses are functions of p_d and position along the pipe circumference, as given by the angle, θ, which is defined in below Figure 2.19.

The equations for the radial and shear stresses are given as follows:

$$\sigma_{rd\theta} = A_{d\sigma} p_d \cos 2\theta \tag{2.45}$$

$$\tau_{d\theta} = A_{dr} p_d \sin 2\theta \tag{2.46}$$

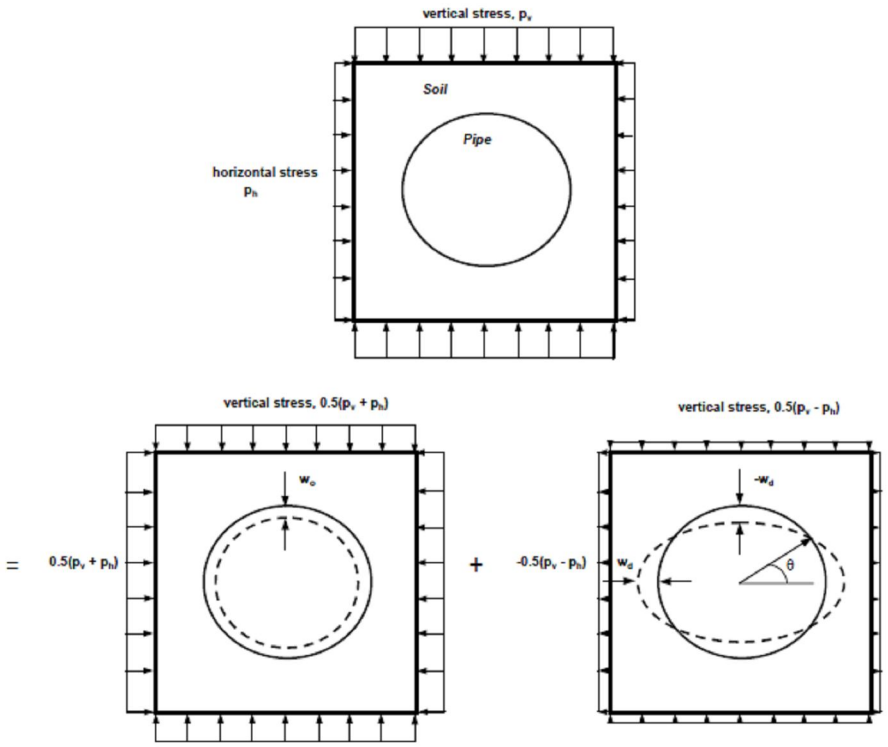

Figure 2.19 The response of a flexible thin pipe to the isotropic and deviatoric components of external loading (Moore, 1993)

In above expressions, $A_{d\sigma}$ and A_{dr} are functions of the relative stiffness of the pipe to the surrounding soil as well as the bond developed between the pipe and the soil. Hoeg (1968) provided theoretical solutions for these two factors, for both cases of a free slip (smooth) and a full bonding (rough) soil-pipe interface. In case of a perfectly rough interface and along the pipe circumference, these two factors are expressed with the following equations:

$$A_{d\sigma} = -(1 - 3a_2 - 4a_3) \tag{2.47}$$

$$A_{dr} = -(1 + 3a_2 + 2a_3) \tag{2.48}$$

$$a_2 = \frac{(1-2v_s)(1-C)F - 0.5(1-2v_s)^2 C + 2}{\left[(3-2v_s) + (1-2v_s)C\right]F + (2.5 - 8v_s + 6v_s^2)C + 6 - 8v_s}$$

$$a_3 = \frac{[1+(1-2v_s)C]F - 0.5(1-2v_s)C - 2}{[(3-2v_s)+(1-2v_s)C]F + (2.5-8v_s+6v_s^2)C + 6 - 8v_s}$$

The maximum radial stress, σ_{rd}, develops at the pipe springline and the minimum stress occurs at both the crown and the bottom of the pipe. The maximum shear stress, τ_d, develops at the crown and the bottom of the pipe, while the minimum shear occurs at the pipe springline.

The moments and thrusts developed due to the pipe stresses for the deviatoric and isotropic external stress sets depend on the position of the point considered on the pipe circumference. The thrusts at the crown and the springline, N_{crown} and N_{spring}, and the corresponding moments attract particular interest. These moments and thrusts can be derived from thin shell theory as follows:

$$N_{crown} = \sigma_0 r + \left[\frac{\sigma_{rd}}{3} - \frac{2\tau_d}{3}\right] r \tag{2.49}$$

$$N_{spring} = \sigma_0 r - \left[\frac{\sigma_{rd}}{3} - \frac{2\tau_d}{3}\right] r \tag{2.50}$$

$$M_{crown} = \left[\frac{\sigma_{rd}}{3} - \frac{\tau_d}{6}\right] r^2 \tag{2.51}$$

$$M_{spring} = -\left[\frac{\sigma_{rd}}{3} - \frac{\tau_d}{6}\right] r^2 \tag{2.52}$$

Deflections may be determined from the pipe stresses by considering the external stress components, w_o, due to the isotropic loading and $w_{d\theta}$, due to the deviatoric loading as follows:

$$w_0 = \frac{\sigma_0 r^2}{EA} \tag{2.53}$$

$$w_{d\theta} = \left[\frac{(2\sigma_{rd} - \tau_d) r^4}{18EI}\right] \cos 2\theta = w_{d\max} \cos 2\theta \tag{2.54}$$

$$w_\theta = \left(w_0 + w_{d\max} \cos 2\theta\right) \tag{2.55}$$

The changes in diameter of the pipe in the vertical and horizontal directions, ΔD_V and ΔD_H respectively, may then be formulated as;

$$\Delta D_V = 2\left(w_0 - w_{d\max}\right) \tag{2.56}$$

$$\Delta D_H = 2\left(w_0 + w_{d\max}\right) \tag{2.57}$$

Moore (1993) demonstrated with a case example that this theory provided far superior predictions of deflections than those produced by the Iowa equation and gave estimates of radial stresses, which reasonably matched those measured.

The significance of hoop stiffness on pipe performance was pointed by Webb, McGrath and Selig (1996). Low hoop stiffness leads to pipe deformation, which helps the distribution of load to the surrounding soil. Hoop stiffness is given as:

$$H = \frac{2E_p A}{D} \tag{2.58}$$

2.1.14 Finite element analysis (FEA)

The finite element analysis technique is a mathematical solution which was primarily developed to solve complex structural systems. The technique is also a very useful tool in geotechnical engineering as well as other areas such as fluid mechanics, thermodynamics, ground water analysis, aerodynamics, etc.

According to finite element method a continuum is divided into a number of (volume) elements. Each element which may be one, two or three dimensions consists of a number of nodes and is connected to each other only at their nodes. Shape functions relate the displacements in the elements and along the element boundaries to the nodal displacements. Displacements may be resulted due to the self weight of the elements or the external loads. The prescribed displacements at the boundaries of the system must be specified as well. After the continuum is idealised and the boundary conditions are specified, an analysis can be performed using the stiffness method. Analyses through stiffness method involve the solution of equilibrium equations for the unknown nodal displacements. The equilibrium

equations in matrix form, consists of a stiffness matrix [K] that relates the nodal displacements (d) to the nodal forces (f). The stiffness matrix is a function of the geometry and the properties of materials. Once the displacements are found from the equilibrium equations, they can be then used to evaluate the element stresses and strains.

One area of development for the use of FEA is in soil-structure interaction mechanics. Each element type may be defined with different stiffness properties. The modelling of the nonlinear stress-strain properties of soil has been accommodated through incremental analysis and an iterative solution scheme.

A variety of commercial finite element programs are currently available in the market. Each of them has advantages and disadvantages depending on the type of problem. Examples to these programs are PLAXIS, which is used in this thesis, CANDE (Culvert Analysis and Design) (Allgood, 1976) (Katona, 1980), PIPE5, which is a version of SAP (Wilson, 1971) modified by the Utah State University researchers for the analysis of flexible pipe, SPIDA (Heger, Liepins, Selig, 1985), which is used for the analysis of buried concrete pipes and some others such as ABAQUS (1998) and ADINA.

2.2 *Performance Limits for Buried Pipes*

The design of buried flexible pipes requires checking for certain performance criteria which are related to the performance limits of a specific product. When a capability of a product is reached or exceeded, it is stated that a performance limit has been reached. For flexible pipes, performance limits are directly related to stress, strain, deflection or buckling. The performance limits that are often considered in design of flexible pipes will be presented below:

2.2.1 Wall Crushing (Stress)

Wall crushing term is used to describe the condition of localized yielding for a ductile material or cracking failure for brittle materials. This type of failure occurs in case a very stiff pipe is deeply buried in a very stiff embedment material. It is characterised by a localised yielding at the pipe's springline as shown in Figure

2.20. The ring compression stress has a primary contribution to this performance limit (Moser and Folkman, 2008):

$$\text{Ring compression} = \frac{P_v D}{2A} \tag{2.59}$$

P_v : Vertical soil pressure

D : Diameter

A : Pipe thickness (cross sectional area) per unit length

The bending stress at the springline can also influence wall crushing (Moser and Folkman, 2008):

$$\text{Bending stress} = \frac{Mt/2}{I} \tag{2.60}$$

M : Bending moment per unit length

t : Wall thickness

I : Moment of inertia of wall cross-section per unit length

Wall crushing is generally the primary performance limit or design basis for rigid or brittle pipe products.

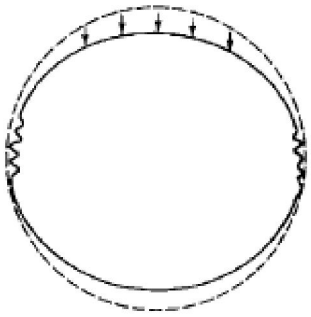

Figure 2.20 Wall crushing at the 3 and 9 o'clock positions. (Moser and Folkman, 2008)

2.2.2 Wall Buckling

Wall buckling is not a strength performance limit; however this failure may occur when the pipe has insufficient stiffness. When the flexible pipes are subjected to internal vacuum, external hydrostatic pressure or high soil pressures in compacted soil, the pipes may buckle as shown in Figure 2.21. For a circular ring in plane

stress, subjected to a uniform external pressure, the critical buckling pressure, P_{cr} is given with following equation (Moser and Folkman, 2008):

$$P_{cr} = \frac{Et^3}{4(1-v^2)R^3} \tag{2.61}$$

E : Young's modulus of the pipe material

t : Wall thickness

v : Poisson's ratio of the pipe material

R : Pipe radius

Meyerhof and Baike (1963) developed the following formula for computing the critical buckling pressure in a buried circular conduit:

$$P_{cr} = 2\sqrt{\frac{E'}{1-v^2}\left(\frac{EI}{R^3}\right)} \tag{2.62}$$

E' : Soil modulus

The Scandinavians have rewritten the above formula for critical buckling pressure as follows:

$$P_{cr} = 1.15\sqrt{P_b E'} \qquad P_b = \frac{2E}{1-v^2}\left(\frac{t}{D}\right)^3 \tag{2.63}$$

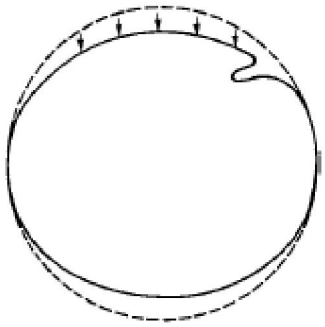

Figure 2.21 Localized wall buckling (Moser and Folkman, 2008)

2.2.3 Overdeflection

The deflection is a design parameter for flexible pipes. It is rarely considered in the design of rigid pipes. Flexible pipe products have design deflection

limits based on the maximum deflection of the pipe with a safety factor. For instance, PVC pipes will not suffer reversal curvature until about 30 percent deflection (Spangler, 1941). Thus, engineers generally consider a 7.5 percent deflection limit which is based on a safety factor of 4. For such products which require a deflection consideration in design, bending stresses or strains may also be a limiting criterion. Figure 2.22 below shows the ring deflection and the reversal of curvature due to over-deflection.

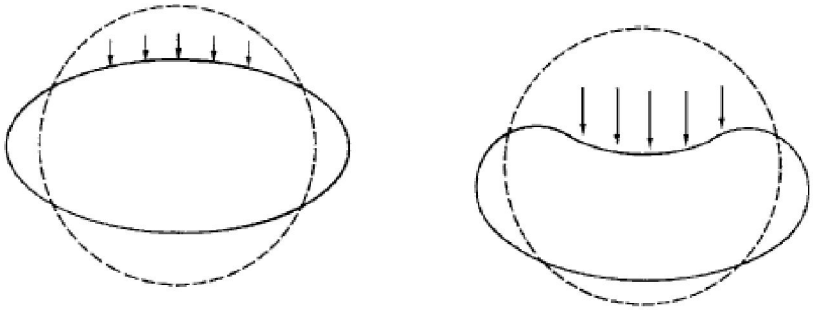

Figure 2.22 Ring deflection and Reversal of curvature due to overdeflection (Moser and Folkman, 2008)

2.2.4 Strain Limit

Since the strain is related to deflection, installation techniques for certain pipe products are proposed in order to limit deflection and thus limit the strain. Generally only brittle, composite, or highly filled materials have installation designs controlled by strain. Moser and Folkman (2008) proposed the following equations to calculate the strains:

$$\text{Bending strain;} \qquad \varepsilon_b = 6\left(\frac{t}{D}\right)\left(\frac{\Delta y}{D}\right) \tag{2.64}$$

$$\text{Ring compression strain;} \qquad \varepsilon_c = \left(\frac{P_v D}{2tE}\right) \tag{2.65}$$

$$\text{Hoop strain (due to internal pressure);} \qquad \varepsilon_p = \left(\frac{PD}{2tE}\right) \tag{2.66}$$

Poisson's circumferential strain; $\varepsilon = -v$ (longitudinal strain) (2.67)

t : Wall thickness

D : Diameter.

Δy : Vertical deflection

P_v : Vertical soil pressure

E : Young's modulus

p : Internal pressure

v : Poisson's ratio

2.2.5 Longitudinal stresses

Longitudinal stresses may be produced by thermal expansion (contraction), longitudinal bending, and Poisson's effect (due to internal pressure). Since the flexible pipes are susceptible to temperature changes, thermal stresses develop. Expansion or contraction movements of the pipe are restrained by the frictional forces caused by the surrounding soil and this may result in a circumferential break. Longitudinal bending or beam action in a pipeline may be caused by: differential settlement of a structure to which the pipe is rigidly connected (e.g. settlement of a manhole), uneven settlement of pipe bedding (e.g. due to erosion of the soil below), ground movement due to tidal water, seasonal rise and fall of soils (e.g. expansive clays), non-uniformity of the foundation, tree-root growth pressure, etc (Moser and Folkman, 2008). Circular and longitudinal split failure modes are presented by Rajani et al. (1995) in Figure 2.23.

2.2.6 Shear loadings

Shear loadings usually accompany longitudinal bending. Therefore, the major causes of shear loading are similarly due to non-uniform bending or differential settlement. Such reasons which develop shear loading can be large, highly variable, and difficult to quantify (Moser and Folkman, 2008). For this reason, shear forces must be minimised by proper design and installation.

2.2.7 Fatigue

If the buried pipes experience a high number of cyclic stresses, pipe materials will

fail at a lower stress (Moser and Folkman, 2008). These cyclic stresses may be caused by water hammers or traffic loads. Cyclic stresses due to traffic loading usually do not cause failure except the case of shallow burials.

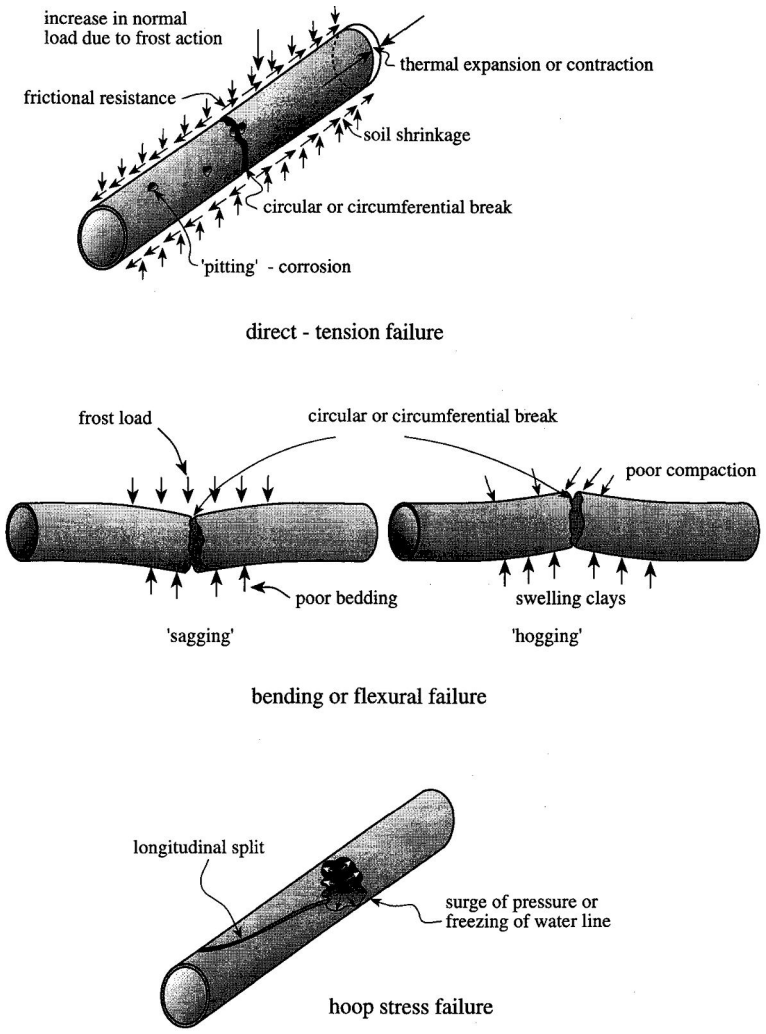

Figure 2.23 Circular and longitudinal split failure modes (Rajani et al., 1995)

2.3 *Modulus of Soil Reaction, E'*

2.3.1 Soil Stiffness

Since the structural integrity of buried flexible pipes mainly comes from the lateral support of the soil, a design parameter indicating the strength of soil is

essential. This design parameter developed by Spangler and Watkins is the modulus of soil reaction, E'.

As previously stated in section 2.1.9, the Modified Iowa Formula includes a term referred to as the modulus of soil reaction, E', and is defined as an empirical value used to express the stiffness of the embedment soil in predicting flexible pipe deflection. E' has also been referred to as the soil modulus or soil stiffness.

The original Iowa formula from Spangler for culvert deflections was as follows:

$$dx=DPK/(EI/r^3 + 0.06ler) \tag{2.68}$$

Spangler (1941) noticed that the ratio of the horizontal pressure acting on the culvert and its associated deflection remained essentially constant. Accordingly, he defined a constant of proportionality which was called the modulus of passive resistance, *e*. Later, it was noticed by Watkins and Spangler (1958) that *e* indeed was not a constant for a given soil, and that *er* (modulus of passive resistance of embedment times mean radius of the pipe) was observed to be more of a constant. Watkins accordingly proposed the use of the current E' as the modulus of soil reaction. Hence the modified Iowa formula was presented as follows:

$$dx=DPK/(EI/r^3 + 0.06l\,E') \tag{2.69}$$

As stated by Watkins and Jeyapalan (2004), this empirical parameter, E', is not a function of the soil alone but of the soil-pipe system and it can only be back-calculated under actual field conditions. Due to its empirical nature, E' parameter, alone brings a wide degree of uncertainty into the design of buried pipelines. The researchers focused on establishing the E' values in the following years and Spangler (1941) was the first one to do this followed by Watkins and Spangler (1958), again followed by Spangler (1969).

The predictions of pipe deflections are sensitive to E'. As stated above, E' is given to be the modulus of passive resistance of embedment, *e*, (units of pressure/length) times the pipe radius, *r*. The maximum soil stiffness at the passive soil condition may not be reached in practice since it can only be achieved at high levels of soil

strain. In fact, the soil modulus, E' is defined based on circumferential strain of the pipe, which is not the usual definition of soil modulus:

$$E' = \frac{p}{\varepsilon_\theta} \tag{2.70}$$

p : Pressure applied to pipe from the side soil

ε_θ : Circumferential pipe strain = $\Delta x/r$ for axial symmetry

As cited by Singh and Pal (1990), Watkins and Spangler (1958) proposed that E' values are reasonably constant for a given soil and degree of compaction. However they noticed that the pipe size also had an effect which leads to different levels of soil resistance. This was probably because of the difference in soil side strains developed in different pipe installations.

There has been attempts to correlate E' with other true soil properties. It was stated by McGrath et al. (1990) that the semi-empirical modulus of soil reaction, E', was not a true material property and that there was no practical test available to calculate it. However, the authors together with Watkins (1988), proposed that E' could be approximated by the constrained soil modulus of a vertically loaded soil in a consolidometer (see Figure 2.24). The constrained or one-dimensional modulus of soil, M_s, is defined as follows:

$$M_s = \frac{\sigma'_v}{\varepsilon_v} = \frac{E_s(1-\nu)}{(1+\nu)(1-2\nu)} \tag{2.71}$$

σ'_v : Effective vertical stress

ε_v : Vertical soil strain

E_s : Young's modulus of soil

ν : Poisson's ratio of soil

The secant modulus over the stress range was argued to define the average sidefill stiffness. The use of the constrained modulus incorporates the non-linear behaviour of the soil subjected to loading.

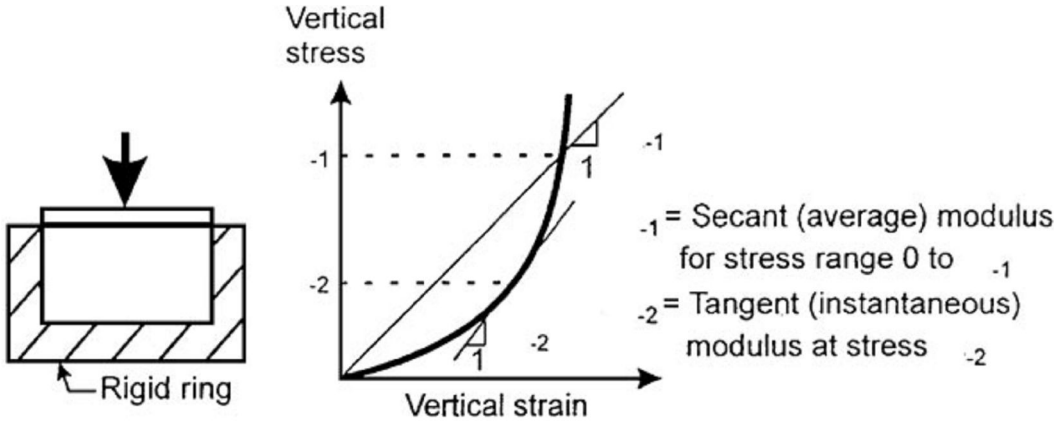

Figure 2.24 Constrained compression test schematic

2.3.2 Variables on Which E' Depends

Watkins and Jeyapalan (2004) cited the discussions for the variables on which E' depends. In order to establish the relationships between E' and the variables on which it depends, researchers used theory of closed-form solutions, finite element studies, model experiments, laboratory tests, and field tests. The type of soil and degree of compaction was never doubted to affect E' values. However, the E' values obtained from various methods ranged several hundred percents. This was making the reliable prediction of deflection impossibly difficult and was discussed by the researchers.

Hartley and Duncan (1987) published their study on steel pipes and established the variation of E' with depth of soil over the pipe. However, the values produced by the study have not been adopted in most of the standards. Hartley and Duncan's work involved finite element analyses and field data collection of the following conditions:

- Steel pipe only,
- r = 24-72 in.,
- H = 5-20 ft,
- PS = 4-136 psi,
- $EI/(0.061\ E'r^3)$ = 0.003-0.656.

As defined in Equation 2.70, E' is conceptually similar to a soil modulus and can be expected to behave similarly. In this regard, just like soil modulus which is dependent on confining pressure or depth of soil column over it, the E' will vary with height of soil

cover above the pipe. Further investigations have been carried out via laboratory and model tests by Shafer (1948), Watkins and Nielson (1964), Meyerhof (1966), Nielson (1967), Krizek et al. (1971), Allgood and Takahashi (1972) and Chambers et al. (1980). Based on the field data, the researchers often concluded that E' did not depend on the depth of soil column. However, they did not realize that the data reduction was somewhat tainted by many unknowns (Watkins and Jeyapalan, 2004). These field data from a wide variety of soil types and installation conditions were compared to carefully controlled laboratory tests and model experiments. Shafer (1948), in a careful reduction of data from a single site, demonstrated that the values of E' varied significantly with height of soil above pipe. The exception for the variation of soil modulus with the depth of soil is for the case of saturated clays which have little possibility of drainage. Thus, all backfill soils around pipes will have E' values varying with depth of soil cover. Additionally, E' values for most native soils will also vary with depth of soil cover. The summary of results from the field data analysis of Jaramillo (1989) was published by Jeyapalan and Jaramillo (1994) and it was established that the E' values also varied significantly with the pipe stiffness and pipe size. Such variation will be studied in the scope of this thesis as well. Jaramillo (1989) worked with field data of the following conditions:

- Plastic pipe only,
- r = 6-18 in.,
- H = 5-30 ft,
- PS = 25-200 psi,
- $EI/(0.061\ E'r^3)$ = 0.015-2.44.

In the work of Leonhardt (1973) which was further presented in *ATV-A-127* (1984), closed-form solutions were used to incorporate the effects of trench width in case the native ground conditions are considerably different from the bedding material conditions.

As cited by McGrath, Chambers and Sharff (1990), the influence of the natural soil forming the trench walls on the lateral soil support has been addressed by Leonhardt. The effective sidefill stiffness is given by ς E', where ς is Leonhardt's correction factor on the modulus of soil reaction, E', as defined in the Iowa formula:

$$\varsigma = \frac{1.662 + 0.639(B/D - 1)}{(B/D - 1) + [1.662 - 0.361(B/D - 1)]\frac{E'}{E_3}} \tag{2.72}$$

ς : Leonhardt's correction factor

E_3 : Young's modulus of the natural soil forming the trench

B : The width of the trench

D : Pipe diameter

In case E' is considerably less than E_3, it can be stated that the trench walls are effectively rigid. If the ratio of trench width to pipe diameter, *B/D* is 2, then the effective modulus for sidefill is 2.3 times E'. The value of ς is reduced as E' approaches the value of E_3 (see Figure 2.25). A wider trench will be affected less and the correction factor may be ignored for a trench width to pipe diameter ratio of 5 or greater.

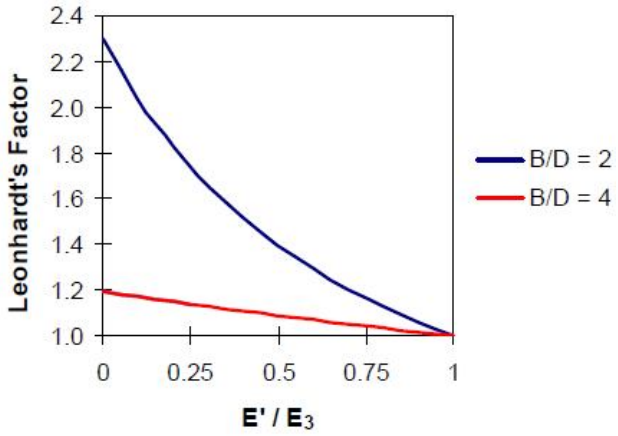

Figure 2.25 Leonhardt's correction factor for different trench geometries

2.3.3 Howard's Modulus of Soil Reaction (E') Values

E' was tried to be measured by many research efforts without much success. The most useful method involves the back calculation of effective E' values through the Iowa formula using the measured deflections of a buried pipe for which installation conditions are known. However, this requires to assume the values for the load, the bedding factor, and the deflection lag factor and the inconsistent

assumptions have led to a variation in reported values of E'.

The most popular form of E' values comes from the empirical data published by Amster K. Howard of the U.S. Bureau of Reclamation. Howard (1977) reported typical values of modulus of soil reaction, which varied with soil type and composition, as well as the degree of soil compaction (see Table 2.6). The moduli were deduced from laboratory tests by the US Bureau of reclamation on a range of pipe diameters and materials, and were complemented by field test data. He assigned values to E', K, and W_c and then used the Iowa formula to calculate a theoretical value of deflection which was then compared with actual measurements. Using the assumed values of E' in Table 2.6 and a bedding constant K = 0.1, Howard was able to correlate the theoretical and empirical results to within ± 2 percent deflection when he used the prism soil load. Howard used a deflection lag factor D_l = 1.5 in his calculations while using the prism load. However, in order to be theoretically correct, a lag factor D_l = 1.0 would have to have been used along with the prism load (Moser and Folkman, 2008).

Although Howard's study provided some useful information to guide designers of flexible pipes, it has created more confusion than settling the ongoing discussions on E'. Therefore, the engineering community has relied on and misused the oversimplified E' values of U.S. Bureau of Reclamation for years. Jeyapalan and Watkins (2004) had done a multitude of pipeline projects around the world, carefully examined the original data used by Howard (1977) and recalculated what E' values are possible. They concluded that the degree of error was totally unacceptable and stated that a reasonable value for E' using Howard's work could only be reached by luck and not via sound engineering principles. They accordingly presented a step-by step methodology in order to build the engineering know how needed to establish E' values on a project-specific basis allowing for most significant factors. The findings of this valuable paper and the step by step methodology will be given in the following section.

Table 2.6 Average Values of Modulus of Soil Reaction, E' (for initial flexible pipe deflection) (Howard, 1977)

Soil type-pipe bedding material (Unified Soil Classification System*)	E′ for degree of compaction of bedding, lb/in²			
	Dumped	Slight, <85% Proctor, <40% relative density	Moderate, 85–95% Proctor, 40–70% relative density	High, >95% Proctor, >70% relative density
Fine-grained soils (LL > 50)† Soils with medium to high plasticity CH, MH, CH-MH	No data available. Consult a competent soils engineer; otherwise, use E′ = 0			
Fine-grained soils (LL < 50) Soils with medium to no plasticity CL, ML, ML-CL with less than 25% coarse-grained particles	50	200	400	1000
Fine-grained soils (LL < 50) Soils with medium to no plasticity CL, ML, ML-CL with more than 25% coarse-grained particles Coarse-grained soils with fines GM, GC, SM, SC contain more than 12% fines	100	400	1000	2000
Coarse-grained soils with little or no fines GW, GP, SW, SP‡ contains less than 12% fines	200	1000	2000	3000
Crushed rock	1000	3000	3000	3000
Accuracy in terms of percentage of deflection§	±2	±2	±1	±0.5

*ASTM D 2487, USBR E-3.
†LL = liquid limit.
‡Or any borderline soil beginning with one of these symbols (i.e., GM-GC, GC-SC).
§For ±1 percent accuracy and predicted deflection of 3 percent, actual deflection would be between 2 and 4 percent.
NOTE: Values applicable only for fills less than 50 ft (15 m). Table does not include any safety factor. For use in predicting initial deflections only, appropriate deflection lag factor must be applied for long-term deflections. If bedding falls on the borderline between two compaction categories, select lower E′ value or average the two values. Percentage Proctor based on laboratory maximum dry density from test standards using about 12,500 ft·lb/ft³ (598,000 J/m³)(ASTM D 698, AASHTO T-99, USBR E-11). 1 lb/in² = 6.9 kN/m².
SOURCE: Amster K. Howard, U.S. Bureau of Reclamation, Denver, "Modulus of Soil Reaction (E′) Values for Buried Flexible Pipe," *J. Geotech. Eng. Div.*, January 1977, pp. 33–43. Reprinted with permission from American Society of Civil Engineers.

2.3.4 Engineering Know How to Establish E' Values

Further to the research efforts presented in Section 2.3.2 and based on the reanalysis of Howard's original data, Jeyapalan and Watkins concluded that the *E′* values proposed by Howard could result in wrongful estimates of buried pipe deflections. Thus, it was proposed that any proper guidance on *E′* for design practice should include a careful consideration of the following factors:

- Native soil type,
- Native soil compaction density,
- Modulus of native soil,
- Trench material type,
- Trench material compaction density,
- Modulus of trench material,

- Size of pipe,
- Pipe stiffness-soil stiffness ratio, $EI/(0.061E'r^3)$.
- Depth of cover,
- Trench width-pipe diameter ratio, and
- Location of water table.

As stated in the article, "*The E' is not a fundamental geotechnical engineering property of the soil. This property can not be measured either in the laboratory or in the field. This is an empirical soil-pipe system parameter, which could be obtained only from back-calculating by knowing the values of other parameters in the modified Iowa equation.*" The authors also added that an experienced soil-pipe interaction design engineer would expect the pipe-soil stiffness ratio to have an effect on the value one uses for E' in design. Such effect of relative stiffness is the subject matter of this thesis.

To determine E' for a buried pipe, separate E' values for the native soil, E'_n and the backfill surrounding the pipe, E'_b must be determined and then combined using the equation:

$$E' = S_c E'_b \tag{2.73}$$

The value of the soil support combining factor, S_c, is given in Table 2.7, as a function of E'_n / E'_b and B_d /D, where B_d = trench width at pipe spring line.

Table 2.8 can be used to obtain the values of modulus of soil reaction of the pipe zone-backfill embedment, E'_b, and that of the native soil, E'_n.

Table 2.7 Use of ATV for trench width effects on E' for open-cut trenches (Jeyapalan and Watkins, 2004)

	S_c for B_d/D					
E'_n/E'_b	1.5	2.0	2.5	3.0	4.0	5.0
0.1	0.15	0.30	0.60	0.80	0.90	1.00
0.2	0.30	0.45	0.70	0.85	0.92	1.00
0.4	0.50	0.60	0.80	0.90	0.95	1.00
0.8	0.85	0.90	0.95	0.98	1.00	1.00
1.5	1.30	1.15	1.10	1.05	1.00	1.00
2.0	1.50	1.30	1.15	1.10	1.05	1.00
3.0	1.75	1.45	1.30	1.20	1.08	1.00
≥5.0	2.00	1.60	1.40	1.25	1.10	1.00

Table 2.8 Modulus of soil reaction for pipe embedment, (Jeyapalan and Watkins, 2004)

	Standard proctor relative compaction density			
Type of soil[a]	85%	90%	95%	100%
CL, ML, CL-ML	3.4(500)	4.8(700)	6.8(1,000)	9.6(1,400)
SM, SC	4.1(600)	6.2(900)	9.3(1,350)	13.6(2,000)
SP, SW, GP, GW	4.8(700)	6.8(1,000)	10.2(1,500)	15.3(2,300)

In summary, the following steps are helpful in establishing reasonable E' values for pipeline design:

- Step 1: Review borings, plans, profiles, and obtain most appropriate standard penetration test blow counts,
- Step 2: Calculate total stress, pore water pressure, effective stress,
- Step 3: Calculate relative density with some judgment,
- Step 4: Estimate standard proctor relative compaction density,
- Step 5: Select E' for native ground conditions using Table 2.8,
- Step 6: Adjust E' to allow for pipe-soil stiffness ratio, size, and other factors,
- Step 7: Repeat the procedure for bedding soil to obtain its E',
- Step 8: Select trial trench width
- Step 9: Obtain factor S_c allowing for native to bedding variation from Table 2.7,
- Step 10: Estimate design E' for the pipe-soil system and adjust up or down.

The design of flexible pipes require checking certain performance criteria such as deflection, buckling, stress and strain and most of these design checks involve the use of design parameter, E'. Therefore, establishing E' values has utmost importance in the design of buried flexible pipes.

CHAPTER 3

PLAXIS FINITE ELEMENT CODE FOR SOIL AND ROCK ANALYSES (PLAXIS 2D VERSION 8)

3.1 *Introduction*

PLAXIS Version 8 is a finite element program specifically developed for the two-dimensional analysis of deformation and stability in geotechnical problems such as the settlement of foundations, the stability of slopes, or the deformation of buried structures. PLAXIS refers to two commonly used idealizations in geotechnical engineering, which are plane strain and axisymmetric analysis. The plane strain idealization is used for structures having a constant cross-section along a significant length (e.g. buried pipes). This model simplifies the problem to two dimensions because it is assumed that the displacements normal to the cross-section are zero. The axisymmetric idealization is used for problems that are symmetrical relative to a central axis. This model simplifies the problem due to the assumption of identical stresses and deformations in any radial direction. Geotechnical applications require to be handled by advanced constitutive models in order to simulate the non-linear, time-dependent and anisotropic behaviour of soils and/or rock. Additionally, special procedures are required to deal with the pore pressures in the soil due to the multi-phase nature of soils. PLAXIS utilizes some well known constitutive models that can deal with various aspects of complex geotechnical structures. Another capability of the program is that the soil-structure interaction can be modelled by PLAXIS. A brief summary of the important features are given below.

3.2 *Short Review of Features*

3.2.1 Graphical input of geometry models

The input of soil layers, structures, construction stages, loads and boundary conditions is based on the CAD (computer aided drawing) program available in PLAXIS. This convenient drawing program allows the detailed modelling of a wide variety of geometry cross-sections. After the structural members, applied loads and prescribed displacements are directly entered to the geometry in the drawing area, a 2D finite element mesh can be easily generated.

3.2.2 Automatic mesh generation

PLAXIS allows automatic generation of unstructured 2D finite element meshes which saves a precious time. This feature enables the automatic generation of a random mesh of triangular elements. Global and local mesh refinement options are available where the stress concentration and large deformations occur.

3.2.3 High order elements

There are two types of triangular elements which are available in PLAXIS to model the deformations and stresses in the soil (Figure 3.1). The standard quadratic 6-node element produces good results. However, the cubic (4^{th} order) 15-node element is even more accurate and produces a smooth distribution of stresses in the soil. In case a very large number of elements are involved in the problem, it might be practical to use the 6-node element since this element type saves computation and time.

3.2.4 Plates

In order to model the bending of retaining walls, tunnel linings, shells and other slender structures, special beam elements are used by PLAXIS. The behaviour of a beam element is defined using a flexural rigidity, a normal stiffness and an ultimate bending moment. Three or five nodes may be used for the beam element depending on the type of elements previously chosen.

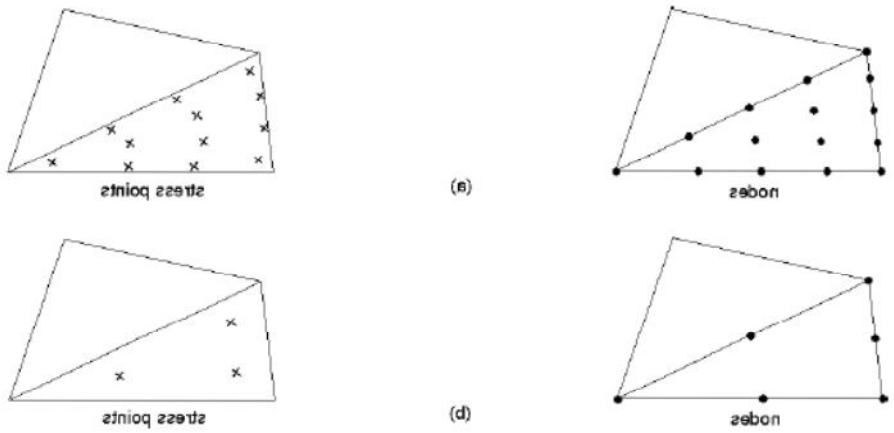

Figure 3.1 a) 15-node triangular elements, b) 6-node triangular element

Each node has three degrees of freedom, two of which are related to the horizontal and vertical displacements, and one related to the rotation. A plastic hinge may also develop when the maximum bending moment or maximum axial force is reached. The weight of the beam, if necessary, can be taken into account with great care. Since the beams are superimposed as a continuum in PLAXIS, they overlap with the soil. Therefore, it is required to subtract the soil unit weight from the unit weight of the beam when the weight of beam is considered in calculation.

The sign convention, coordinate system and the indication of positive stress components in PLAXIS are demonstrated below in Figure 3.2:

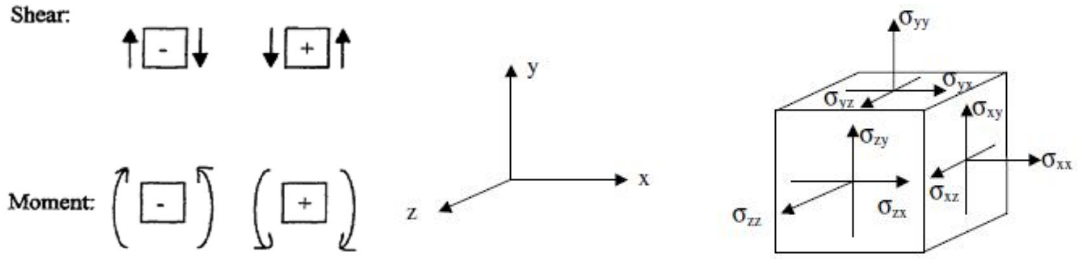

Figure 3.2 Sign convention in PLAXIS

3.2.5 Interfaces

Soil-structure interaction can be modelled with joint elements available in PLAXIS. For instance, these joint or interface elements may be used to simulate

the thin zone of shearing material at the contact between a pipe structure and the surrounding soil. Values of interface friction angle and adhesion are generally not the same as those of the surrounding soil. Usually, the strength of the interface is less than the strength of the soil. Therefore, a reduction factor is applied to the friction angle and the cohesion of the soil resulting in the properties of the interface.

3.2.6 Tunnels

PLAXIS includes a convenient option to create circular and non-circular tunnels using arcs and lines. The tunnel lining and the interaction with the surrounding soil may be modelled using plates and interfaces. Fully isoparametric elements are used to model the curved boundaries within the mesh. The deformations that occur as a result of various methods of tunnel construction are analysed by way of various methods implemented in the program. The tunnel lining is defined by segments of curved beam elements (plates). These curved beam elements may also be used to model pipe materials with the input of necessary flexural rigidity and normal stiffness parameters.

3.2.7 Advanced soil models

PLAXIS offers a variety of advanced soil models as well as some simple models. The well-known Mohr-Coulomb model is the simplest model available. This model gives a good approximation of the ultimate load in simple problems and should be used for a first analysis of the problem considered. In case of more complex problems which involve non-linear behaviour, time-dependent behaviour or unloading-reloading residual strain, more advanced models are required for the simulation. A Soft-Soil model which is based on the Cam-Clay model (Burland 1965, 1967) can be used to model the primary compression of normally consolidated soft soils. Furthermore, secondary compression can also be modelled by the use of Soft-Soil-Creep model. In addition to the soft soils, the behaviour of stiffer soils can be simulated by the Hardening-Soil model of Schanz (1998), which is based on the well-known Hyperbolic model (Duncan and Chang, 1970) and gives good results. Details of the Hardening Soil Model will be presented in Chapter 4.

3.2.8 Automatic load stepping

PLAXIS can be run in an automatic step size and automatic time step selection mode. This feature allows optimising the step size to get an efficient and robust calculation process. In case the load increments are too small, many steps are required and the computation may take a significant time. On the other side, too large increments would require an excessive number of iteration to reach equilibrium, and the solution could even diverge. There are three possible outcomes of the automatic load stepping procedure at which a series of iterations are carried out to reach equilibrium. As described in the user manual of PLAXIS, these outcomes are:

Case 1: In case the solution reaches equilibrium within a number of iterations that is less than the desired minimum control parameter (the default value is 4, but can be changed manually), then the calculation step is assumed to be too small. In this case, the size of the load increment is multiplied by two and further iterations are applied to reach equilibrium.

Case 2: In case the solution fails to converge within a desired maximum number of iterations (the default value is 10, but can be changed manually), then the calculation step is assumed to be too large. In this case, the size of the increment is reduced by a factor of two and the iteration procedure is continued.

Case 3: In case the number of required iterations lies between the desired minimum and the desired maximum, then the size of the load increment is assumed to be satisfactory. After the iterations are complete, the next calculation step begins. The initial size of this calculation step is made equal to the size of the previous successful step.

3.2.9 Staged construction

This powerful feature of PLAXIS allows for a realistic assessment of stress and deformation results. The staged construction procedure simulates the construction, excavation, and backfill processes by activating, deactivating and changing the properties of soil clusters, structural elements and applied loads during the

calculation. For example, soil clusters, defined within the geometry, are deactivated to simulate the excavation. Structural elements can also be deactivated at the proper stages of construction.

3.2.10 Updated Lagrangian analysis

PLAXIS has a special option for the analysis of large displacement problems. The updated Lagrangian analysis continuously updates the mesh during the calculation. This option is available for all types of calculations; however it was not used in the finite element analysis of the pipes in this study.

3.2.11 Presentation of results

PLAXIS has powerful graphical features for the presentation of computational results. A view of the deformed mesh is initially presented. Then, it is possible to visualise the total, horizontal, vertical and incremental deformations in the form of vectors, contour lines, or shaded areas. Additionally, the effective and total stresses are shown by principal stresses, mean contour lines, or mean shaded areas. For the structural and interface elements, it is possible to visualise deformations, bending moments, shear stresses and normal stresses. The output presentation for the underground water flow and pore water pressure are also available. In addition, a special curve program included in PLAXIS allows to present load or time versus displacement, and stress-strain diagrams for special points of interest. This presentation is especially practical and useful to analyse the behaviour of soils locally.

CHAPTER 4

MODELLING THE BEHAVIOUR OF SOIL

4.1 *Introduction*

As explained in previous chapter, PLAXIS is a finite element code for geotechnical applications in which soil models are used to simulate the soil behaviour. The selection of the most appropriate soil model which adequately defines the soil behaviour is important to get the most accurate results. In this study, three certain types of soils, i.e. Kanto loam, crushed stone, and basalt aggregate are required to be modelled for the analysis of buried pipe installations. The soil model available in PLAXIS, which simulates most adequately the behaviour, is the Hardening-Soil model. Additionally, the triaxial stiffness parameter, E_{50} which is an input parameter in Hardening-Soil model is of particular interest since the pipe-soil stiffness ratio, $S_r = PS/E_{50}$ which is defined for the purpose of this study refers to its value. Therefore, the Hardening-Soil model is explained in detail in this chapter.

4.2 *The Hardening - Soil Model (Isotropic Hardening)*

The Hardening-Soil model is an advanced constitutive model, included in PLAXIS. This model takes into account the hardening behaviour of soil and uses a non-associated flow rule. Some principles of the plasticity theory should be reviewed to understand the hardening behaviour and the non-associated flow rule. First, elastic and plastic deformations develop in soils when they are subjected to shear forces. In case the stress levels are not below a yield surface, only elastic or recoverable deformations develop. However, in case the stress levels are equal to or higher than the yield surface, then both elastic and plastic deformations develop.

Plastic deformation implies that a portion of the deformation is not recoverable. Second, a flow rule relates the direction of the vector of plastic strain increment to the yield surface. According to an associated flow rule, a vector of plastic strain increment is perpendicular to the yield surface. However, according to a non-associated flow rule, a vector of plastic strain increment is not perpendicular to the yield surface. If the yield surface increases in size while the plastic straining develops in the soil, hardening behaviour happens. In other words, after unloading/reloading, the soil will yield at a higher stress level than the previous stress level, which caused yielding. A hardening law relates the magnitude of the plastic strain to the magnitude of the stress increment.

Two main types of hardening can be defined as shear hardening and compression hardening. Shear hardening is used to model irreversible strains resulted from the primary deviatoric loading; whilst the compression hardening is used to model irreversible strains resulted from primary compression in oedometer and isotropic loading. Both types are included in PLAXIS (PLAXIS V8, 2002).

It is advised to use the Mohr-Coulomb model for a quick and first analysis of the problem considered. The Mohr-Coulomb model is practical and useful to analyse simple problems, or in cases where there is not enough data about the soil characteristics. However; it is not capable to simulate the behaviour of soil at different stress levels very well and is not realistic. It is also referred as an elastic-perfectly plastic model since the soil strain can only be elastic before the yield surface or perfectly plastic when the stress level exceeds the yield surface. In a perfectly plastic model, the yield surface is fixed and is not affected by the plastic straining. Therefore, it is not possible to model the hardening behaviour of soils. The elastic-perfectly plastic Mohr-Coulomb model is idealised from the standard drained triaxial tests as in Figure 4.1.

The Cam-clay model, which is also included in PLAXIS, was originally developed for soft clays. It was later improved and the modified Cam-Clay model was proposed by Roscoe and Burland (1968).

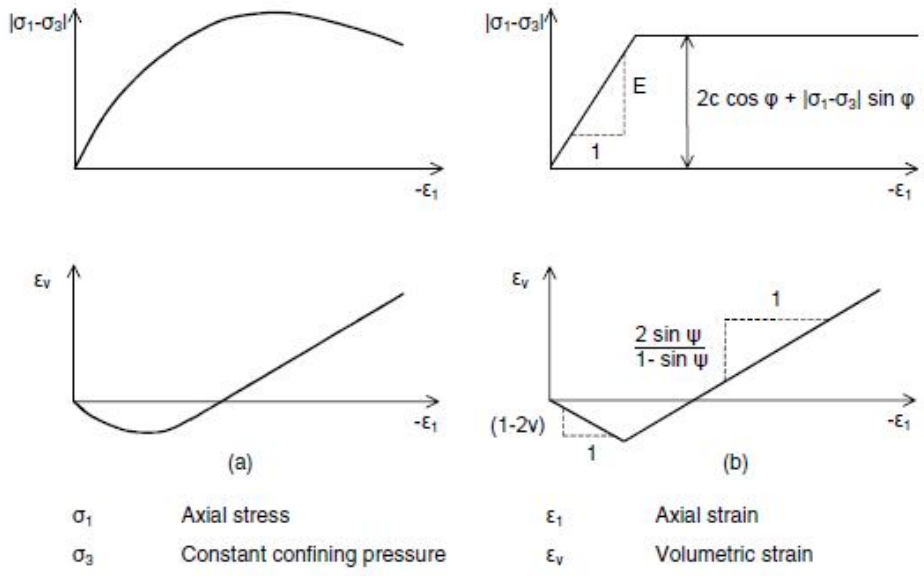

Figure 4.1 (a) Results from standard drained triaxial tests, (b) elastic-plastic model (PLAXIS V8 Reference Manual, 2002)

The Hardening-Soil model can be used for simulating the behaviour of different types of soils, both soft soils and stiff soils (Schanz, 1998 – PLAXIS V8, 2002). In summary, the model was formulated as per the classical theory of plasticity. In the model, total strains are calculated using a stress dependent stiffness which is different for loading and unloading cases. The plastic strains are calculated by introducing a multi-surface yield criterion and isotropic hardening is assumed. The model also includes soil dilatancy and has a non-associated flow rule. Some basic characteristics of the model are:

- Stress dependent stiffness according to a power law.
- Plastic straining due to primary deviatoric loading.
- Plastic straining due to primary compression.
- Elastic unloading - reloading condition.
- Failure according to Mohr-Coulomb theory.

4.2.1 Hyperbolic relationship for standard drained triaxial test

Although it is a superior model, the Hardening-Soil model is based on the well-known Hyperbolic model by Duncan and Chang (1970). Therefore, the hyperbolic

relationship will be first reviewed before presenting the details of Hardening-Soil model.

Over a wide range of stresses, the soil behaviour is non-linear, inelastic, and dependent on the degree of the confining pressure. Kondner (1963) found that the non-linear stress-strain relationship for both clay and sand can be approximated by a hyperbolic curve with a high degree of accuracy. In a standard drained triaxial test, the stress-strain relationship, i.e. the relationship between the vertical strain, ε_1, and the deviatoric stress, q, tends to yield curves described by the following equation and shown in Figure 4.2:

$$-\varepsilon_1 = \frac{1}{2E_{50}} \frac{q}{1 - q/q_a} \qquad \text{for: } q < q_f \tag{4.1}$$

E_{50} : The confining stress dependent stiffness modulus for primary loading.

$$E_{50} = E_{50}^{ref} \left(\frac{c\cos\varphi - \sigma_3' \sin\varphi}{c\cos\varphi + p^{ref} \sin\varphi} \right)^m \tag{4.2}$$

E_{50}^{ref} : Reference stiffness modulus corresponding to the reference confining pressure, p^{ref}. In PLAXIS, the default value of p^{ref} is 100 kPa.

σ_3' : Minor principal stress (confining pressure in a triaxial test). Negative for compression.

m : The amount of stress dependency of soils is given by the power m. For soft clays, the power should be taken equal to 1.0. Janbu (1963) reports values of m around 0.5 for Norwegian sands and silts, whilst Von Soos (1980) reports various different values in the range 0.5<m<1.0 (PLAXIS V8, 2002).

q : Deviatoric stress

q_a : Asymptotic value of the shear strength = q_f / R_f. In PLAXIS, the default value of the failure ratio, R_f is 0.9.

q_f : Utimate deviatoric stress

$$q_f = (c\cot\varphi - \sigma_3) \frac{2\sin\varphi}{1 - \sin\varphi} \tag{4.3}$$

The relationship for q_f is based on the Mohr-Coulomb failure criterion and involves the strength parameters, c and φ. When q is equal to or higher than q_f, the failure criterion is reached and perfectly plastic yielding accurs.

For unloading/reloading stress paths, another stress-dependent stiffness modulus is used:

$$E_{ur} = E_{ur}^{ref} \left(\frac{c\cos\varphi - \sigma_3' \sin\varphi}{c\cos\varphi + p^{ref} \sin\varphi} \right)^m \tag{4.4}$$

E_{ur}^{ref} : The reference Young's modulus for unloading and reloading, corresponding to the reference pressure p^{ref}. In PLAXIS, the default setting is $E_{ur}^{ref} = 3\,E_{50}^{ref}$.

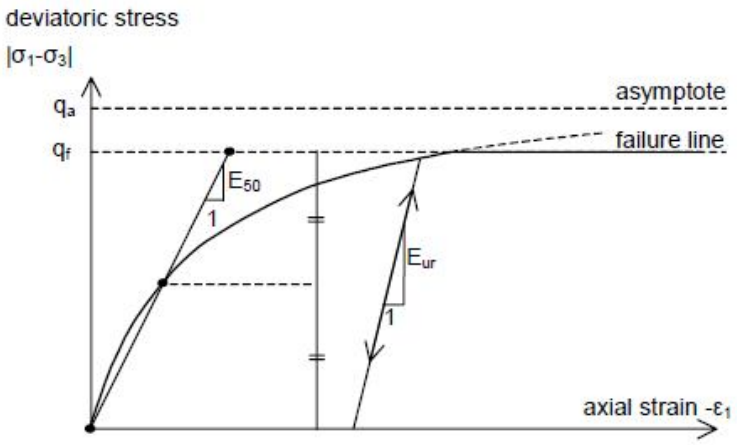

Figure 4.2 Hyperbolic stress-strain relation in primary loading for a standard drained triaxial test (PLAXIS V8, 2002)

4.2.2 Approximation of Hyperbola by the Hardening-Soil Model

In this section, the Hardening-Soil model will be described and it will be shown that the model gives hyperbolic stress-strain curve of Equation 4.1 while considering the stress-strain behaviour of soils in standard drained triaxial tests. For plastic strains, the following form yield function is used:

$$f = \bar{f} - \gamma_p \tag{4.5}$$

where $\bar{f}$ is a function of stress and γ_p is a function of plastic strains:

$$\bar{f} = \frac{1}{E_{50}} \frac{q}{1 - q/q_a} - \frac{2q}{E_{ur}} \qquad \gamma^p = -(2\varepsilon_1^p - \varepsilon_v^p) \approx -2\varepsilon_1^p \tag{4.6}$$

For stiff soils, the value of the volumetric plastic strain (ε_v^p) generally tend to be small, therefore the following approximation can be made: $\gamma_p = -2\varepsilon_1^p$ (PLAXIS V8, 2002).

Primary loading of a standard drained triaxial test implies that the yield function $\bar{f}$=0, or $\gamma_p = \bar{f}$. Accordingly, it follows from Equation 4.6 that:

$$-\varepsilon_1^p \approx \frac{1}{2}\bar{f} = \frac{1}{2E_{50}} \frac{q}{1 - q/q_a} - \frac{q}{E_{ur}} \tag{4.7}$$

Plastic strains develop in primary loading alone. However, the elastic strains develop in both primary loading and unloading/reloading. For drained triaxial stress paths with σ_3' =σ_2' = constant, the elastic Young's modulus for unloading/reloading is constant and the elastic strains are given by the following equations:

$$-\varepsilon_1^e = \frac{q}{E_{ur}} \qquad -\varepsilon_2^e = -\varepsilon_3^e = -\nu_{ur} \frac{q}{E_{ur}} \tag{4.8}$$

ν_{ur} : Unloading / Reloading Poisson's ratio

It should be noted that for the first stage of isotropic compression (with consolidation), the strain is considered fully elastic according to Hooke's law, and it is not included in Equation 4.8. For the deviatoric loading stage of triaxial test, the axial strain is given by the summation of the elastic component and the plastic component according to equation:

$$-\varepsilon_1 = -\varepsilon_1^e - \varepsilon_1^p \approx \frac{1}{2E_{50}} \frac{q}{1 - q/q_a} \tag{4.9}$$

It is concluded that the Equation 4.9 above is the hyperbolic equation described in Equation 4.1. Therefore, it is made clear that the Hardening-Soil model produces hyperbolic stress-strain curves under standard drained triaxial testing conditions.

4.2.3 Plastic Volumetric Strain for Triaxial States of Stress

The Hardening-Soil model involves a non-associated flow rule relating an increment of volumetric plastic strain to an increment of axial plastic strain:

$$\dot{\varepsilon}_v^p = \sin\psi_m \dot{\gamma}^p \tag{4.10}$$

ψ_m: Mobilised dilation angle

$$\sin\psi_m = \frac{\sin\varphi_m - \sin\varphi_{cv}}{1 - \sin\varphi_m \sin\varphi_{cv}} \tag{4.11}$$

φ_{cv}: Material constant representing the critical state friction angle, and being independent of the density.

φ_m: Mobilised friction angle

$$\sin\varphi_m = \frac{\sigma_1' - \sigma_3'}{\sigma_1' + \sigma_3' - 2c\cot\varphi} \tag{4.12}$$

These equations correspond to the stress-dilatancy theory by Rowe (PLAXIS V8, 2002). This theory implies that the material contracts for small stress ratios ($\varphi_m < \varphi_{cv}$) and dilates for high stress ratios ($\varphi_m > \varphi_{cv}$). The value of φ_{cv} can be computed from the previous equations if the user provides input data on the ultimate fiction angle and the ultimate dilatancy angle:

$$\sin\varphi_{cv} = \frac{\sin\varphi - \sin\psi}{1 - \sin\varphi\sin\psi} \tag{4.13}$$

4.2.4 Parameters of the Hardening-Soil Model

Failure parameters (as in Mohr-Coulomb model):

c : (Effective) Cohesion [kN/m^2]

□ : (Effective) Angle of internal friction [^{0}]

ψ : Angle of dilatancy [^{0}]

Basic parameters for soil stiffness:

E_{50}^{ref} : Secant modulus in standard drained triaxial tests [kN/m^2]

E_{oed}^{ref} : Tangent modulus for primary oedometer loading [kN/m^2]

m : Power for stress-level dependency of tangent modulus [dimensionless]

Advanced parameters:

E_{ur}^{ref} : Unloading/Reloading modulus (default $E_{ur}^{ref} = 3\,E_{50}^{ref}$) [kN/m^2]

v_{ur} : Poisson's ratio for unloading/reloading (default $v_{ur} = 0.2$) [kN/m^2]

p^{ref} : Reference stress for modulus (default p^{ref} = 100) [kN/m^2]

K_0^{nc} : K_0 value for normal consolidation (default K_0^{nc} = 1 -sin□ [-]

R_f : Failure ratio q_f / q_a (default $R_f = 0.9$) [-]

$\sigma_{tension}$: Tensile strength (default $\sigma_{tension}$=0 stress units) [kN/m^2]

$c_{increment}$: Increase of cohesion with depth (default $c_{increment} = 0$) [kN/m^2]

In the elastoplastic Hardening-Soil model, there is no fixed relationship between the drained triaxial stiffness E_{50} and the oedometer stiffness E_{oed} for one dimensional compression modulus for primary oedometer loading. These parameters have to be input by the user independently. The tangent stiffness modulus for one-dimensional compression is given by the following equation and shown in Figure 4.3:

$$E_{oed} = E_{oed}^{ref}\left(\frac{c\cos\varphi - \sigma_1' \sin\varphi_1}{c\cos\varphi + p^{ref}\sin\varphi}\right)^m \tag{4.14}$$

E_{oed}^{ref}: Tangent stiffness modulus at a vertical stress of $-\sigma_1' = p^{ref}$

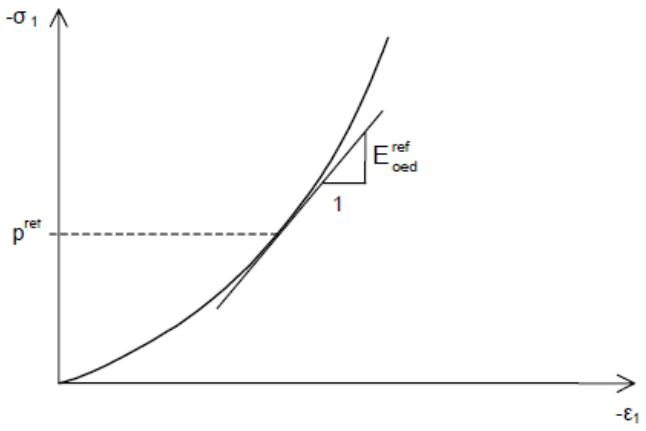

Figure 4.3 Definition of E_{oed}^{ref} in oedometer test results (PLAXIS V8, 2002).

A dilatancy cut-off option which is controlled by an initial void ratio and a maximum void ratio is also included in PLAXIS. Extensively sheared soil can not dilate indefinitely; therefore, a dilatancy cut-off set the dilation angle to zero when the maximum void ratio is reached Figure 4.4 shows a volumetric strain-axial strain curve for standard triaxial test including a dilatancy cut-off.

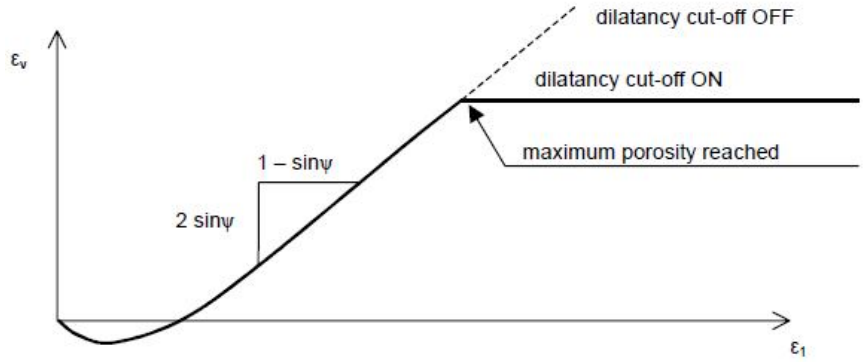

Figure 4.4 Resulting strain curve for a standard drained triaxial test when including dilatancy cut-off (PLAXIS V8, 2002).

The void ratio is related to the volumetric strain by the following relationship:

$$-\left(\varepsilon_v - \varepsilon_v^{init}\right) = \left(\frac{1+e}{1+e_{init}}\right) \tag{4.15}$$

where an increment of ε_v is positive for dilatancy.

4.2.5 Cap Yield Surface in Hardening-Soil Model

The yield condition $f = 0$, at a constant hardening parameter γ_p, defines a yield surface. Successive yield surfaces at different constant hardening parameter are shown in Figure 4.5. These yield surfaces explain the plastic strain occurring in deviatoric loading. However, they do not explain the plastic volumetric strain measured in isotropic compression. Another yield surface is then defined to close the elastic region in the direction of isotopic compression. This second yield surface is called the cap yield surface, and it makes possible the formulation of a model with independent input of the secant modulus in standard drained triaxial tests (E_{50}^{ref}) and the tangent modulus for primary oedometer loading (E_{oed}^{ref}). E_{50}^{ref} controls the plastic strains associated to the shear yield surface, and E_{oed}^{ref} controls the plastic

strains associated with the cap yield surface.

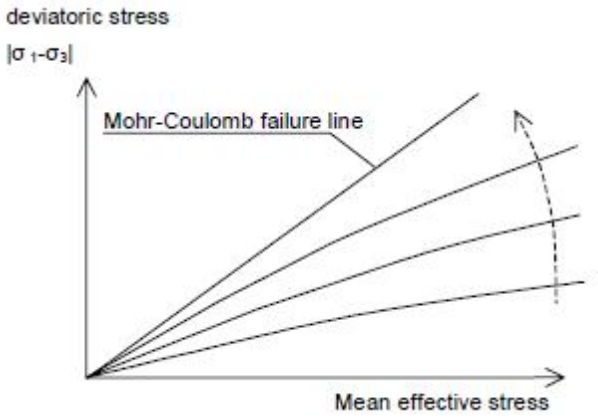

Figure 4.5 Successive yield surfaces for various constant values of the hardening parameter γ^p

The definition of the cap yield surface is similar to the equation of an ellipse:

$$f_c = \frac{\tilde{q}^2}{\alpha^2} + p^2 - p_p^2 \tag{4.16}$$

α : Cap parameter related to K_0^{nc} and defining the aspect ratio of the ellipse

p : $-(\sigma_1 + \sigma_2 + \sigma_3)/3$

$\tilde{q}$: Special stress measure for deviatoric stress = $\sigma_1 + (\delta-1)\,\sigma_2 - \delta\,\sigma_3$

δ : $(3+\sin\varphi)/(3-\sin\varphi)$

p_p : Isotropic pre-consolidation stress determining the magnitude of the yield cap or the ellipse. This parameter is provided by the PLAXIS initial stresses procedure

$\tilde{q}$ is a special stress measure for deviatoric stresses and it yields $\tilde{q} = -(\sigma_1 - \sigma_3)$ for the special case of triaxial compression ($-\sigma_1 > -\sigma_2 = -\sigma_3$), and yields $\tilde{q} = -\delta(\sigma_1 - \sigma_3)$ for triaxial extension ($-\sigma_1 = -\sigma_2 > -\sigma_3$). In addition, a hardening law relating p_p, to volumetric cap strain ε_v^{pc} defines the yield cap:

$$\varepsilon_v^{pc} = \frac{\beta}{m+1}\left(\frac{p_p}{p^{ref}}\right)^{m+1} \tag{4.17}$$

β : Cap parameter related to the tangent modulus for primary oedometer loading.

The ellipse is used both as a yield surface and as a plastic potential surface:

$$\dot{\varepsilon}^{pc} = \lambda \frac{\partial f_c}{\partial \sigma} \qquad \lambda = \frac{\beta}{2p}\left(\frac{p_p}{p^{ref}}\right)^m \frac{\dot{p}_p}{p^{ref}} \tag{4.18}$$

Figure 4.6 shows the two yield surfaces $\tilde{q}$ - p plane, and figure 4.7 shows the surfaces in principal stress space.

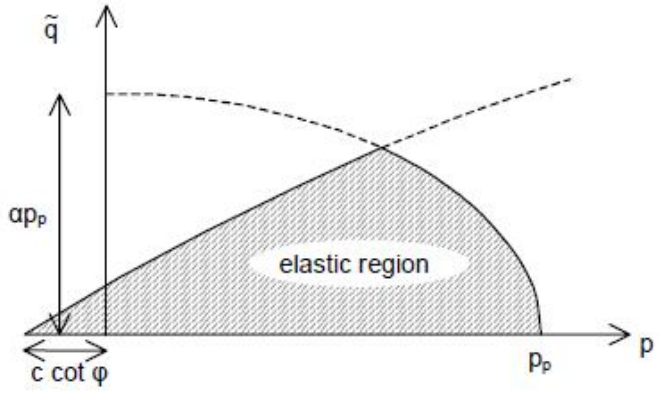

Figure 4.6 Yield surface and cap yield surface in the Hardening-Soil model (PLAXIS V8, 2002).

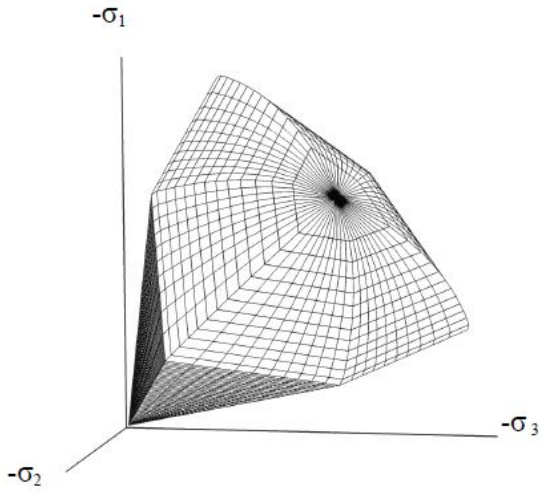

Figure 4.7 Yield surface and cap yield surface in principal stress space in the Hardening-Soil model (PLAXIS V8, 2002).

The grain size distribution of the crushed stone as well as the stress-strain curve produced in the drained triaxial test on crushed stone at a confining pressure of 100 kPa and a relative density of 89% are shown in Figures 4.8 and 4.9.

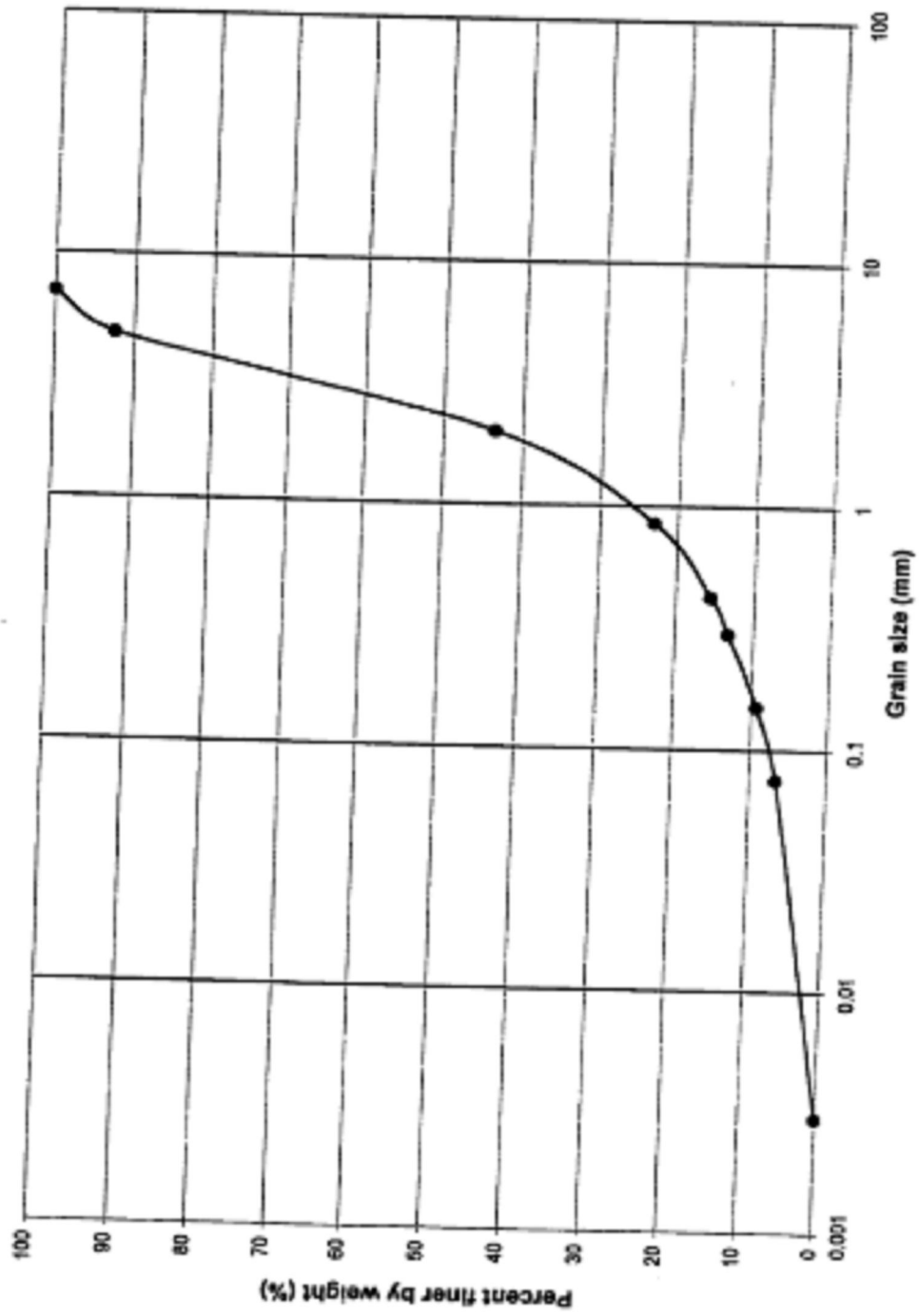

Figure 4.8 Grain size distribution of the crushed stone

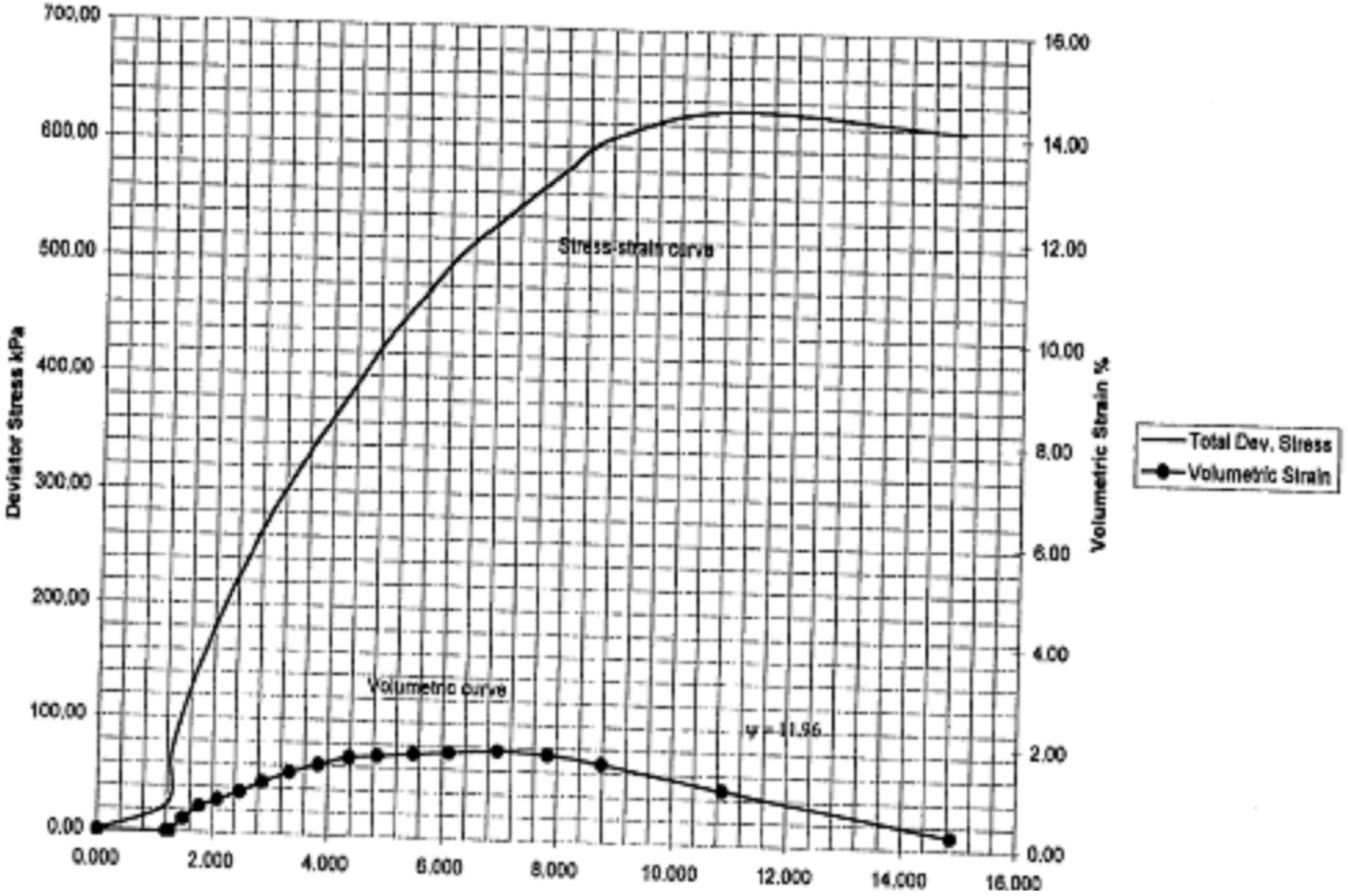

Figure 4.9 Drained triaxial test on crushed stone at a confining pressure of 100 kPa and a relative density of 89%

CHAPTER 5

FINITE ELEMENT ANALYSES

5.1 *Analysis Approach*

The modulus of soil reaction values proposed in Howard's E' table (1977) does not account for a number of important parameters and may be misleading in predicting the deformations of buried flexible pipes in real site conditions. It is an established fact that the pipe-soil relative stiffness is an important determining factor in the loads and deformations developed on buried pipes and it certainly has an effect which should be considered in the selection of modulus of soil reaction values. Therefore it was required to conduct a parametric study for a number of trench pipe-soil cases with differing pipe-soil relative stiffness in order to find out its effect on the loads and deformations on the buried pipes as well as its effect on the range of back-calculated E' values for a certain embedment condition.

The work presented in this thesis deals with the trench-pipe installation problem by developing reasonable models which include all the key factors in analyses and design of buried flexible pipes, using the finite element method (FEM). The use of a numerical approach is reasonable, considering the number of parameters involved and the complex interaction between the soil and the pipe with differing stiffnesses. The reliance on FEM for such problems in geotechnical engineering has increased in reliability and practicality as the analysis tools and computational capabilities have increased. The results of finite element calculations are used to find out the effect of relative stiffness on the behaviour of buried flexible pipes and the deformation predictions are used

to back-calculate the E' values from the Iowa formula.

5.2 *Description of the Problem and Relative Stiffness Parameters*

In addition to the description of relative stiffness parameter investigated in this thesis, the various pipe, soil, and trench dimensions and characteristic properties are described in this section. The schematic trench installation geometry and associated parameters were shown in Figure 2.11 (the zones within a backfill). The trench pipe-soil configurations of the finite element models used in this study are presented in Figures 5.1 and 5.2.

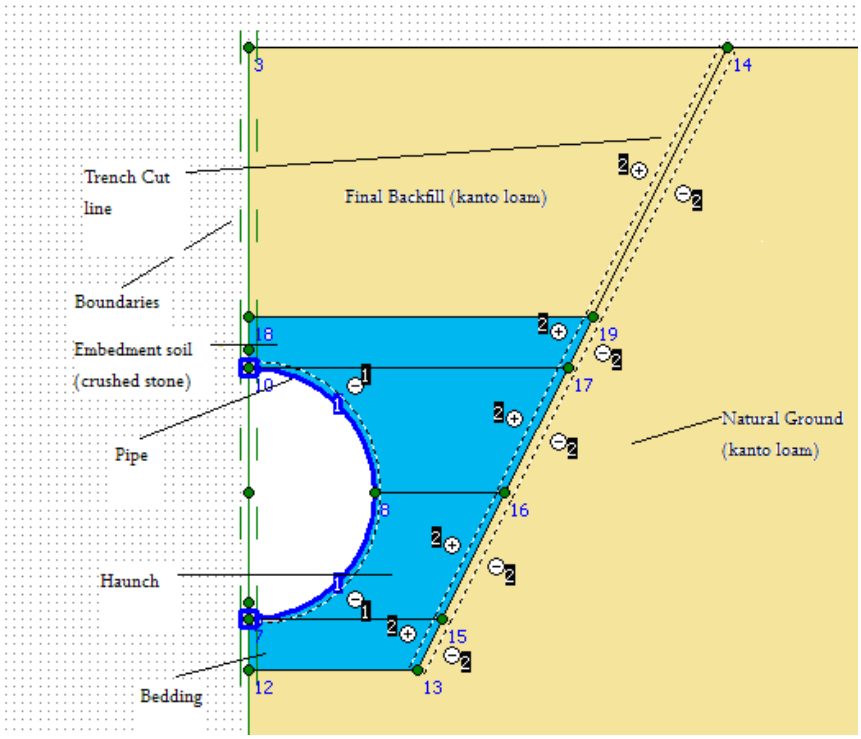

Figure 5.1 Finite Element Model of Trench Pipe-Soil System_Model 1

The main parameter investigated in this study is the pipe-soil relative stiffness. Pipe stiffness and soil stiffness concepts are discussed in a previous chapter in detail. In order to establish a practical reference for comparison, E_{50}^{ref} defined as 'the reference stiffness modulus corresponding to a confining reference pressure' is used to represent the soil stiffness. This is also reasonable as it is used as an input parameter in the Hardening-Soil model of PLAXIS which was explained in detail

in previous chapter. Pipe stiffness is kept as it is defined in Equation 2.15. Therefore, the pipe-soil stiffness ratio (S_r) defined for the purpose of this study is as follows:

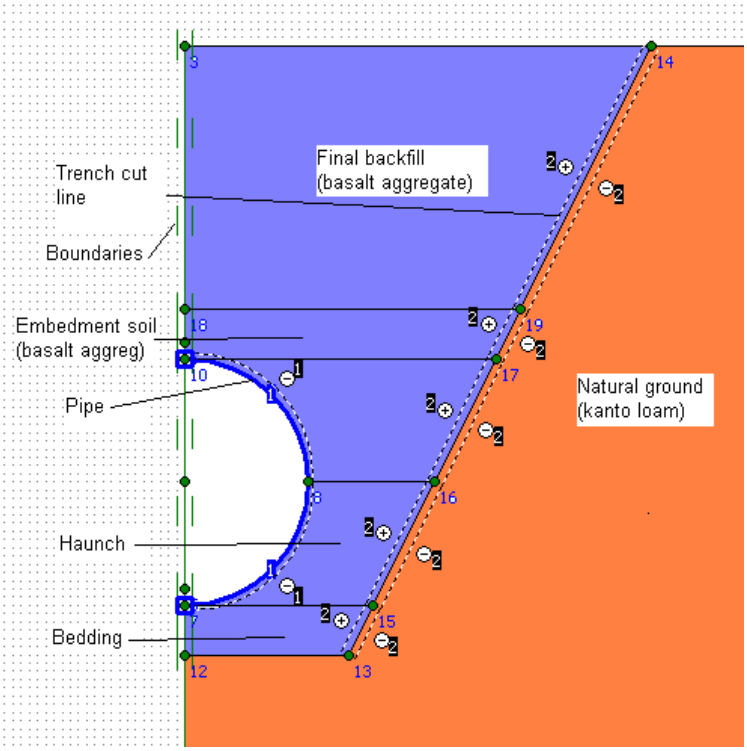

Figure 5.2 Finite Element Model of Trench Pipe-Soil System_Model 2

$$S_r = \frac{PS}{E_{50}} = \frac{EI / 0.149r^3}{E_{50}} \tag{5.1}$$

In case of Model 1, the value of E_{50}^{ref} for the embedment soil (crushed stone) is constant to be 5602 kPa as it is adopted from the measurements of standard drained triaxial tests by Mohri and Kawabata (1995). For the case of Model 2, the value of E_{50}^{ref} for the embedment soil (basalt aggregate) is also constant to be 42,500 kPa which was measured by Kaya (2004) from the laboratory triaxial tests. Since the soil stiffness is assumed to be the same in all cases, the relative stiffness can be altered by way of changing the pipe stiffness parameters, i.e. pipe material type, diameter and wall thickness.

Three pipe material types; concrete, polyethylene (PE), and ductile iron with

significantly different moduli of elasticity, E, were considered in this study. Three conduit diameters, D (0.5, 1.0 and 1.5m), were analysed for each material type. The corresponding pipe-wall thicknesses, t, were representatively selected to conform to the range of general standards. Accordingly, the wall thickness was assigned for each diameter D, such that the diameter to thickness ratio D/t ranges from 10 to 30 (5 cases) for the concrete pipes, 10 to 20 (5 cases) for the PE pipes, and 40 to 100 (5 cases) for ductile iron pipes. The trench widths at the bottom were assumed to be 1.0m, 1.5m and 2.0m for D=0.5m, 1.0m and 1.5m respectively based on general site applications. The slope of the trenches were assumed to be 1H:2V which leaded to varying average trench widths, B_d = 0.9m, 1.4m and 1.9m for D=0.5m, 1.0m and 1.5m respectively. The height of fill above the pipe, H, is the same with the average trench width, B_d since the fill height to trench width ratio $H/B_d = 1$ is kept constant in all cases. In total, 45 trench pipe-soil cases were analysed separately for both Model 1 and Model 2 using the finite element method and compared with conventional solutions (3 Material types x 3 Diameters x 5 Wall Thicknesses). The dimension ratio D/t and the previously defined pipe-soil stiffness ratio, S_r, are the main parameters for which the trench-pipe behaviour and results will be studied, the deflections will be predicted and the range of E' values will be back-calculated for the given embedment material.

5.3 *Two Dimensional Finite Element Analyses by PLAXIS*

The trench-pipe installation cases, including the construction phasing and sequences are numerically simulated by the finite element method. The modelling and analyses were carried out using PLAXIS 2D Version 8 which is a comprehensive soil-structure interaction finite element analysis (FEA) and design program. The programme simulates the non-linear nature of the problem analysed. Especially, it accounts for large deformation analysis and includes the Hardening-Soil constitutive model which is used in this study. PLAXIS is also very useful in rationally simulating the interaction between soil and pipe and provides for the interface elements described earlier. Furthermore, it allows for complex plastic computation procedures such as defining and activating loading phases at different stages or steps of the analysis, which is typical in the

simulation of trench-pipe installation problems. Further details of above and other features of the programme were discussed in a previous chapter. General settings and input parameters of the analyses carried out are hereby presented in detail. Additionally, some of the graphical presentations of results are given in order to be representative for other analyses.

5.3.1 General Settings and Boundary Conditions

5.3.1.1 Plane Strain Model

The aim of the analyses is to predict the deflections and the loads of a buried flexible pipe, considering the stages of construction and the pipe-soil interaction. In the analyses, only earth loading is considered, which is assumed to be uniform along the pipe length. For this type of analysis the pipe will be subjected to loads that act only in the x and y direction, and that the trench-pipe system (pipe and backfill material) has a cross-sectional area which is constant along an indefinite length in the z direction. This nature of the problem allows assuming the state of strain normal to the x-y plane ε_z and the shear strains γ_{xz} and γ_{yz} to be zero. This state of strain is called the plane strain condition and simplifies the calculation to a two dimensional analysis. Plane strain model is used for these analyses.

5.3.1.2 Elements

For the modelling of deformations and stresses in the analyses, the fifteen-node triangular element is selected in order to get the most accurate results. This type of element provides a fourth order interpolation involving twelve Gaussian integration points (stress points).

5.3.1.3 Geometry

In addition to the plane strain simplification, the symmetrical nature of the problem allows for one half of the pipe-soil system to be modelled. The total area of the problem studied has to be wide enough to make sure that the displacements at the extreme boundaries would be almost zero. Accordingly, an area of thirty meters wide by fifteen meters deep which is large enough to avoid any effect of the boundaries on the pipe displacements was selected. In the first analysis of

polyethylene pipes (Pipe Analysis_PE1), the horizontal displacements at the ground surface are almost zero at about fifteen meters from the centre of the ditch. The dimensions are shown in Figure 5.4.

For the purpose of simulating the staged construction and defining different layers of soil, the trench should be divided into several horizontal layers. Therefore, 5 main soil layers depending on the geometry of the trench pipe-soil system were defined. Normally, the dimensions of these layers shall follow the specifications provided in the pipe installation standards. Backfill material is required to be compacted in layers of specified thicknesses as described by the standards. However, for the sake of simplicity and practicality and considering that the effect of compaction was not taken into account in this study, the dimensions do not strictly follow a certain standard. Three different diameters of pipe sets (D=0.5m, 1.0m and 1.5m) were analysed in this study. For all three diameters, the trench was assumed to be backfilled with crushed stone beginning from 0.3m below the pipe invert level (bedding) up to 0.3m above the pipe crown level in Model 1. In case of Model 2, it was assumed that the trench was backfilled with basalt aggregate from the bottom of trench (0.3m below the pipe invert level) till the natural ground level. Since the ratio of fill height to average trench width, i.e. H/B_d=1 ratio was kept constant in all cases, the fill heights were determined depending on to the average trench widths for each diameter and the dimensions of the trench pipe-soil systems were modelled accordingly. The stages of construction (Table 5.1 and Table 5.2) and the cross section of the geometry of the trenches are presented below (Figure 5.3).

Table 5.1 Stages of Construction_Model 1

Stage	Stage of Construction	H (for D=0.5)	H (for D=1.0)	H (for D=1.5)
1	Initial Condition (Natural Ground)	15.0	15.0	15.0
2	Excavation Phase (Kanto Loam)	11.3	12.3	13.3
3	Bedding (Crushed Stone)	11.6	12.6	13.6
4	Installation of pipe with Haunch zone (Crushed Stone)	12.35	13.1	13.85
5	Backfill Phase 1 (Crushed Stone)	13.1	13.6	14.1
6	Backfill Phase 2 (Crushed Stone)	13.4	13.9	14.4
7	Backfill Phase 3 (Kanto Loam)	15.0	15.0	15.0

Table 5.2 Stages of Construction_Model 2

Stage	Stage of Construction	H (for D=0.5)	H (for D=1.0)	H (for D=1.5)
1	Initial Condition (Natural Ground)	15.0	15.0	15.0
2	Excavation Phase (Kanto Loam)	11.3	12.3	13.3
3	Bedding (Basalt Aggregate)	11.6	12.6	13.6
4	Installation of pipe with Haunch zone (Crushed Stone)	12.35	13.1	13.85
5	Backfill Phase 1 (Basalt Aggregate)	13.1	13.6	14.1
6	Backfill Phase 2 (Basalt Aggregate)	13.4	13.9	14.4
7	Backfill Phase 3 (Basalt Aggregate)	15.0	15.0	15.0

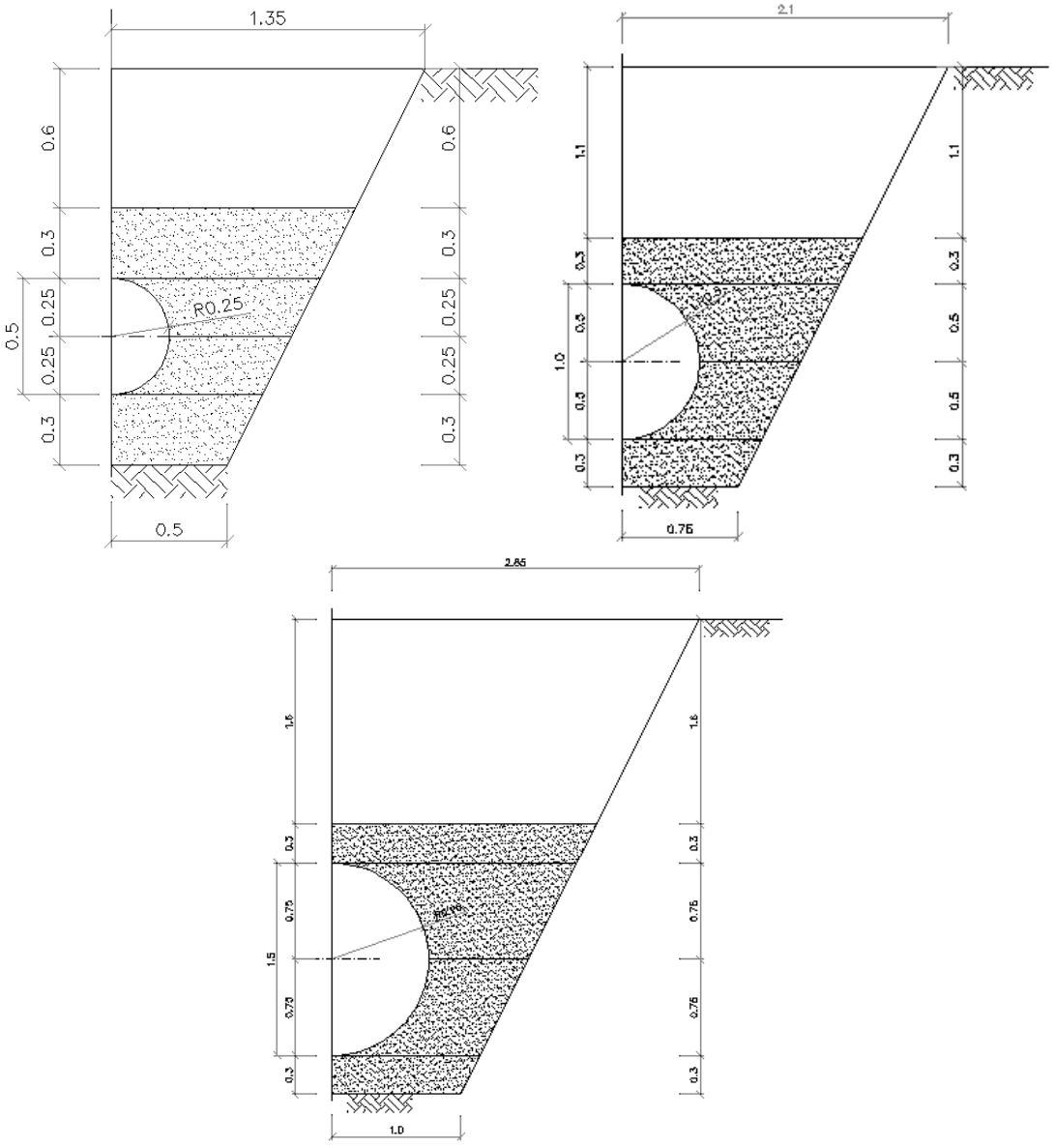

Figure 5.3 Trench geometries for D=0.5, 1.0 and 1.5m

5.3.1.4 Pipe

The curved beam elements available in the tunnel feature of PLAXIS were utilized to represent the pipe in the ground. These beams are real plate in the out of plane direction and can therefore be used to adequately model the pipe. Five-node beam elements, with eight stress points, are used together with the fifteen-node soil elements. In PLAXIS, beam elements deflect when they are subjected to both shear forces and bending moments.

5.3.1.5 Mesh Generation

A sensitivity analysis of the mesh using 15-node triangle elements for the soil and for the pipe was conducted. Mesh generation in finite element programmes is often cumbersome. Fortunately, PLAXIS automatically creates a random mesh. An option is available to refine the mesh where stress concentration and large deformations occur. In the case of a buried pipe analysis, the mesh is refined within the trench zone and close to the pipe, where most of the stress change and deformation occur. A coarser mesh is used away from the trench. Additionally, options are available to refine the mesh around lines and points which are of interest. In this study, in order to increase the accuracy of results, the mesh around the pipe crown, spring line and pipe invert points as well as around the pipe beams were refined locally. The meshes for the soil clusters within the trench were individually refined as well.

5.3.1.6 Boundaries

Standard boundaries are used in the far field and below the pipe. The vertical boundaries at the side allow vertical displacement of the soil while the horizontal boundaries at the bottom are assigned fixed. The standard fixities in PLAXIS include a horizontal displacement equal to zero for the extreme x-coordinates of the total geometry, a vertical and horizontal displacement equal to zero for the lowest y-coordinate of the total geometry, and a rotation equal to zero for beams that extend to the boundary of the geometry. These boundary conditions are suitable for most geotechnical problems, and they are also well fitting to the problem analysed in this study.

5.3.1.7 Interface Elements

In order to model the pipe-soil interaction between the pipe and the embedment material, interface elements are required around the pipe. They are also required around the trench cut line to model the soil-soil interaction between the backfill material and the natural ground. A strength reduction factor which is thought to be suitable is used to model the roughness of the interface. This factor relates the friction angle and the adhesion of the interface to the friction angle and the cohesion of the soil. When using the fifteen-node soil element, five pairs of nodes and five stress points define the interface element.

As suggested by NCHRP Report 116 (1971), the interface between pipe and soil should be properly modelled to simulate the large relative deformations expected between two materials of varying stiffnesses. The use of interface elements with a strength reduction factor of 0.4 to 0.8 is recommended. In the current analyses, the reduction factor is fixed to 0.5 for all trench cases, which implies that the interface elements will have half of the strength characteristics of those of the adjacent soil clusters. In such case, the elasticity of the interface allows both slipping (relative displacement parallel to the interface) and gapping (relative displacements perpendicular to the interface) to occur which would be expected.

The interface elements enhance the flexibility of the mesh. A sudden change in soil conditions may occur between the layers of backfill material and the side of trench. In such cases, it is useful to add an interface which would allow the flexibility of mesh and prevent any failure. Therefore, interface elements were added between the backfill material and the side of the trench. The reduction factor is the same for all the interface elements in a specific type of soil. In this case, the reduction factor for the interface between the backfill and the side of the trench is the same as the reduction factor of 0.5 for the interface between the pipe and the backfill material.

The interface soil-soil and pipe-soil elements are indicated by dashed lines in Figures 5.1 and 5.2.

5.3.1.8 Ground Water Table (Phreatic line)

The water table is taken at the bottom of the geometry, fifteen meters below the soil surface. Therefore the analyses are in dry soil conditions and water does not have an effect on the stress distribution around the pipe.

5.3.2 Input Parameters

5.3.2.1 Hardening-Soil Model Parameters

The modelling of the soil materials present in the typical trench installation is performed using the Hardening-Soil constitutive model. The Hardening-Soil parameters for Model 1 are adopted from a previous study of Mohri and Kawabata who used Kanto Loam as the natural ground and Crushed Stone as the embedment material in their buried pipe analyses. Stress–strain curves for standard drained triaxial tests allow finding the failure envelope and the strength parameters such as friction angle and cohesion. The friction angles for Kanto Loam and Crushed Stone are 17.86^0 and 28.19^0 respectively, and the cohesion values are 13.13 kPa and 40.61 kPa respectively. Although the value of cohesion seems to be high for crushed stone, it provides comparable results in the finite element analysis using the Hardening-Soil model. Another set of hardening-soil model parameters for basalt aggregate which was studied by Kaya (2004) are also used to run the same 45 analyses for Model 2. Although the value of cohesion is again recorded to be high, i.e. 36 kPa, it is input in the value of 1 kPA (approximately zero) in the analyses conducted for Model 2.

The primary deviatoric loading curve at a confining pressure of 100 kPa is needed for the determination of an important parameter for the Hardening Soil Model. This parameter is the reference stiffness modulus, E_{50}^{ref} corresponding to a confining reference pressure of 100 kPa, and is defined by a slope of a secant line passing by the origin and the point on the stress-strain curve where 50% of the failure value is reached. It is also called secant modulus, and it is found to be 11554 kPa for the Kanto Loam, and 5602 kPa for the Crushed Stone (adopted from Mohri and Kawabata, 1995) analysed in Model 1. In case of Model 2, the secant modulus E_{50}^{ref} is

taken to be 42,500 kPa for basalt aggregate as measured by Kaya (2004). The default value of the reference Young's modulus for unloading and reloading E_{ur}^{ref} in PLAXIS, corresponding to the reference pressure of 100 kPa, is used. The default elastic unloading/reloading modulus is equal to 3 E_{50}^{ref} .

The tangent stiffness for primary oedometer loading E_{oed}^{ref} *is* chosen to be equal to the secant modulus in standard drained triaxial test E_{50}^{ref} . This is the default value in PLAXIS.

In PLAXIS, it is advised to use a value of m = 0.5 for stress-level dependency of stiffness used in the hardening soil model. All the other settings such as the Poisson's ratio for unloading-reloading, v, K_0 value for normal consolidation (based on Jacky's formula, 1-sinφ), and the failure ratio R_f are set to the default value. A summary of the input parameters is presented in Table 5.3 below. The input parameters for the basalt aggregate which is used in verification analyses are also given in the same table.

Table 5.3 Summary of the input parameters for the Hardening Soil Model

Parameters	Kanto Loam	Crushed Stone	Basalt Agg.
Unit weight, γ_{dry} (kN/m^3)	12.27	16.35	16.87
Wet unit weight, γ_{wet} (kN/m^3)	13.72	20.08	16.87
Friction angle, φ^o	17.86	28.19	46.50
Cohesion, c (kPa)	13.13	40.61	1.00
Dilation angle, ψ^o	0.0	0.0	0.0
Secant modulus, E_{50}^{ref} (kPa)	11,632.08	5,604.86	42,500
Primary compression modulus E_{oed}^{ref} (kPa)	11,632.08	5,604.86	42,050
Elastic unloading & reloading modulus E_{ur}^{ref} (kPa)	34,896.24	16,814.40	145,000
Stress-level dependency, m	0.5	0.5	0.5
Failure ratio, R_f	0.9	0.9	0.9
Poisson's ratio for unloading/reloading, v	0.2	0.2	0.2
K_o(l-sinφ)	0.693	0.528	0.296

5.3.2.2 Pipe Parameters

Three pipe material types - concrete, polyethylene (PE), and ductile iron - with significantly different moduli of elasticity, *E,* were considered in this study. The parameters of interest describing their response, namely, the Young's modulus, *E,* and Poisson's ratio, *v,* as well as the material unit weight, γ used for the various types considered are listed in Table 5.4.

Table 5.4 Pipe material properties

Pipe Material Type	γ (kN/m3)	E (kPA)	*v*
Concrete	25	$2x10^7$	0.15
Polyethylene	19	$1x10^6$	0.45
Ductile Iron	78.5	$2x10^8$	0.30

PLAXIS uses curved beam elements based on the Mindlin's theory (PLAXIS V8, 2002) to simulate a pipe. The input parameters for the beam elements are: Normal stiffness, EA, Flexural rigidity, EI, Equivalent thickness, d_{eq}, Weight, W and Poisson's ratio, v.

The weight of the beam is not considered in this analysis. From the user manual of PLAXIS, the beam thickness d_{eq} is calculated from $d_{eq} = \sqrt{12EI / EA}$. Three conduit diameters, *D* (0.5, 1.0 and 1.5m), were analysed for each material type. The corresponding pipe wall thickness was assigned for each diameter *D*, such that the diameter to thickness ratio *D/t* ranges from 10 to 30 (5 cases) for the concrete pipes, 10 to 20 (5 cases) for the PE pipes, and 40 to 100 (5 cases) for ductile iron pipes. The normal stiffness, *EA* and flexural rigidity, *EI* of the pipe is different for these cases depending on the wall thickness. As defined previously, the moment of inertia is $I=t^3/12$ for a solid pipe wall of unit length. The input parameters for each type of material corresponding to their diameters and *D/t* ratios are given in below Tables 5.5 to 5.13.

Table 5.5 Input parameters for concrete pipe, D=1.5m

Parameters	*D/t=10*	*D/t=15*	*D/t=20*	*D/t=25*	*D/t=30*
Normal stiffness, EA (kN/m)	3,000,000	2,000,000	1,500,000	1,200,000	1,000,000
Flexural Rigidity, EI (kNm^2/m)	5,625.00	1,666.67	703.13	360.00	208.33
Equivalent thickness, d_{eq}, (m)	0.150	0.100	0.075	0.060	0.050
Weight, W (kN/m^2)	0	0	0	0	0
Poisson's ratio, v	0.15	0.15	0.15	0.15	0.15

Table 5.6 Input parameters for concrete pipe, D=1.0m

Parameters	*D/t=10*	*D/t=15*	*D/t=20*	*D/t=25*	*D/t=30*
Normal stiffness, EA (kN/m)	2,000,000	1,333,333	1,000,000	800,000	666,666
Flexural Rigidity, EI (kNm^2/m)	1,666.67	493.83	208.33	106.67	61.73
Equivalent thickness, d_{eq}, (m)	0.100	0.067	0.050	0.040	0.033
Weight, W (kN/m^2)	0	0	0	0	0
Poisson's ratio, v	0.15	0.15	0.15	0.15	0.15

Table 5.7 Input parameters for concrete pipe, D=0.5m

Parameters	*D/t=10*	*D/t=15*	*D/t=20*	*D/t=25*	*D/t=30*
Normal stiffness, EA (kN/m)	1,000,000	666,667	500,000	400,000	333,333
Flexural Rigidity, EI (kNm^2/m)	208.33	61.73	26.04	13.33	7.72
Equivalent thickness, d_{eq}, (m)	0.050	0.033	0.025	0.020	0.017
Weight, W (kN/m^2)	0	0	0	0	0
Poisson's ratio, v	0.15	0.15	0.15	0.15	0.15

Table 5.8 Input parameters for polyethylene pipe, D=1.5m

Parameters	*D/t=10*	*D/t=12.5*	*D/t=15*	*D/t=17.5*	*D/t=20*
Normal stiffness, EA (kN/m)	150,000	120,000	100,000	85,714	75,000
Flexural Rigidity, EI (kNm^2/m)	281.25	144.00	83.33	52.48	35.16
Equivalent thickness, d_{eq}, (m)	0.150	0.120	0.100	0.086	0.075
Weight, W (kN/m^2)	0	0	0	0	0
Poisson's ratio, v	0.45	0.45	0.45	0.45	0.45

Table 5.9 Input parameters for polyethylene pipe, D=1.0m

Parameters	*D/t=10*	*D/t=12.5*	*D/t=15*	*D/t=17.5*	*D/t=20*
Normal stiffness, EA (kN/m)	100,000	80,000	66,667	57,143	50,000
Flexural Rigidity, EI (kNm^2/m)	83.33	42.67	24.69	15.55	10.42
Equivalent thickness, d_{eq}, (m)	0.100	0.080	0.067	0.057	0.050
Weight, W (kN/m^2)	0	0	0	0	0
Poisson's ratio, v	0.45	0.45	0.45	0.45	0.45

Table 5.10 Input parameters for polyethylene pipe, D=0.5m

Parameters	*D/t=10*	*D/t=12.5*	*D/t=15*	*D/t=17.5*	*D/t=20*
Normal stiffness, EA (kN/m)	50,000	40,000	33,333	28,571	25,000
Flexural Rigidity, EI (kNm^2/m)	10.42	5.33	3.09	1.94	1.30
Equivalent thickness, d_{eq}, (m)	0.050	0.040	0.033	0.029	0.025
Weight, W (kN/m^2)	0	0	0	0	0
Poisson's ratio, v	0.45	0.45	0.45	0.45	0.45

Table 5.11 Input parameters for ductile iron pipe, D=1.5m

Parameters	*D/t=40*	*D/t=55*	*D/t=70*	*D/t=85*	*D/t=100*
Normal stiffness, EA (kN/m)	7,500,000	5,454,545	4,285,714	3,529,412	3,000,000
Flexural Rigidity, EI (kNm^2/m)	878.91	338.09	163.99	91.59	56.25
Equivalent thickness, d_{eq}, (m)	0.038	0.027	0.021	0.018	0.015
Weight, W (kN/m^2)	0	0	0	0	0
Poisson's ratio, v	0.30	0.30	0.30	0.30	0.30

Table 5.12 Input parameters for ductile iron pipe, D=1.0m

Parameters	*D/t=40*	*D/t=55*	*D/t=70*	*D/t=85*	*D/t=100*
Normal stiffness, EA (kN/m)	5,000,000	3,636,364	2,857,143	2,352,941	2,000,000
Flexural Rigidity, EI (kNm^2/m)	260.42	100.18	48.59	27.14	16.67
Equivalent thickness, d_{eq}, (m)	0.025	0.018	0.014	0.012	0.010
Weight, W (kN/m^2)	0	0	0	0	0
Poisson's ratio, v	0.30	0.30	0.30	0.30	0.30

Table 5.13 Input parameters for ductile iron pipe, D=0.5m

Parameters	*D/t=40*	*D/t=55*	*D/t=70*	*D/t=85*	*D/t=100*
Normal stiffness, EA (kN/m)	2,500,000	1,818,182	1,428,571	1,176,471	1,000,000
Flexural Rigidity, EI (kNm^2/m)	32.55	12.52	6.07	3.39	2.08
Equivalent thickness, d_{eq}, (m)	0.013	0.009	0.007	0.006	0.005
Weight, W (kN/m^2)	0	0	0	0	0
Poisson's ratio, v	0.30	0.30	0.30	0.30	0.30

5.3.2.3 Interface Parameters

As explained previously, the interface reduction factor is fixed to 0.5 for all trench cases in this study. This implies that the interface elements will have half of the strength characteristics of those of the adjacent soil clusters. In such case, the elasticity of the interface allows both slipping (relative displacement parallel to the interface) and gapping (relative displacements perpendicular to the interface) to occur as would be expected.

The reduction factor is the same for all the interface elements in a specific type of soil. In this case, the reduction factor for the interface between the backfill and the side of the trench is the same as the reduction factor of 0.5 for the interface between the pipe and the backfill material.

5.3.3 Trench Pipe-Soil Cases for Analysis

In total, 45 trench-pipe cases for both Model 1 and Model 2 were analysed using the finite element method (3 Material types x 3 Diameters x 5 Wall Thicknesses). These 45 analyses classified as per the pipe size, material and stiffness allowed investigating the effect of pipe-soil relative stiffness on the loads and deformations developed on buried pipes. The general set-up and parameters of these 45 cases are tabulated in the results tabulated for Model 1 and Model 2 in Tables 6.1 and 6.3.

5.3.4 Calculation

Among the different types of calculation available in PLAXIS, the most suitable type for the analyses in this study is the Plastic Calculation, because the analyses include elastic-plastic behaviour. Another option which may be chosen in PLAXIS is the Load Advancement Ultimate Level algorithm. In this calculation, step size is automatically determined and the calculation is terminated when the following criteria are satisfied:

- The maximum specified number of additional calculation steps has been applied.
- The total specified load has been applied
- A collapse load has been reached. Collapse is assumed when the applied load reduces in magnitude in two successive calculation steps.

Table 5.14 below shows the calculation phases used to simulate the staged construction in analyses.

Table 5.14 Calculation phases for Analyses

Stage of Construction	Phase No	Start from	Calculation	Loading Input	First	Last
Initial Condition (Natural Ground)	0	N/A	N/A	N/A	0	0
Excavation Phase (Kanto Loam)	1	0	Plastic	Staged construction	1	2
Bedding (Crushed Stone or Basalt Ag)	2	1	Plastic	Staged construction	3	4
Installation of pipe with Haunch zone (Crushed Stone or Basalt Ag.)	3	2	Plastic	Staged construction	5	6
Backfill Phase 1 (Crushed Stone or Basalt Ag.)	4	3	Plastic	Staged construction	7	8
Backfill Phase 2 (Crushed Stone or Basalt Ag.)	5	4	Plastic	Staged construction	9	10
Backfill Phase 3 (Kanto Loam or Basalt Ag.)	6	5	Plastic	Staged construction	11	12

5.3.5 Presentation of geometry and output results

The results in PLAXIS can be presented graphically in different formats. First, a view of the deformed mesh is presented. Second, it is possible to visualise the total, incremental, horizontal and vertical deformations by vectors, contour lines, or shaded areas. Third, the effective and total stresses are shown in the form of principal stresses, mean contour lines, or mean shaded areas. It is possible to visualise deformations, bending moments, shear stresses and normal stresses for structural and interface elements. Underground water flow and pore pressure outputs are also available. In addition, PLAXIS includes a special curve program to visualise load or time versus displacement, and stress-strain diagrams. This information is particularly useful to analyse local behaviour of soils.

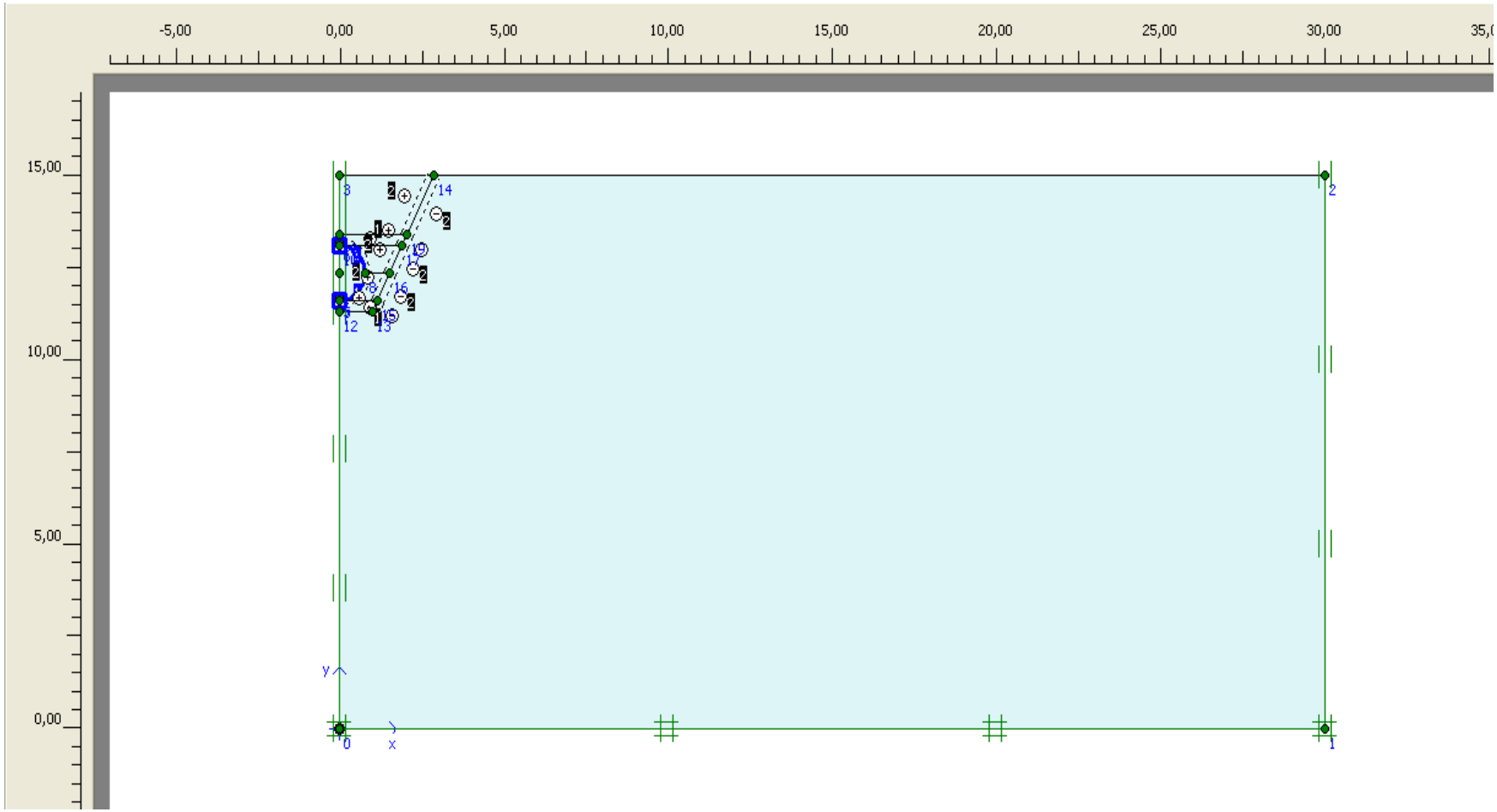

Figure 5.4 Geometry and boundary conditions

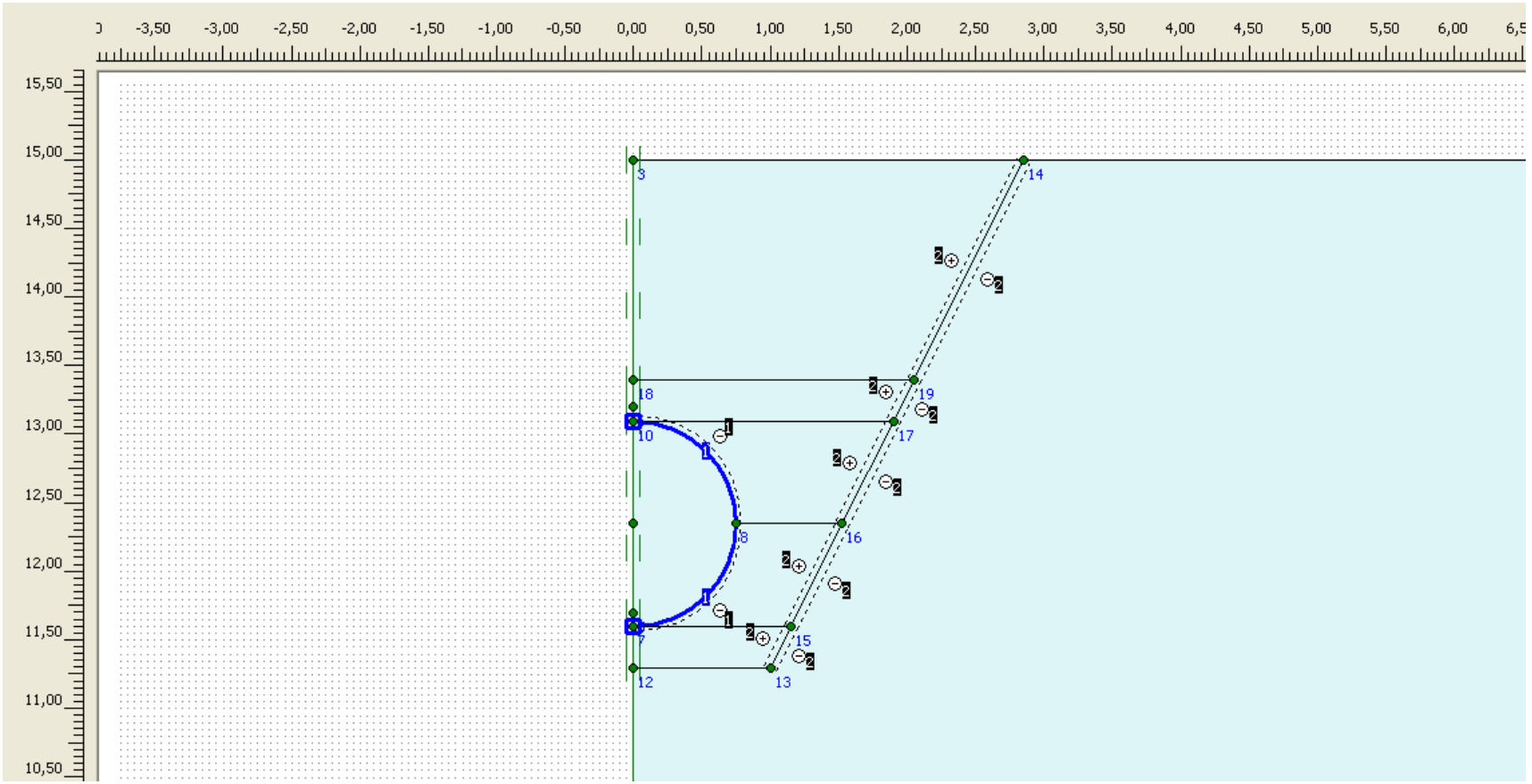

Figure 5.5 Enlarged geometry and boundary conditions in the analyses of pipes, D=1.5m

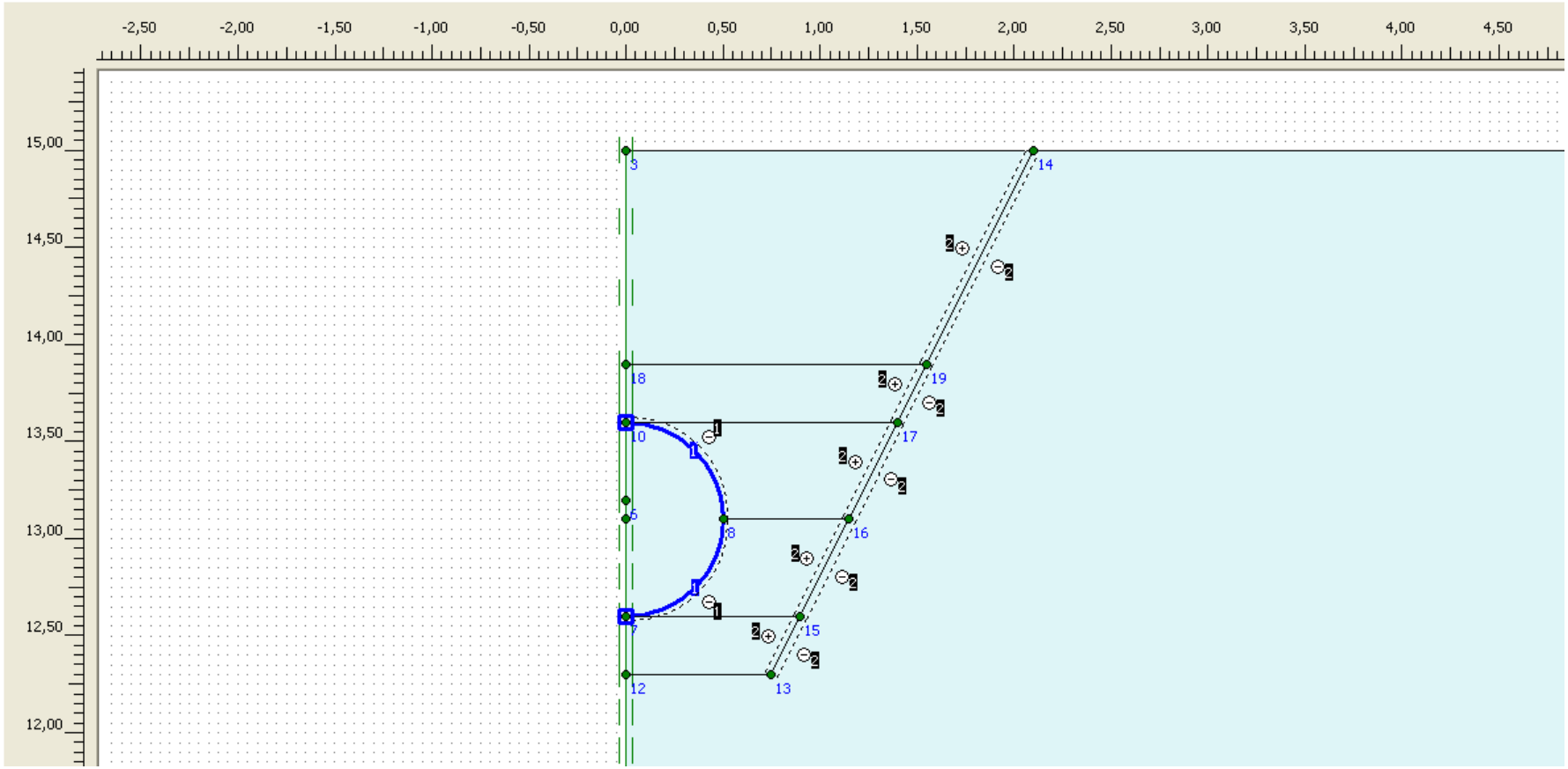

Figure 5.6 Enlarged geometry and boundary conditions in the analyses of pipes, D=1.0m

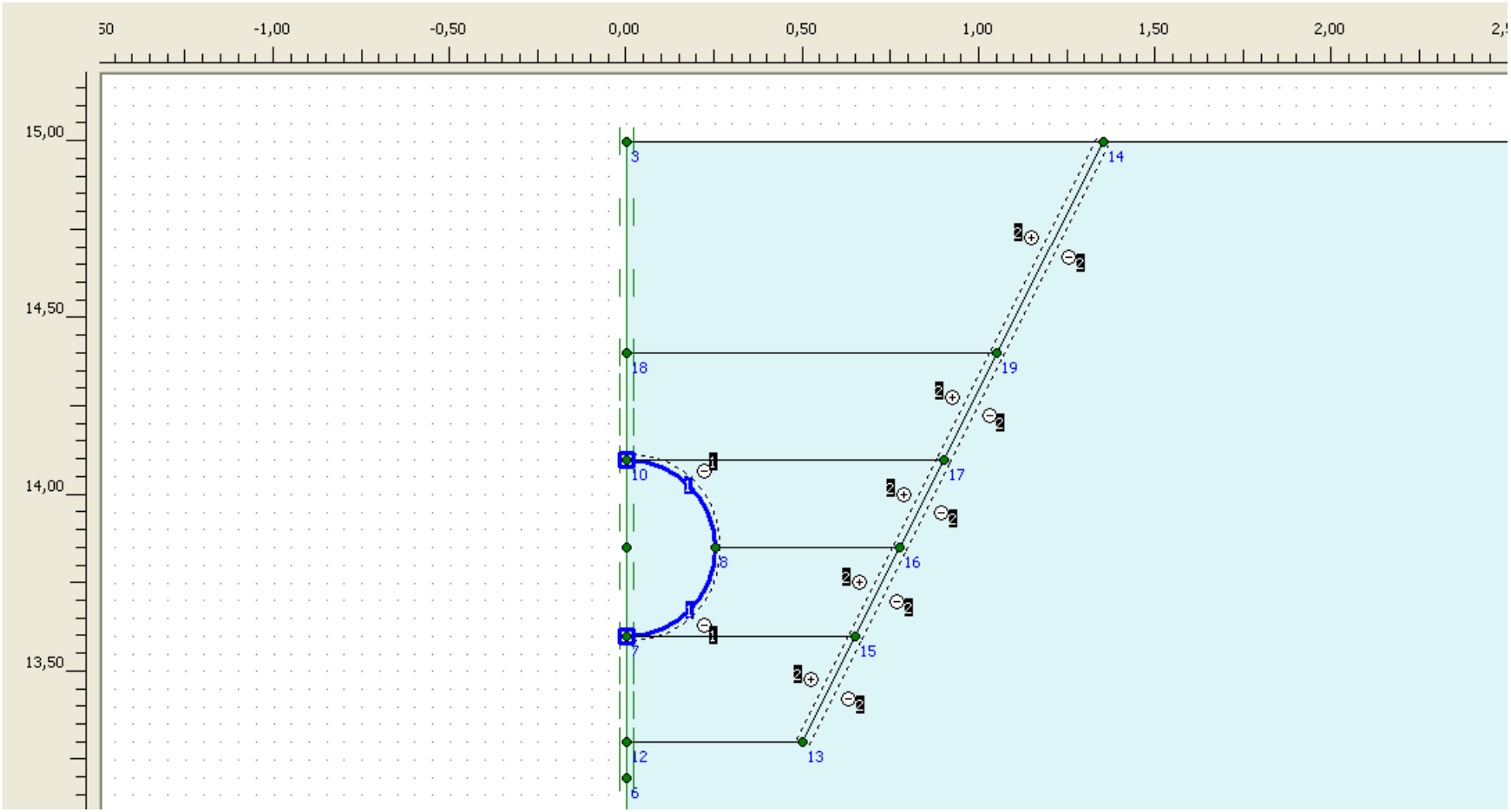

Figure 5.7 Enlarged geometry and boundary conditions in the analyses of pipes, D=0.5m

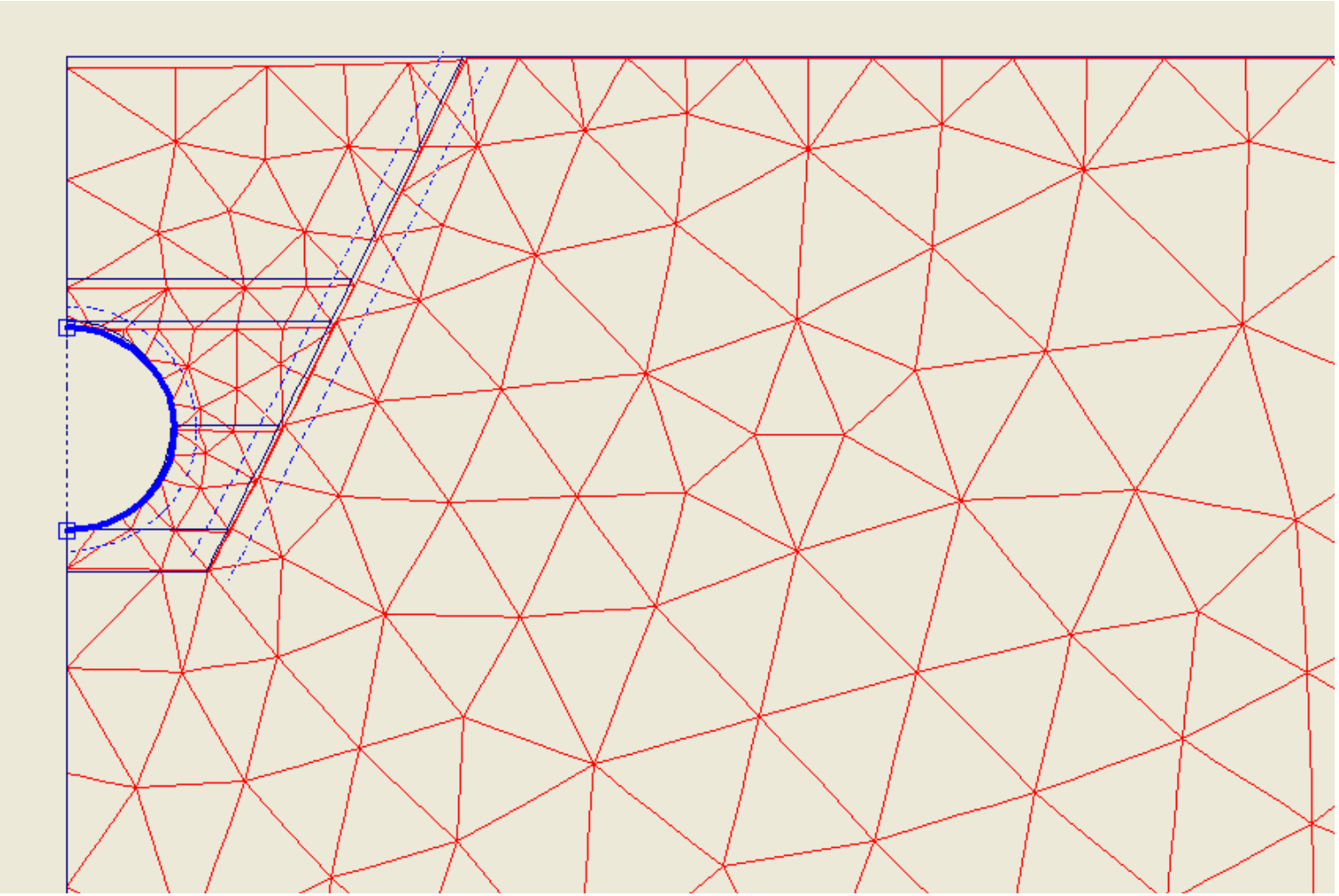

Figure 5.8 Mesh deformed in Analysis_PE1_Model 1 (deformations are scaled to 10 times)

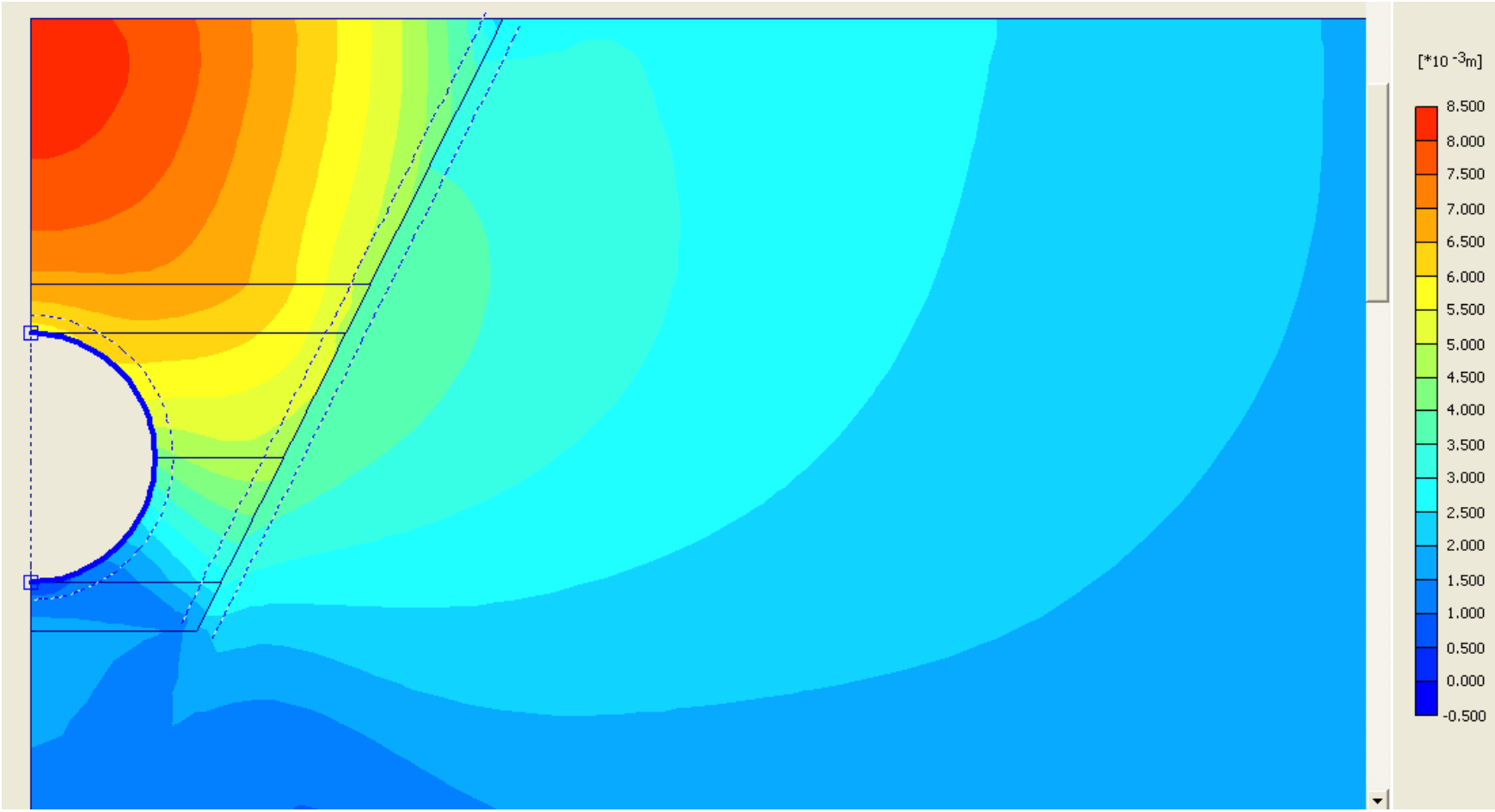

Figure 5.9 Total displacements for Analysis_PE1_Model 1 (Shadings presentation)

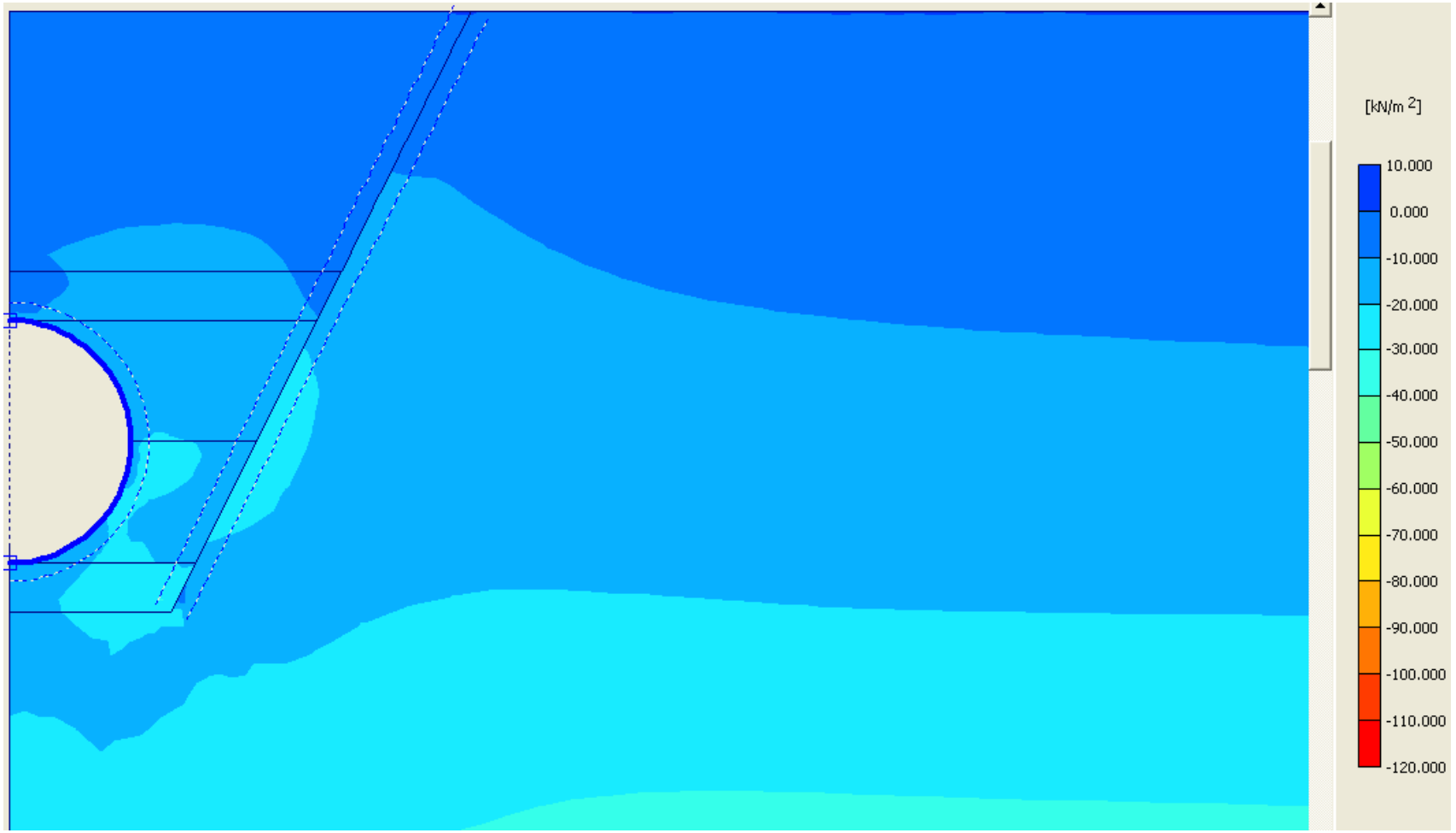

Figure 5.10 Total Stresses around pipe for Analysis_PE1_Model 1 (Shadings presentation)

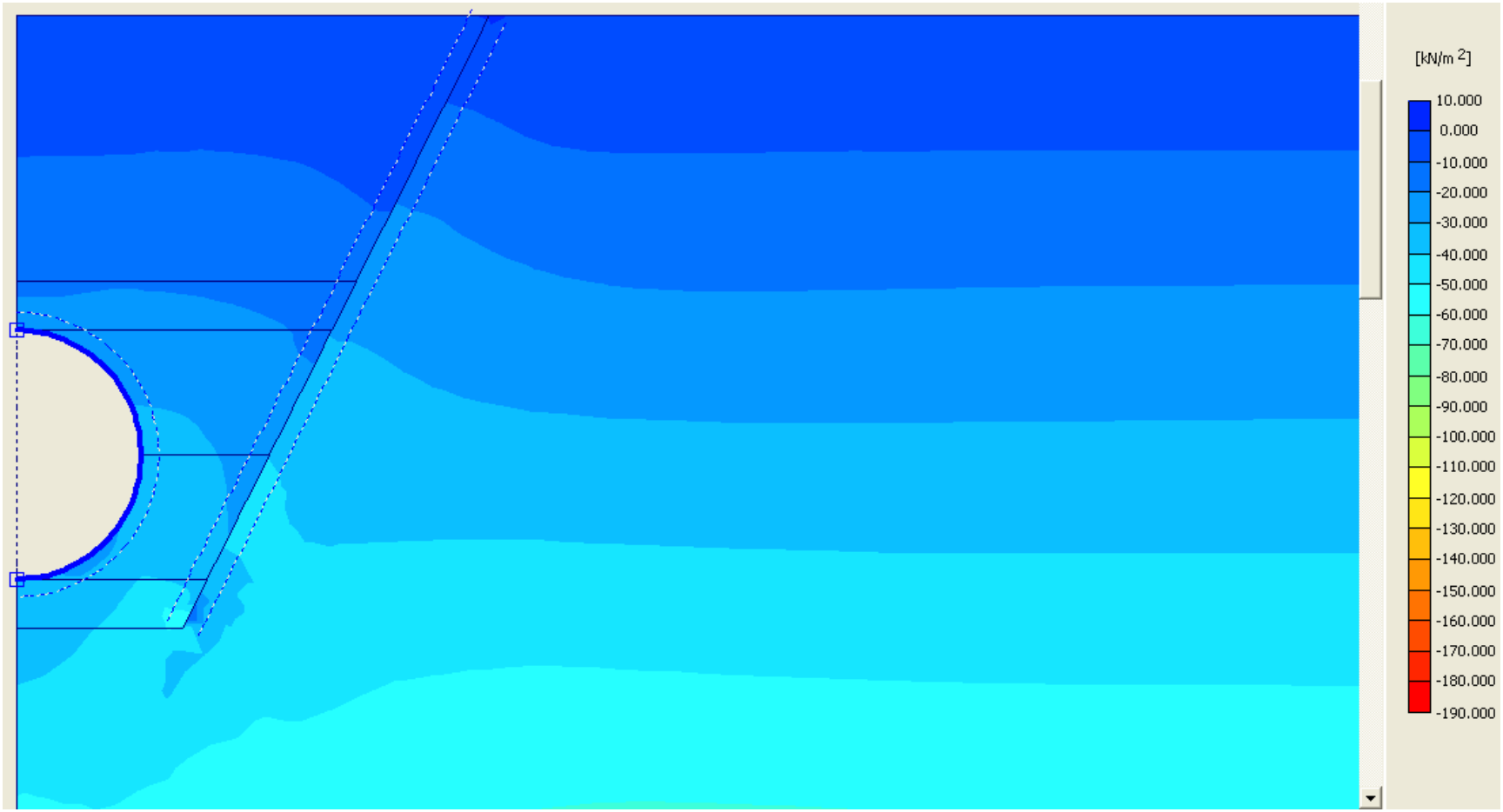

Figure 5.11 Cartesian Total Vertical Stresses, σ_{yy} for Analysis_PE1_Model 1 (Shadings presentation)

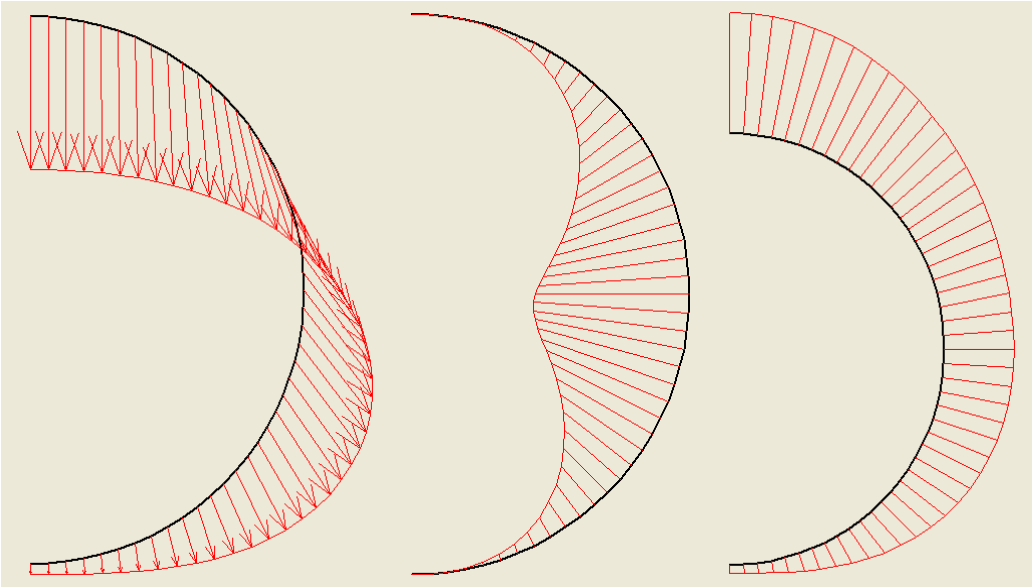

Figure 5.12 Total, Horizontal and Vertical Displacements for Analysis_PE1_Model 1 (Plate displacements presentation)

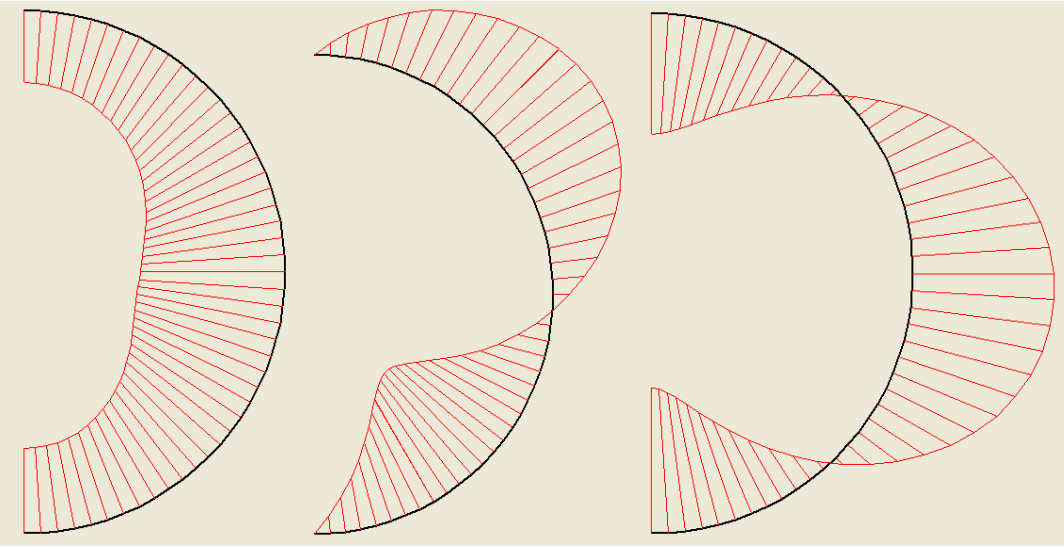

Figure 5.13 Axial forces, shear forces and bending moments for Analysis_PE1_Model 1 (Plate forces presentation)

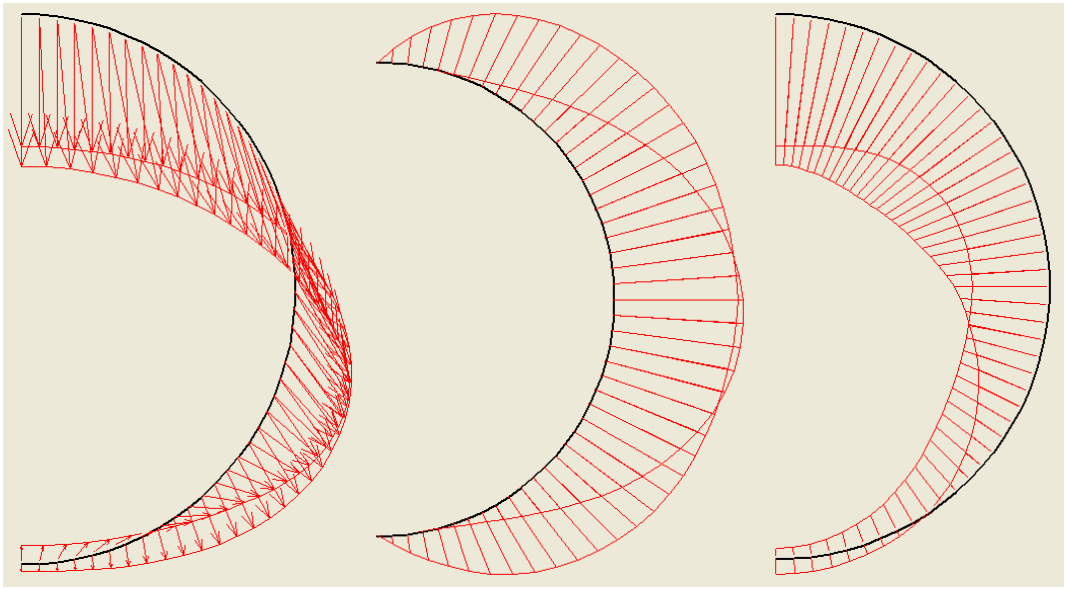

Figure 5.14 Total, Horizontal and Vertical Displacements at the Interface for Analysis_PE1_Model 1 (Interface displacements presentation)

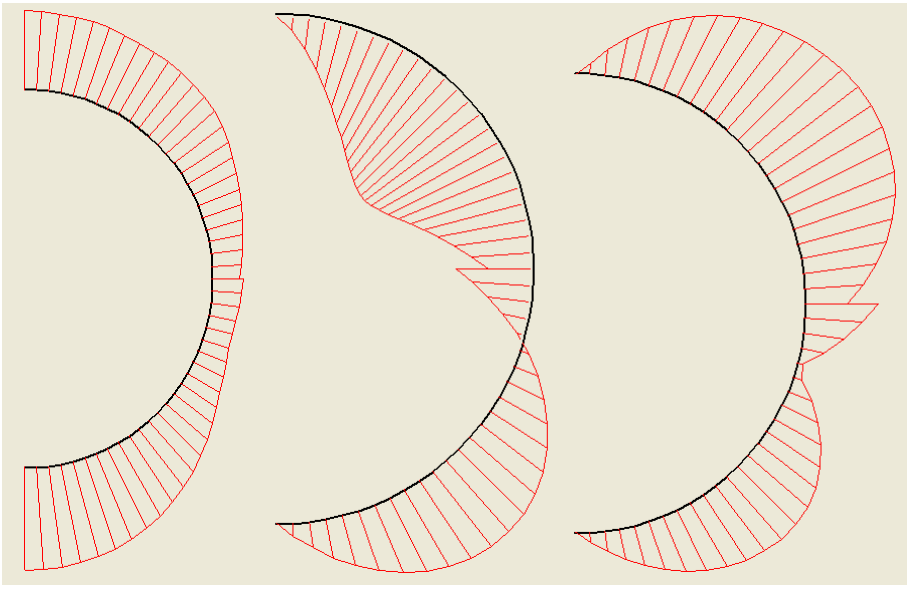

Figure 5.15 Effective normal stresses, shear stresses and relative shear stresses at the Interface for Analysis_PE1_Model 1(Interface stresses presentation)

CHAPTER 6

RESULTS AND DISCUSSION

Numerical results for the trench pipe-soil cases were obtained using the PLAXIS finite element code as per the details and methodology described in previous chapter. The groups of analyses contain three main pipe types (Concrete, Polyethylene, Ductile Iron) and three diameters (D=1,5m, 1,0m and 0,5m). For each diameter within a material type, five different *D/t* ratios which respectively correspond to the same pipe-soil stiffness ratios (S_r) were defined to allow the comparison of deformations and loads on pipes based on the relative stiffness parameter. In order to allow for comparison between the earth load estimates based on the conventional method and the analyses conducted using the FEM, the vertical stress at the crown is used to obtain an estimate of the vertical earth load, by multiplying the stress by the pipe diameter, D. The numerical results obtained from FEA for the pipe deformations at the crown, invert and spring line as well as the vertical total stresses at the pipe crown level for Model 1 and Model 2 are tabulated in Tables 6.1 and 6.3 respectively.

6.1 *Pipe Deformations*

6.1.1 Numerical Results and Discussion

The deformations of the pipes follow a general trend as per the stages of the construction. Since the compaction process is not simulated in this study, the deformations are due to the earth loads only. The pipes elongated during the placement of the haunch zone because of the lateral earth pressure applied by the side fill and then they deflected because of the earth pressure over the pipe's crown. The elongation is defined as an increase in the vertical or horizontal

diameter of the pipe and the deflection is defined as a decrease in vertical or horizontal diameter. The elongations are considered positive and the deflections are considered negative. The deformation results tabulated in Table 6.1 are the final values when the backfill reached the ground surface. The deflections in vertical direction are measured from the changes in the level of pipe crown (Point A) and the pipe invert (Point B). Due to the symmetrical nature of the problem, total horizontal elongation is two times the value recorded for pipe springline (Point C). Based on these measurements at the reference points on the pipe (Figure 6.1), the results for the horizontal and vertical deformations as well as the respective percent deflections are tabulated along with the conventional results in Table 6.2.

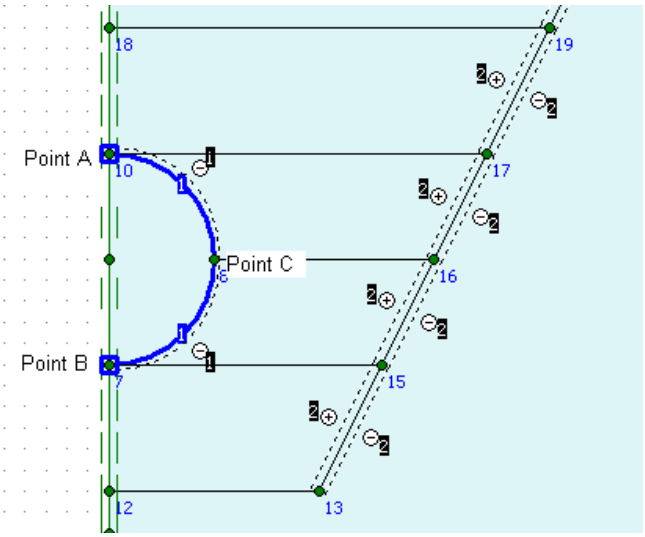

Figure 6.1 Point A, B, C – Reference points for measurement

The percent deflections range in 0.02%-0.38% for the concrete pipes, 0.18%-0.61% for the polyethylene pipes and 0.09%-0.56% for the ductile iron pipes. This small degree of deformations is an expected result since the trench-pipe cases involve a shallow burial and the pipes deform only under the earth loads.

Although the vertical and horizontal deflections are almost equal for small deflections, vertical deflection was reported by Watkins, Spangler and others as a better predictor of pipe performance (Moser and Folkman, 2008). Accordingly, the FEA results of vertical pipe deformations in terms of percent deflections ($\Delta y/D$) are

compared to the relative stiffness parameter (S_r) as they are plotted in Figures 6.3, 6.4 and 6.5 for the Concrete, Polyethylene and Ductile Iron pipes respectively. The pipe diameter and *D/t* ratio have contribution to the pipe-soil stiffness ratio, S_r and considering the other elements related to the pipe diameter such as trench geometry, individual curves are obtained for each pipe size analysed.

The individual curves for each pipe material type are somewhat parallel and as a general trend, the percent deflection at a certain pipe-soil stiffness ratio is higher for a larger diameter pipe in all the analyses. It should be noted that the fill height is equal to the average trench width (*H/Bd=1*) in all trench pipe-soil cases which implies that the depth of burial for a greater diameter and hence greater trench width is higher than a smaller diameter. Therefore, this simple observation is an expected result as the depth of burial has a direct effect on the loads applied on the pipe. On the other side, whenever the percent deflections are checked as the pipe-soil stiffness ratio, S_r decreases; it is observed that the deflection differences with respect to the diameters increase and the curves start to deviate much more from each other. This behaviour leads to the conclusion that the effect of pipe size (diameter) is more pronounced in lower degrees of relative stiffness and the pipes with greater diameters tend to deflect more than smaller diameter pipes which have the same pipe-soil stiffness ratio.

Another observation in terms of the effect of pipe material type can be drawn when the tendency of the curves are checked. It is pointed that the slope of the curves for the concrete pipes are initially increasing with the decrease in relative stiffness. Contrarily, the curves tend to flatten and their slope decreases in case of polyethylene pipes. For the ductile iron pipes, the tendency of the curves is similar to polyethylene pipes, however with a higher degree of slope between the concrete and polyethylene pipes. This behaviour implies that the deflections of the pipes tend to reach a maximum level as the relative stiffness decreases. In this regard, the results for the ductile iron pipes which present a case between the concrete and polyethylene pipes is justified given the resulting intermediate stiffness.

In case the results for all pipe types and pipe diameters are rearranged in a logarithmic plot as in Figure 6.2, some indicative trends with regard to the pipe

material type and pipe size are observed in support of the above results. Different types of pipe materials used in the study complement each other to form a continuous set of overlapping data, when expressed in terms of pipe-soil stiffness ratio ranging from 0.5913 to 15.9657.

The continuous set of data produces three individual curves corresponding to each diameter. As an expected result within each curve, the maximum deflections are observed for the polyethylene pipes, the minimum deflections are recorded for concrete pipes and the deflections for ductile iron pipes which have an intermediate stiffness produces in between results. The curves are somewhat parallel; however the differences in deflections tend to decrease as the pipe-soil stiffness ratio increases (pipes become more rigid). This implies that the effect of pipe diameter is less pronounced for relatively stiffer pipes and the pipe deflections converge to a minimum value.

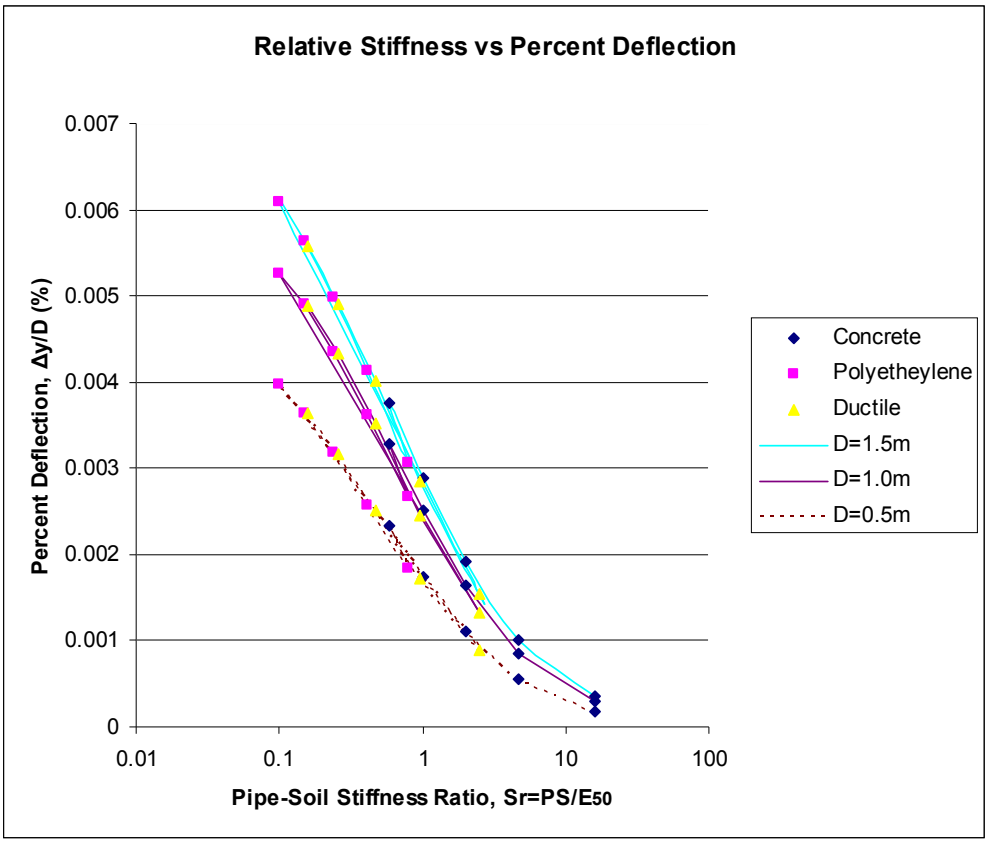

Figure 6.2 Relative Stiffness vs Percent Deflection (for all pipe types and diameters)_Model 1

Table 6.1 Results from Finite Element Analyses_Model 1

SN	Analysis	Material Type	Diameter D (m)	D/t ratio	Pipe-Soil Stiffness Ratio, Sr	FEA RESULTS			
						Vertical Total Stress at Pipe Crown, Pt A (kPa)	Vertical Deflection at Pipe Crown, Pt A (mm)	Vertical Deflection at Pipe Invert, Pt B (mm)	Horizontal Deflection at Pipe Springline, Pt C (mm)
1	Analysis_C1	Concrete	1.5	10	15.9657	-30.267	-2.050	-1.518	0.257
2	Analysis_C2	Concrete	1.5	15	4.7306	-29.415	-2.755	-1.237	0.743
3	Analysis_C3	Concrete	1.5	20	1.9957	-28.027	-3.721	-0.847	1.416
4	Analysis_C4	Concrete	1.5	25	1.0218	-26.546	-4.753	-0.430	2.144
5	Analysis_C5	Concrete	1.5	30	0.5913	-25.009	-5.677	-0.039	2.812
6	Analysis_C6	Concrete	1.0	10	15.9657	-22.120	-1.500	-1.205	0.144
7	Analysis_C7	Concrete	1.0	15	4.7306	-21.858	-2.076	-1.221	0.421
8	Analysis_C8	Concrete	1.0	20	1.9957	-20.796	-2.694	-1.046	0.816
9	Analysis_C9	Concrete	1.0	25	1.0218	-19.826	-3.371	-0.862	1.250
10	Analysis_C10	Concrete	1.0	30	0.5913	-18.121	-3.976	-0.692	1.647
11	Analysis_C11	Concrete	0.5	10	15.9657	-12.870	-0.938	-0.845	0.046
12	Analysis_C12	Concrete	0.5	15	4.7306	-12.535	-1.066	-0.787	0.139
13	Analysis_C13	Concrete	0.5	20	1.9957	-11.921	-1.256	-0.701	0.277
14	Analysis_C14	Concrete	0.5	25	1.0218	-11.238	-1.469	-0.602	0.437
15	Analysis_C15	Concrete	0.5	30	0.5913	-10.284	-1.676	-0.508	0.592
16	Analysis_PE1	Polyethylene	1.5	10	0.7983	-26.157	-4.946	-0.341	2.210
17	Analysis_PE2	Polyethylene	1.5	12.5	0.4087	-24.770	-6.072	0.135	3.003
18	Analysis_PE3	Polyethylene	1.5	15	0.2365	-22.732	-6.969	0.494	3.627
19	Analysis_PE4	Polyethylene	1.5	17.5	0.1490	-20.947	-7.715	0.736	4.114
20	Analysis_PE5	Polyethylene	1.5	20	0.0998	-20.406	-8.215	0.923	4.446
21	Analysis_PE6	Polyethylene	1.0	10	0.7983	-19.044	-3.465	-0.802	1.298
22	Analysis_PE7	Polyethylene	1.0	12.5	0.4087	-17.605	-4.186	-0.561	1.784

Table 6.1 (continued)

SN	Analysis	Material Type	Diameter D (m)	D/t ratio	Pipe-Soil Stiffness Ratio, Sr	FEA RESULTS			
						Vertical Total Stress at Pipe Crown, Pt A (kPa)	Vertical Deflection at Pipe Crown, Pt A (mm)	Vertical Deflection at Pipe Invert, Pt B (mm)	Horizontal Deflection at Pipe Springline, Pt C (mm)
23	Analysis_PE8	Polyethylene	1.0	15	0.2365	-16.482	-4.526	-0.181	2.151
24	Analysis_PE9	Polyethylene	1.0	17.5	0.1490	-16.006	-4.967	-0.059	2.441
25	Analysis_PE10	Polyethylene	1.0	20	0.0998	-15.210	-5.073	0.177	2.630
26	Analysis_PE11	Polyethylene	0.5	10	0.7983	-11.061	-1.502	-0.582	0.456
27	Analysis_PE12	Polyethylene	0.5	12.5	0.4087	-9.991	-1.755	-0.469	0.645
28	Analysis_PE13	Polyethylene	0.5	15	0.2365	-8.858	-1.956	-0.368	0.804
29	Analysis_PE14	Polyethylene	0.5	17.5	0.1490	-7.782	-2.120	-0.301	0.930
30	Analysis_PE15	Polyethylene	0.5	20	0.0998	-8.717	-2.246	-0.255	1.026
31	Analysis_DI1	Ductile Iron	1.5	40	2.4946	-28.582	-3.331	-1.009	1.148
32	Analysis_DI2	Ductile Iron	1.5	55	0.9596	-26.553	-4.725	-0.443	2.134
33	Analysis_DI3	Ductile Iron	1.5	70	0.4655	-24.512	-5.942	0.077	3.022
34	Analysis_DI4	Ductile Iron	1.5	85	0.2600	-22.859	-6.886	0.459	3.709
35	Analysis_DI5	Ductile Iron	1.5	100	0.1597	-21.290	-7.641	0.712	4.231
36	Analysis_DI6	Ductile Iron	1.0	40	2.4946	-21.169	-2.565	-1.233	0.661
37	Analysis_DI7	Ductile Iron	1.0	55	0.9596	-20.065	-3.242	-0.785	1.229
38	Analysis_DI8	Ductile Iron	1.0	70	0.4655	-17.901	-4.065	-0.551	1.773
39	Analysis_DI9	Ductile Iron	1.0	85	0.2600	-16.616	-4.561	-0.235	2.201
40	Analysis_DI10	Ductile Iron	1.0	100	0.1597	-15.445	-4.914	-0.037	2.495
41	Analysis_DI11	Ductile Iron	0.5	40	2.4946	-12.196	-1.178	-0.737	0.221
42	Analysis_DI12	Ductile Iron	0.5	55	0.9596	-11.254	-1.465	-0.605	0.434
43	Analysis_DI13	Ductile Iron	0.5	70	0.4655	-10.159	-1.740	-0.480	0.643
44	Analysis_DI14	Ductile Iron	0.5	85	0.2600	-8.981	-1.957	-0.372	0.818
45	Analysis_DI15	Ductile Iron	0.5	100	0.1597	-8.000	-2.125	-0.303	0.952

Table 6.2 Percent deflections from FEA and Conventional methods_Model 1

SN	Analysis	Material Type	Diameter D (m)	D/t ratio	Pipe-Soil Stiffness Ratio, Sr	FEA RESULTS				CONVENTIONAL	
						Horizontal Elongation, Δx (mm)	Percent Deflection, Δx/D (%)	Vertical Deflection, Δy (mm)	Percent Deflection, Δy/D (%)	IOWA formula, Δy/D (%)	WATKINS Soil-Strain, Δy/D (%)
1	Analysis_C1	Concrete	1.5	10	15.9657	0.515	0.03%	-0.532	0.04%	0.02%	0.05%
2	Analysis_C2	Concrete	1.5	15	4.7306	1.485	0.10%	-1.518	0.10%	0.07%	0.15%
3	Analysis_C3	Concrete	1.5	20	1.9957	2.832	0.19%	-2.874	0.19%	0.15%	0.32%
4	Analysis_C4	Concrete	1.5	25	1.0218	4.288	0.29%	-4.323	0.29%	0.29%	0.53%
5	Analysis_C5	Concrete	1.5	30	0.5913	5.624	0.37%	-5.638	0.38%	0.46%	0.75%
6	Analysis_C6	Concrete	1.0	10	15.9657	0.287	0.03%	-0.295	0.03%	0.02%	0.04%
7	Analysis_C7	Concrete	1.0	15	4.7306	0.841	0.08%	-0.855	0.09%	0.05%	0.11%
8	Analysis_C8	Concrete	1.0	20	1.9957	1.632	0.16%	-1.648	0.16%	0.12%	0.24%
9	Analysis_C9	Concrete	1.0	25	1.0218	2.500	0.25%	-2.509	0.25%	0.21%	0.40%
10	Analysis_C10	Concrete	1.0	30	0.5913	3.294	0.33%	-3.284	0.33%	0.35%	0.57%
11	Analysis_C11	Concrete	0.5	10	15.9657	0.092	0.02%	-0.094	0.02%	0.01%	0.02%
12	Analysis_C12	Concrete	0.5	15	4.7306	0.277	0.06%	-0.279	0.06%	0.03%	0.08%
13	Analysis_C13	Concrete	0.5	20	1.9957	0.555	0.11%	-0.555	0.11%	0.08%	0.16%
14	Analysis_C14	Concrete	0.5	25	1.0218	0.873	0.17%	-0.867	0.17%	0.14%	0.27%
15	Analysis_C15	Concrete	0.5	30	0.5913	1.184	0.24%	-1.168	0.23%	0.23%	0.38%
16	Analysis_PE1	Polyethylene	1.5	10	0.7983	4.420	0.29%	-4.605	0.31%	0.36%	0.63%
17	Analysis_PE2	Polyethylene	1.5	12.5	0.4087	6.006	0.40%	-6.207	0.41%	0.63%	0.92%
18	Analysis_PE3	Polyethylene	1.5	15	0.2365	7.254	0.48%	-7.463	0.50%	0.95%	1.15%
19	Analysis_PE4	Polyethylene	1.5	17.5	0.1490	8.228	0.55%	-8.451	0.56%	1.28%	1.31%
20	Analysis_PE5	Polyethylene	1.5	20	0.0998	8.892	0.59%	-9.138	0.61%	1.59%	1.43%
21	Analysis_PE6	Polyethylene	1.0	10	0.7983	2.596	0.26%	-2.663	0.27%	0.27%	0.47%
22	Analysis_PE7	Polyethylene	1.0	12.5	0.4087	3.568	0.36%	-3.625	0.36%	0.47%	0.69%

Table 6.2 (continued)

SN	Analysis	Material Type	Diameter D (m)	D/t ratio	Pipe-Soil Stiffness Ratio, Sr	FEA RESULTS					
						Horizontal Elongation, Δx (mm)	Percent Deflection, Δx/D (%)	Vertical Deflection, Δy (mm)	Percent Deflection, Δy/D (%)	IOWA formula, Δy/D (%)	WATKINS Soil-Strain, Δy/D (%)
23	Analysis_PE8	Polyethylene	1.0	15	0.2365	4.302	0.43%	-4.345	0.43%	0.71%	0.86%
24	Analysis_PE9	Polyethylene	1.0	17.5	0.1490	4.882	0.49%	-4.908	0.49%	0.96%	0.99%
25	Analysis_PE10	Polyethylene	1.0	20	0.0998	5.260	0.53%	-5.250	0.53%	1.19%	1.07%
26	Analysis_PE11	Polyethylene	0.5	10	0.7983	0.912	0.18%	-0.920	0.18%	0.18%	0.31%
27	Analysis_PE12	Polyethylene	0.5	12.5	0.4087	1.289	0.26%	-1.286	0.26%	0.31%	0.46%
28	Analysis_PE13	Polyethylene	0.5	15	0.2365	1.608	0.32%	-1.588	0.32%	0.47%	0.57%
29	Analysis_PE14	Polyethylene	0.5	17.5	0.1490	1.859	0.37%	-1.819	0.36%	0.64%	0.66%
30	Analysis_PE15	Polyethylene	0.5	20	0.0998	2.052	0.41%	-1.991	0.40%	0.80%	0.72%
31	Analysis_DI1	Ductile Iron	1.5	40	2.4946	2.296	0.15%	-2.322	0.15%	0.12%	0.27%
32	Analysis_DI2	Ductile Iron	1.5	55	0.9596	4.268	0.28%	-4.282	0.29%	0.30%	0.56%
33	Analysis_DI3	Ductile Iron	1.5	70	0.4655	6.044	0.40%	-6.019	0.40%	0.57%	0.86%
34	Analysis_DI4	Ductile Iron	1.5	85	0.2600	7.418	0.49%	-7.345	0.49%	0.89%	1.11%
35	Analysis_DI5	Ductile Iron	1.5	100	0.1597	8.462	0.56%	-8.353	0.56%	1.23%	1.29%
36	Analysis_DI6	Ductile Iron	1.0	40	2.4946	1.321	0.13%	-1.332	0.13%	0.09%	0.20%
37	Analysis_DI7	Ductile Iron	1.0	55	0.9596	2.458	0.25%	-2.457	0.25%	0.23%	0.42%
38	Analysis_DI8	Ductile Iron	1.0	70	0.4655	3.546	0.35%	-3.514	0.35%	0.43%	0.64%
39	Analysis_DI9	Ductile Iron	1.0	85	0.2600	4.402	0.44%	-4.326	0.43%	0.67%	0.83%
40	Analysis_DI10	Ductile Iron	1.0	100	0.1597	4.990	0.50%	-4.877	0.49%	0.92%	0.97%
41	Analysis_DI11	Ductile Iron	0.5	40	2.4946	0.441	0.09%	-0.441	0.09%	0.06%	0.13%
42	Analysis_DI12	Ductile Iron	0.5	55	0.9596	0.868	0.17%	-0.861	0.17%	0.15%	0.28%
43	Analysis_DI13	Ductile Iron	0.5	70	0.4655	1.285	0.26%	-1.260	0.25%	0.28%	0.43%
44	Analysis_DI14	Ductile Iron	0.5	85	0.2600	1.635	0.33%	-1.585	0.32%	0.44%	0.55%
45	Analysis_DI15	Ductile Iron	0.5	100	0.1597	1.904	0.38%	-1.822	0.36%	0.61%	0.65%

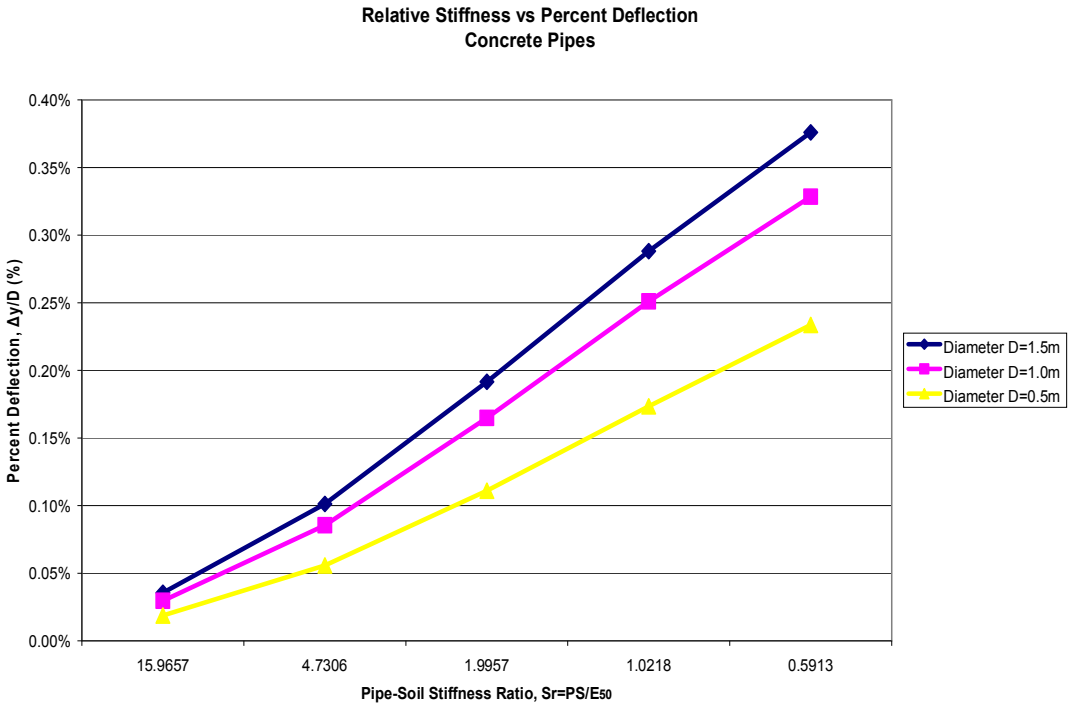

Figure 6.3 Relative Stiffness vs Percent Deflection (Concrete Pipes)_Model 1

Figure 6.4 Relative Stiffness vs Percent Deflection (Polyethylene Pipes)_Model 1

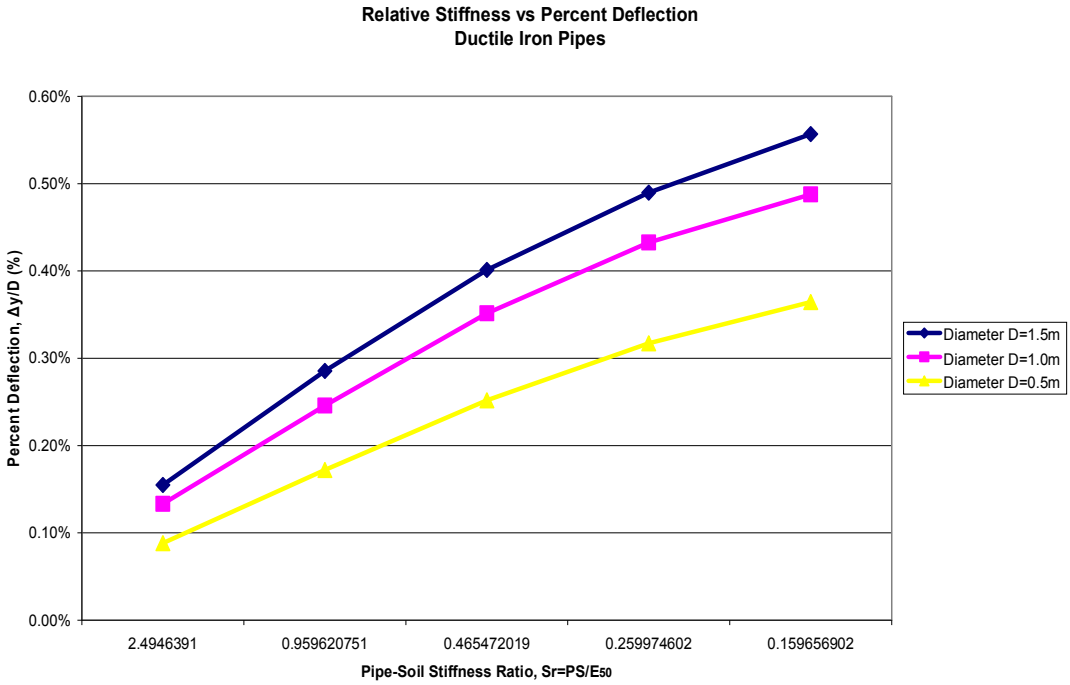

Figure 6.5 Relative Stiffness vs Percent Deflection (Ductile Iron Pipes)_Model 1

The above results and discussion were based on the numerical analyses of the finite element Model 1 at which the embedment material was crushed stone and the final backfill was kanto loam. The numerical results of the analyses conducted for Model 2 are tabulated in Tables 6.3 and Table 6.4. Based on these results, the figures demonstrating the change of percent deflections with respect to the relative stiffness parameter are plotted (Figures 6.6, 6.7, 6.8, 6.9). Again, the results for all pipe types and pipe diameters are rearranged in a logarithmic plot and some indicative trends with regard to the pipe material type and pipe size are observed. Similar to the results of Model 1, different types of pipe materials used in the study complement each other to form a continuous set of overlapping data with the difference that pipe-soil stiffness ratio ranges at a different interval (0.013 to 2.105). The continuous set of data again produces three individual curves corresponding to each diameter and the indicative trends presented by these curves are in similar nature to those of Model 1.

Table 6.3 Results from Finite Element Analyses_Model 2

SN	Analysis	Material Type	Diameter D (m)	D/t ratio	Pipe-Soil Stiffness Ratio, Sr	FEA RESULTS			
						Vertical Total Stress at Pipe Crown, Pt A (kPa)	Vertical Deflection at Pipe Crown, Pt A (mm)	Vertical Deflection at Pipe Invert, Pt B (mm)	Horizontal Deflection at Pipe Springline, Pt C (mm)
1	Analysis_C1	Concrete	1.5	10	15.9657	-30.267	-2.050	-1.518	0.257
2	Analysis_C2	Concrete	1.5	15	4.7306	-29.415	-2.755	-1.237	0.743
3	Analysis_C3	Concrete	1.5	20	1.9957	-28.027	-3.721	-0.847	1.416
4	Analysis_C4	Concrete	1.5	25	1.0218	-26.546	-4.753	-0.430	2.144
5	Analysis_C5	Concrete	1.5	30	0.5913	-25.009	-5.677	-0.039	2.812
6	Analysis_C6	Concrete	1.0	10	15.9657	-22.120	-1.500	-1.205	0.144
7	Analysis_C7	Concrete	1.0	15	4.7306	-21.858	-2.076	-1.221	0.421
8	Analysis_C8	Concrete	1.0	20	1.9957	-20.796	-2.694	-1.046	0.816
9	Analysis_C9	Concrete	1.0	25	1.0218	-19.826	-3.371	-0.862	1.250
10	Analysis_C10	Concrete	1.0	30	0.5913	-18.121	-3.976	-0.692	1.647
11	Analysis_C11	Concrete	0.5	10	15.9657	-12.870	-0.938	-0.845	0.046
12	Analysis_C12	Concrete	0.5	15	4.7306	-12.535	-1.066	-0.787	0.139
13	Analysis_C13	Concrete	0.5	20	1.9957	-11.921	-1.256	-0.701	0.277
14	Analysis_C14	Concrete	0.5	25	1.0218	-11.238	-1.469	-0.602	0.437
15	Analysis_C15	Concrete	0.5	30	0.5913	-10.284	-1.676	-0.508	0.592
16	Analysis_PE1	Polyethylene	1.5	10	0.7983	-26.157	-4.946	-0.341	2.210
17	Analysis_PE2	Polyethylene	1.5	12.5	0.4087	-24.770	-6.072	0.135	3.003
18	Analysis_PE3	Polyethylene	1.5	15	0.2365	-22.732	-6.969	0.494	3.627
19	Analysis_PE4	Polyethylene	1.5	17.5	0.1490	-20.947	-7.715	0.736	4.114
20	Analysis_PE5	Polyethylene	1.5	20	0.0998	-20.406	-8.215	0.923	4.446
21	Analysis_PE6	Polyethylene	1.0	10	0.7983	-19.044	-3.465	-0.802	1.298
22	Analysis_PE7	Polyethylene	1.0	12.5	0.4087	-17.605	-4.186	-0.561	1.784

Table 6.3 (continued)

SN	Analysis	Material Type	Diameter D (m)	D/t ratio	Pipe-Soil Stiffness Ratio, Sr	FEA RESULTS			
						Vertical Total Stress at Pipe Crown, Pt A (kPa)	Vertical Deflection at Pipe Crown, Pt A (mm)	Vertical Deflection at Pipe Invert, Pt B (mm)	Horizontal Deflection at Pipe Springline, Pt C (mm)
23	Analysis_PE8	Polyethylene	1.0	15	0.2365	-16.482	-4.526	-0.181	2.151
24	Analysis_PE9	Polyethylene	1.0	17.5	0.1490	-16.006	-4.967	-0.059	2.441
25	Analysis_PE10	Polyethylene	1.0	20	0.0998	-15.210	-5.073	0.177	2.630
26	Analysis_PE11	Polyethylene	0.5	10	0.7983	-11.061	-1.502	-0.582	0.456
27	Analysis_PE12	Polyethylene	0.5	12.5	0.4087	-9.991	-1.755	-0.469	0.645
28	Analysis_PE13	Polyethylene	0.5	15	0.2365	-8.858	-1.956	-0.368	0.804
29	Analysis_PE14	Polyethylene	0.5	17.5	0.1490	-7.782	-2.120	-0.301	0.930
30	Analysis_PE15	Polyethylene	0.5	20	0.0998	-8.717	-2.246	-0.255	1.026
31	Analysis_DI1	Ductile Iron	1.5	40	2.4946	-28.582	-3.331	-1.009	1.148
32	Analysis_DI2	Ductile Iron	1.5	55	0.9596	-26.553	-4.725	-0.443	2.134
33	Analysis_DI3	Ductile Iron	1.5	70	0.4655	-24.512	-5.942	0.077	3.022
34	Analysis_DI4	Ductile Iron	1.5	85	0.2600	-22.859	-6.886	0.459	3.709
35	Analysis_DI5	Ductile Iron	1.5	100	0.1597	-21.290	-7.641	0.712	4.231
36	Analysis_DI6	Ductile Iron	1.0	40	2.4946	-21.169	-2.565	-1.233	0.661
37	Analysis_DI7	Ductile Iron	1.0	55	0.9596	-20.065	-3.242	-0.785	1.229
38	Analysis_DI8	Ductile Iron	1.0	70	0.4655	-17.901	-4.065	-0.551	1.773
39	Analysis_DI9	Ductile Iron	1.0	85	0.2600	-16.616	-4.561	-0.235	2.201
40	Analysis_DI10	Ductile Iron	1.0	100	0.1597	-15.445	-4.914	-0.037	2.495
41	Analysis_DI11	Ductile Iron	0.5	40	2.4946	-12.196	-1.178	-0.737	0.221
42	Analysis_DI12	Ductile Iron	0.5	55	0.9596	-11.254	-1.465	-0.605	0.434
43	Analysis_DI13	Ductile Iron	0.5	70	0.4655	-10.159	-1.740	-0.480	0.643
44	Analysis_DI14	Ductile Iron	0.5	85	0.2600	-8.981	-1.957	-0.372	0.818
45	Analysis_DI15	Ductile Iron	0.5	100	0.1597	-8.000	-2.125	-0.303	0.952

Table 6.4 Percent deflections from FEA and Conventional methods_Model 2

SN	Analysis	Material Type	Diameter D (m)	D/t ratio	Pipe-Soil Stiffness Ratio, Sr	FEA RESULTS				CONVENTIONAL	
						Horizontal Elongation, Δx (mm)	Percent Deflection, Δx/D (%)	Vertical Deflection, Δy (mm)	Percent Deflection, Δy/D (%)	IOWA formula, Δy/D (%)	WATKINS Soil-Strain, Δy/D (%)
1	Analysis_C1	Concrete	1.5	10	2.1055	0.925	0.06%	-0.934	0.06%	0.03%	0.06%
2	Analysis_C2	Concrete	1.5	15	0.6239	2.310	0.15%	-2.320	0.15%	0.09%	0.20%
3	Analysis_C3	Concrete	1.5	20	0.2632	3.852	0.26%	-3.842	0.26%	0.20%	0.42%
4	Analysis_C4	Concrete	1.5	25	0.1348	5.246	0.35%	-5.200	0.35%	0.37%	0.70%
5	Analysis_C5	Concrete	1.5	30	0.0780	6.432	0.43%	-6.345	0.42%	0.61%	0.99%
6	Analysis_C6	Concrete	1.0	10	2.1055	0.478	0.05%	-0.480	0.05%	0.02%	0.05%
7	Analysis_C7	Concrete	1.0	15	0.6239	1.238	0.12%	-1.236	0.12%	0.06%	0.15%
8	Analysis_C8	Concrete	1.0	20	0.2632	2.116	0.21%	-2.101	0.21%	0.15%	0.31%
9	Analysis_C9	Concrete	1.0	25	0.1348	2.922	0.29%	-2.881	0.29%	0.28%	0.51%
10	Analysis_C10	Concrete	1.0	30	0.0780	3.582	0.36%	-3.507	0.35%	0.45%	0.73%
11	Analysis_C11	Concrete	0.5	10	2.1055	0.108	0.02%	-0.108	0.02%	0.01%	0.03%
12	Analysis_C12	Concrete	0.5	15	0.6239	0.304	0.06%	-0.303	0.06%	0.04%	0.09%
13	Analysis_C13	Concrete	0.5	20	0.2632	0.561	0.11%	-0.555	0.11%	0.09%	0.20%
14	Analysis_C14	Concrete	0.5	25	0.1348	0.820	0.16%	-0.808	0.16%	0.18%	0.33%
15	Analysis_C15	Concrete	0.5	30	0.0780	1.050	0.21%	-1.026	0.21%	0.29%	0.47%
16	Analysis_PE1	Polyethylene	1.5	10	0.1053	5.376	0.36%	-5.436	0.36%	0.47%	0.82%
17	Analysis_PE2	Polyethylene	1.5	12.5	0.0539	6.758	0.45%	-6.814	0.45%	0.82%	1.20%
18	Analysis_PE3	Polyethylene	1.5	15	0.0312	7.792	0.52%	-7.856	0.52%	1.24%	1.50%
19	Analysis_PE4	Polyethylene	1.5	17.5	0.0196	8.542	0.57%	-9.098	0.61%	1.67%	1.72%
20	Analysis_PE5	Polyethylene	1.5	20	0.0132	8.892	0.59%	-9.362	0.62%	2.08%	1.87%
21	Analysis_PE6	Polyethylene	1.0	10	0.1053	2.990	0.30%	-2.984	0.30%	0.34%	0.61%
22	Analysis_PE7	Polyethylene	1.0	12.5	0.0539	3.786	0.38%	-3.758	0.38%	0.61%	0.88%

Table 6.4 (continued)

SN	Analysis	Material Type	Diameter D (m)	D/t ratio	Pipe-Soil Stiffness Ratio, Sr	FEA RESULTS					
						Horizontal Elongation, Δx (mm)	Percent Deflection, Δx/D (%)	Vertical Deflection, Δy (mm)	Percent Deflection, Δy/D (%)	IOWA formula, Δy/D (%)	WATKINS Soil-Strain, Δy/D (%)
23	Analysis_PE8	Polyethylene	1.0	15	0.0312	4.392	0.44%	-4.341	0.43%	0.91%	1.10%
24	Analysis_PE9	Polyethylene	1.0	17.5	0.0196	4.852	0.49%	-4.793	0.48%	1.23%	1.27%
25	Analysis_PE10	Polyethylene	1.0	20	0.0132	5.122	0.51%	-5.045	0.50%	1.53%	1.38%
26	Analysis_PE11	Polyethylene	0.5	10	0.1053	0.912	0.18%	-0.845	0.17%	0.22%	0.39%
27	Analysis_PE12	Polyethylene	0.5	12.5	0.0539	1.120	0.22%	-1.109	0.22%	0.39%	0.57%
28	Analysis_PE13	Polyethylene	0.5	15	0.0312	1.330	0.27%	-1.306	0.26%	0.59%	0.71%
29	Analysis_PE14	Polyethylene	0.5	17.5	0.0196	1.487	0.30%	-1.450	0.29%	0.79%	0.81%
30	Analysis_PE15	Polyethylene	0.5	20	0.0132	1.602	0.32%	-1.551	0.31%	0.99%	0.89%
31	Analysis_DI1	Ductile Iron	1.5	40	0.3290	3.272	0.22%	-3.263	0.22%	0.16%	0.35%
32	Analysis_DI2	Ductile Iron	1.5	55	0.1266	5.224	0.35%	-5.162	0.34%	0.40%	0.73%
33	Analysis_DI3	Ductile Iron	1.5	70	0.0614	6.790	0.45%	-6.668	0.44%	0.74%	1.12%
34	Analysis_DI4	Ductile Iron	1.5	85	0.0343	7.930	0.53%	-7.762	0.52%	1.16%	1.45%
35	Analysis_DI5	Ductile Iron	1.5	100	0.0211	8.740	0.58%	-8.061	0.54%	1.61%	1.69%
36	Analysis_DI6	Ductile Iron	1.0	40	0.3290	1.778	0.18%	-1.766	0.18%	0.12%	0.26%
37	Analysis_DI7	Ductile Iron	1.0	55	0.1266	2.910	0.29%	-2.863	0.29%	0.29%	0.54%
38	Analysis_DI8	Ductile Iron	1.0	70	0.0614	3.822	0.38%	-3.728	0.37%	0.55%	0.83%
39	Analysis_DI9	Ductile Iron	1.0	85	0.0343	4.456	0.45%	-4.311	0.43%	0.86%	1.07%
40	Analysis_DI10	Ductile Iron	1.0	100	0.0211	4.912	0.49%	-4.725	0.47%	1.18%	1.24%
41	Analysis_DI11	Ductile Iron	0.5	40	0.3290	0.460	0.09%	-0.455	0.09%	0.08%	0.16%
42	Analysis_DI12	Ductile Iron	0.5	55	0.1266	0.816	0.16%	-0.802	0.16%	0.19%	0.34%
43	Analysis_DI13	Ductile Iron	0.5	70	0.0614	1.121	0.22%	-1.090	0.22%	0.35%	0.53%
44	Analysis_DI14	Ductile Iron	0.5	85	0.0343	1.353	0.27%	-1.301	0.26%	0.55%	0.69%
45	Analysis_DI15	Ductile Iron	0.5	100	0.0211	1.521	0.30%	-1.448	0.29%	0.76%	0.80%

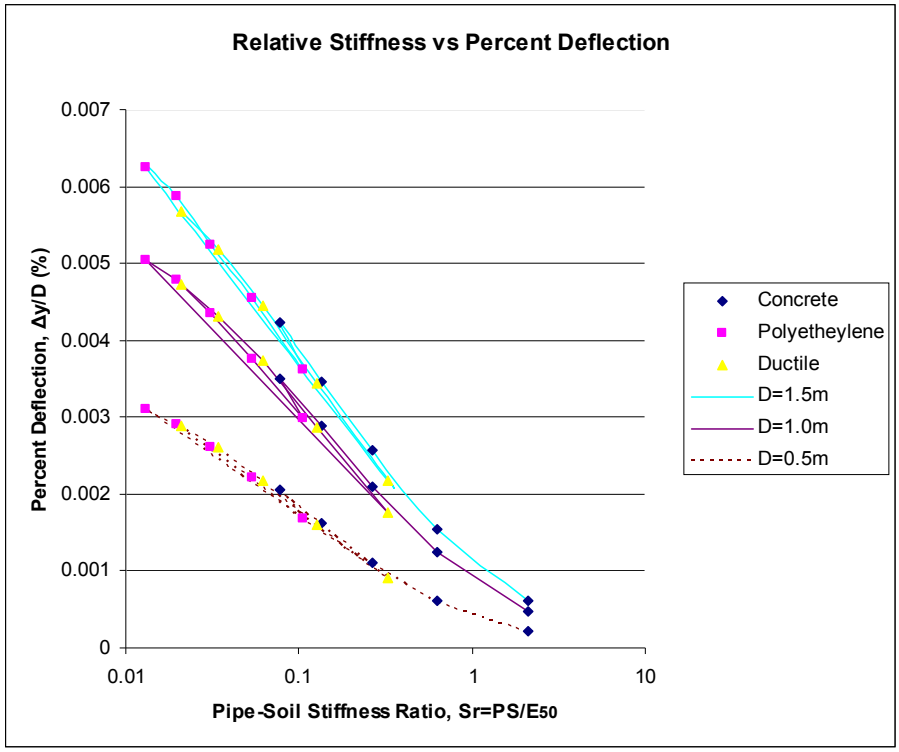

Figure 6.6 Relative Stiffness vs Percent Deflection (for all pipe types and diameters)_Model 2

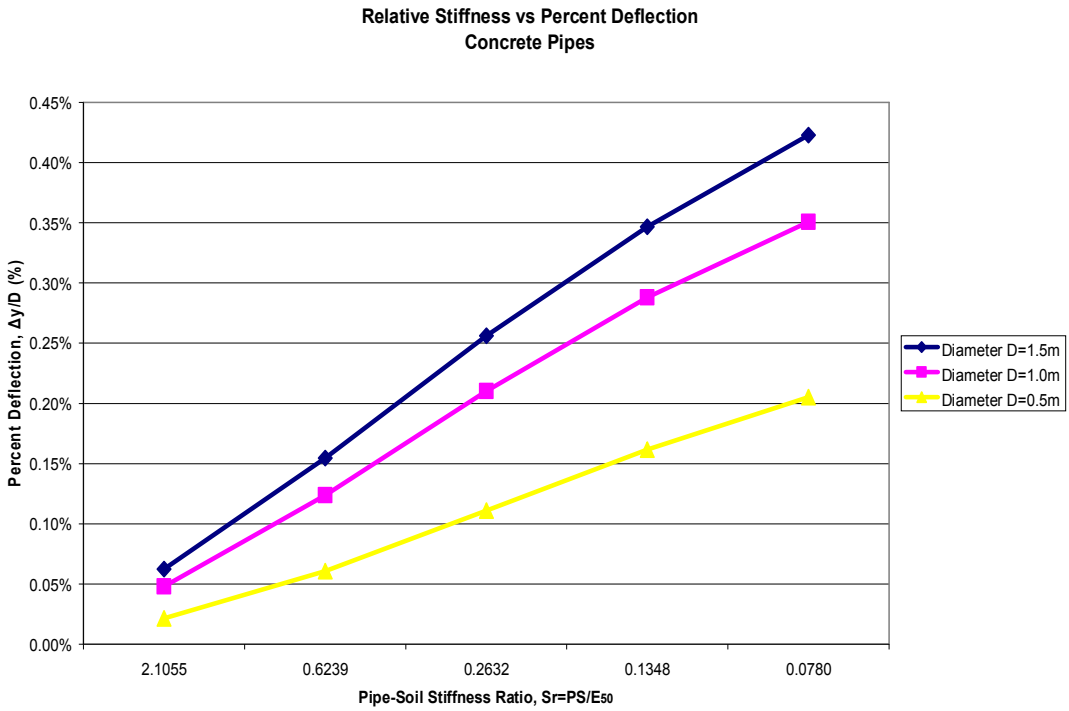

Figure 6.7 Relative Stiffness vs Percent Deflection (Concrete Pipes)_Model 2

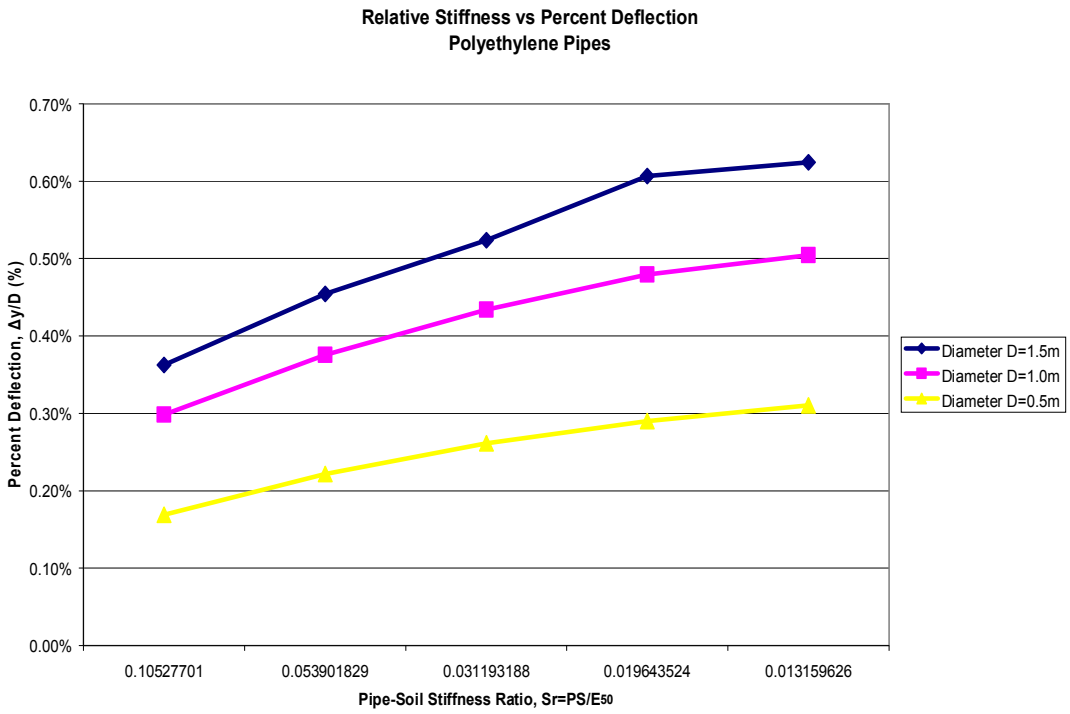

Figure 6.8 Relative Stiffness vs Percent Deflection (PE Pipes)_Model 2

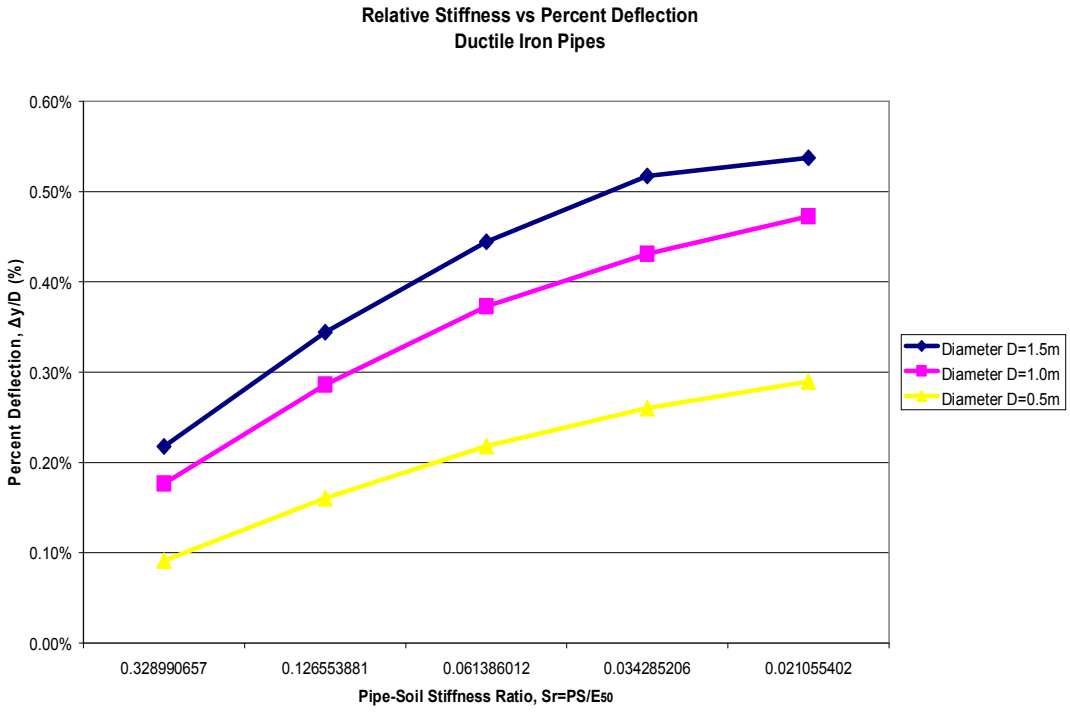

Figure 6.9 Relative Stiffness vs Percent Deflection (DI Pipes)_Model 2

6.1.2 Conventional Results and Discussion

The deflection results from modified Iowa formula of Watkins are essential as the modulus of soil reaction, E' which is the subject matter in this study is defined in the Iowa formula. The parameters used in the modified Iowa formula for the cases dealt within this study are:

$$\Delta x/D = D_l PK/(EI/r^3 + 0.06l\,E')$$

- D_l : 1.0 (Deflection lag factor)
- P=γH: Prism load, 36.81 kPa (D=1.5m); 18.40 kPa (D=1.0m); 6.13 kPA (D=0.5m) for Model 1.
- K : 0.1 (Bedding constant)
- EI : As previously tabulated in Tables 5.4 to 5.12 for each trench-pipe case.
- r^3 : for r=0.75 m, 0.5m and 0.25m
- E' : 1400 kPa (Howards, 1977)
- Δx/ Δy : 0.913 (Spangler, 1941)

The conventional results of Iowa formula tabulated in Table 6.2 are compared to those of finite element analyses for Model 1 in below Figures 6.10, 6.11 and 6.12 which are again demonstrating the change of percent deflections with respect to the pipe-soil stiffness ratio. In the application of modified Iowa formula, the modulus of soil reaction, E' value was taken 1.4 MPa as proposed by Howard.

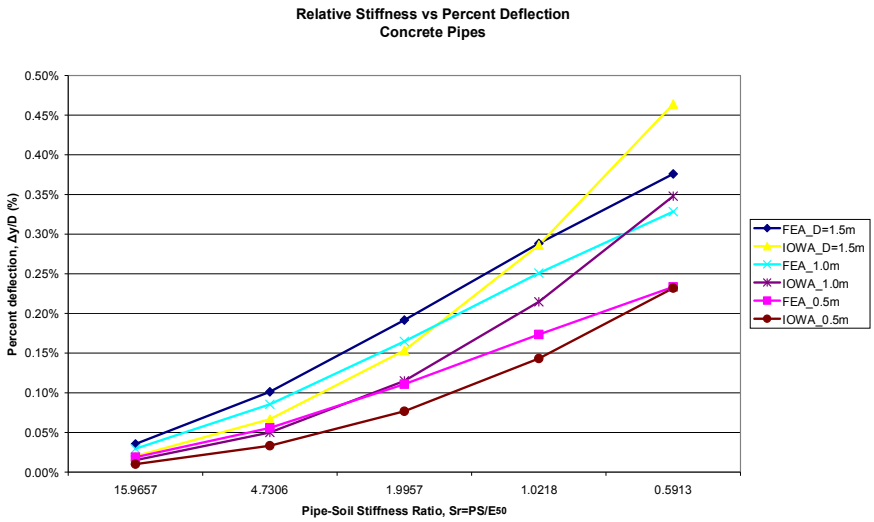

Figure 6.10 Comparison of FEA and Conventional results - Relative Stiffness vs Percent Deflection (Concrete Pipes)_Model 1

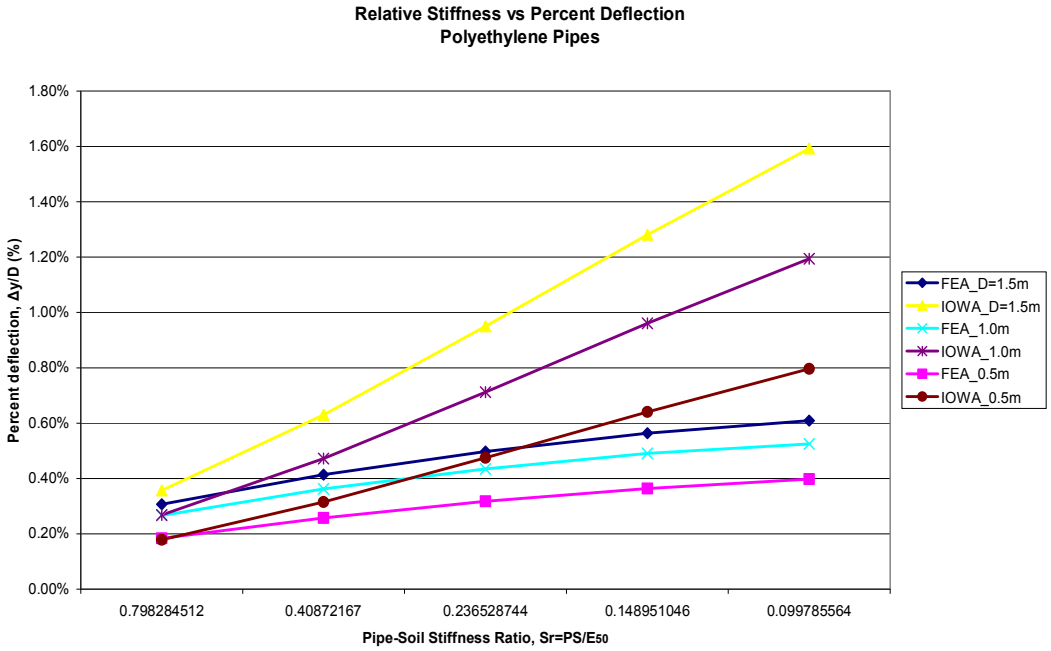

Figure 6.11 Comparison of FEA and Conventional results - Relative Stiffness vs Percent Deflection (Polyethylene Pipes)_Model 1

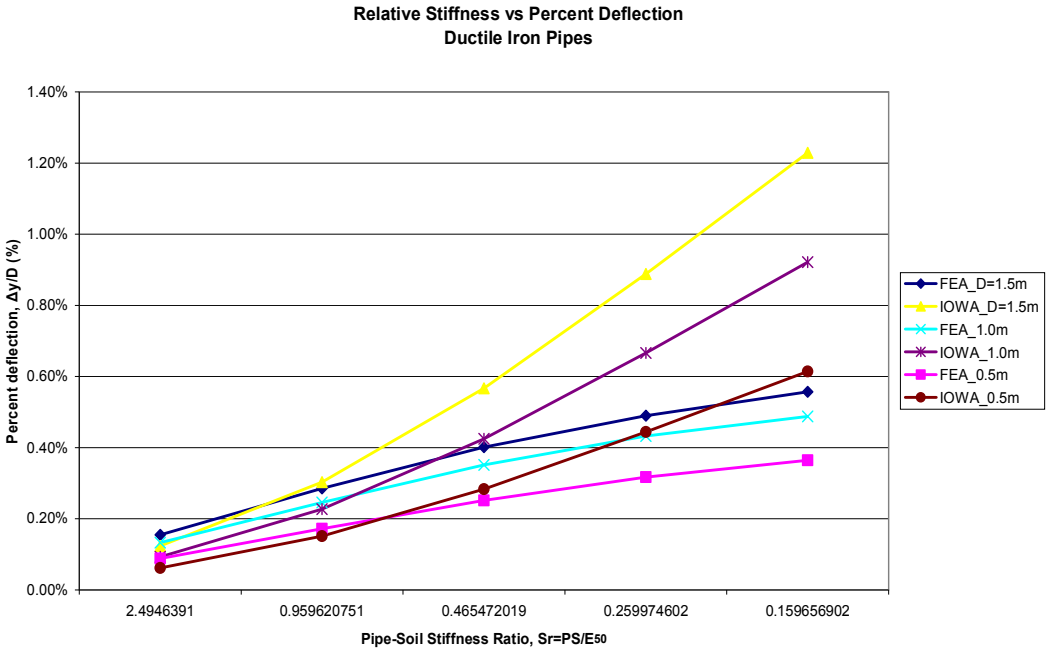

Figure 6.12 Comparison of FEA and Conventional results - Relative Stiffness vs Percent Deflection (Ductile Iron Pipes)_Model 1

In case of the concrete pipes, when the deflection curves obtained from the results of FEA and the modified Iowa formula are compared, it is observed that the Iowa formula initially predicts smaller deflections compared to that of the FEM at higher degrees of pipe-soil stiffness ratio. As the relative stiffness decreases, percent deflection curves predicted by the Iowa formula tend to have an increasing slope and intersect the FEM curve at a lower degree of relative stiffness. After the intersection point corresponding to the pipe-soil stiffness ratio where the two methods predict the same deflections is reached, the deflection estimates from the Iowa formula become greater than that of FEM estimates with an increasing rate as the relative stiffness decreases (pipes become more flexible). When the intersection points of the curves are checked, it is observed that the curves intersect at a higher stiffness ratio for larger diameter pipes. In the current analyses for concrete pipes, the curves intersect around the stiffness ratio values of 1.05, 0.75 and 0.58 for diameters D=1.5m, 1.0m and 0.5m respectively.

When the same is checked for the polyethylene pipes, it is observed that the curves obtained from Iowa formula are more of a linear type. Again, the Iowa curves which initially predict smaller deflections have greater slopes than the FEM curves (increases with a higher rate) and intersect the FEM curves close to the highest relative stiffness levels only (within the stiffness range analysed). Once the curves intersect each other, the Iowa formula starts to estimate greater deflections than that of FEM with an increasing rate at lower degrees of relative stiffness (as the pipes become more flexible). The values of pipe-soil stiffness ratios corresponding to the intersection points of curves and where the deflection predictions of the Iowa formula equals to that of the FEM are 0.79 and 0.75 for diameters D=1.0m and 0.5m respectively. The curves do not intersect for D=1.5m in the range of relative stiffness analysed in this study; however it is obvious that the curves crosses at a higher relative stiffness value.

The deflection curves obtained for ductile iron pipes present behaviour in between concrete and polyethylene pipes. The slopes of the Iowa curves increases slightly as the relative stiffness decreases and the intersection points are shifted to a lower stiffness ratio. Similarly, the deflection predictions of Iowa formula are smaller

than that of the FEM for a relative stiffness higher than the intersection value and they are greater for a relative stiffness lower than the intersection value.

As a general comment, it can be concluded that the conventional results obtained from Iowa formula are sensitive to the pipe material type and pipe size. It is observed in all cases that the Iowa formula which initially predicts smaller deflections than that of FEM tends to overestimate the deflections with an increasing rate at lower degrees of relative stiffness. This implies that the Iowa formula gives more compatible results with FEM in case of relatively stiffer pipes. For more flexible pipes, the use of deflection predictions from Iowa formula yields conservative results. When the pipe size is considered, it is again observed in all cases that as the pipe diameter increases the Iowa formula tends to start overestimating the deflections at a higher pipe-soil stiffness ratio. This can be interpreted that the flexibility of pipes are more pronounced for larger diameters and the use of estimates from Iowa formula yields conservative results for a greater range of relative stiffness.

In addition to Iowa formula, the deflection predictions from the results of Watkins-soil strain theory are tabulated in Table 6.2 for comparison purposes. The importance of Watkins soil strain theory is that it expresses the deflection in terms of the Stiffness Ratio, R_s (This is the ratio of soil stiffness E_s to pipe-ring stiffness EI/D^3). As the major concern in this study is the effect of pipe-soil relative stiffness, it is worth giving the results from Watkins' soil strain theory. The parameters are as follows:

$$\frac{\Delta y}{D\varepsilon} = \frac{R_s}{30 + R_s}$$

R_s : Stiffness ratio, $R_s = E'/S$

S : EI/D^3 (As tabulated)

E' : 1400 kPa (Howard 1977)

ε' : Vertical soil strain, ε' = w/E'

w : Vertical soil stress above pipe

As a representative example, the results of Watkins's soil strain theory for typically flexible polyethylene pipes are plotted together with the results of Iowa formula and FEA in Figure 6.13. Within the range of relative stiffness analysed in this study, the Watkins soil strain theory predicts greater deflections compared to the

results of FEA. Similar to the case of Iowa formula, the deflection curve of Watkins theory deviates more from FEM curve as the pipe-soil stiffness ratio decreases. In case it is compared to the Iowa formula, it is observed that Watkins's soil strain theory overestimates deflections for relatively high stiffness ratios and underestimates deflections for more flexible pipes.

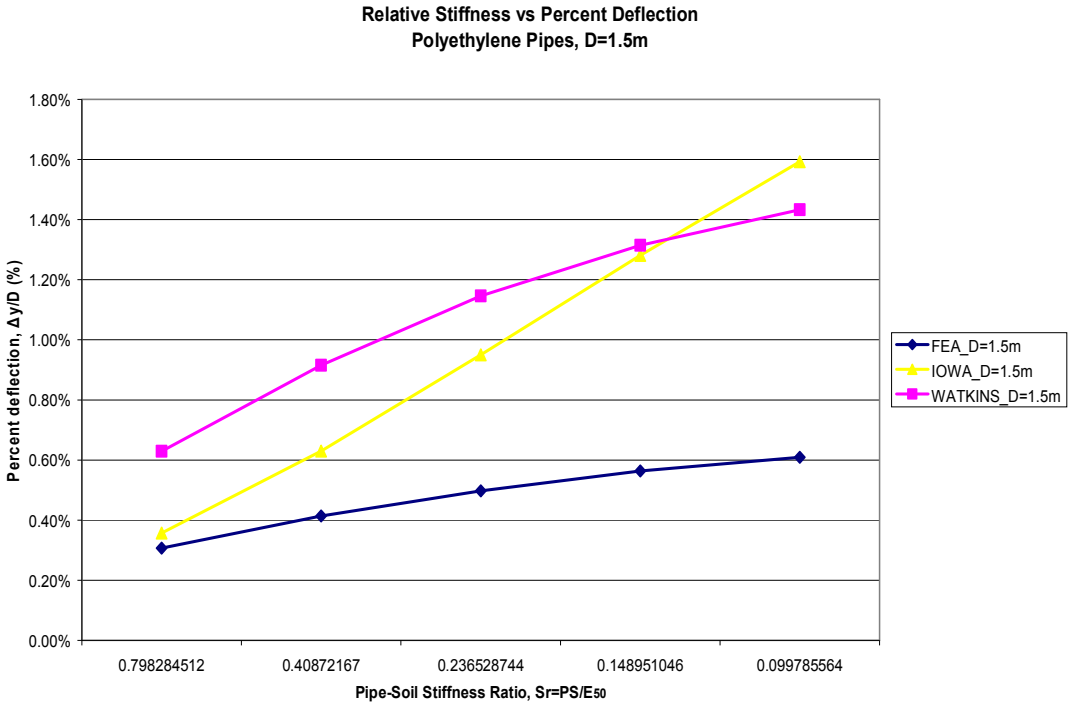

Figure 6.13 Comparison of FEA and Conventional results - Relative Stiffness vs Percent Deflection (Polyethylene Pipes)_Model 1

In Model 2 both the embedment and backfill material are assumed to be formed by basalt aggregate. Using the results yielded by conventional method as given in Table 6.4, similar figures are reproduced and it is observed that the graphical results are of same in nature as those produced for Model 1 (Figures 6.14, 6.15, 6.16 and 6.17).

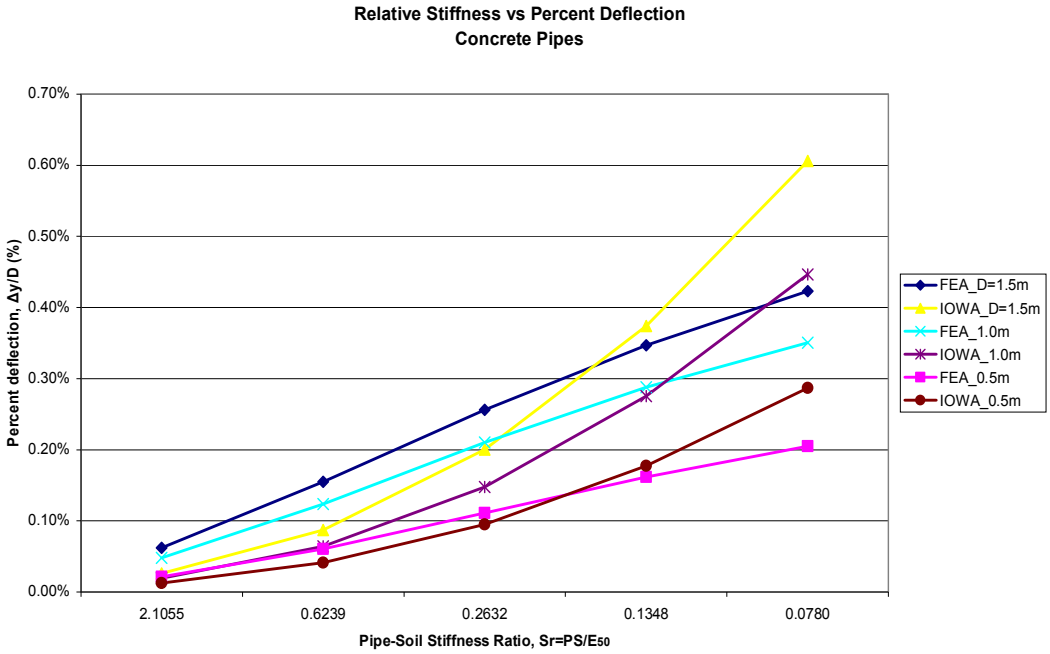

Figure 6.14 Comparison of FEA and Conventional results - Relative Stiffness vs Percent Deflection (Concrete Pipes)_Model 2

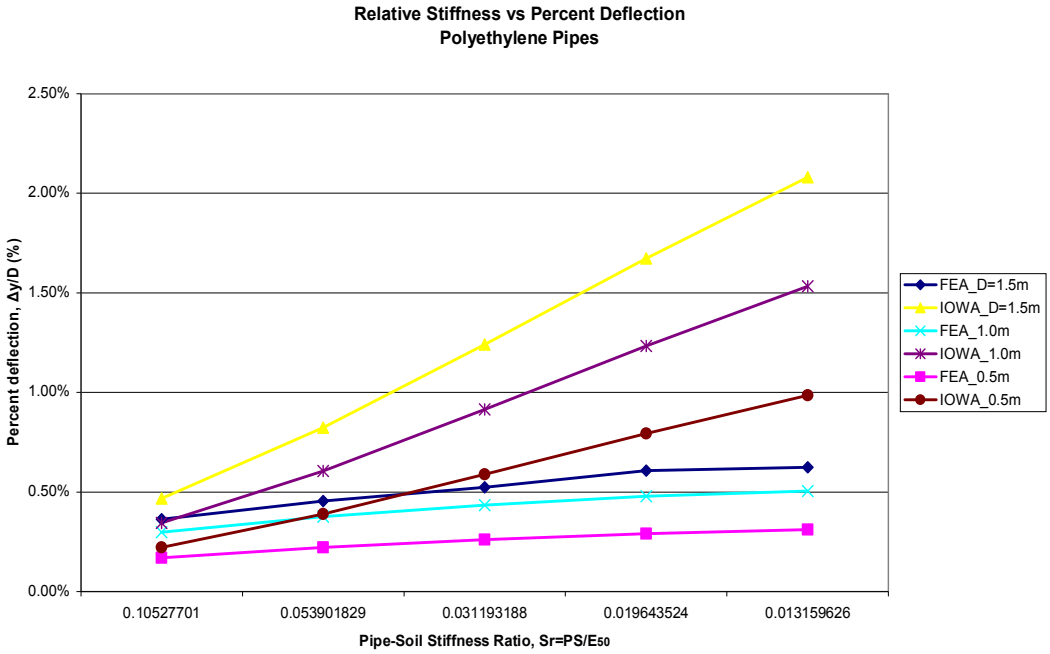

Figure 6.15 Comparison of FEA and Conventional results - Relative Stiffness vs Percent Deflection (Polyethylene Pipes) _Model 2

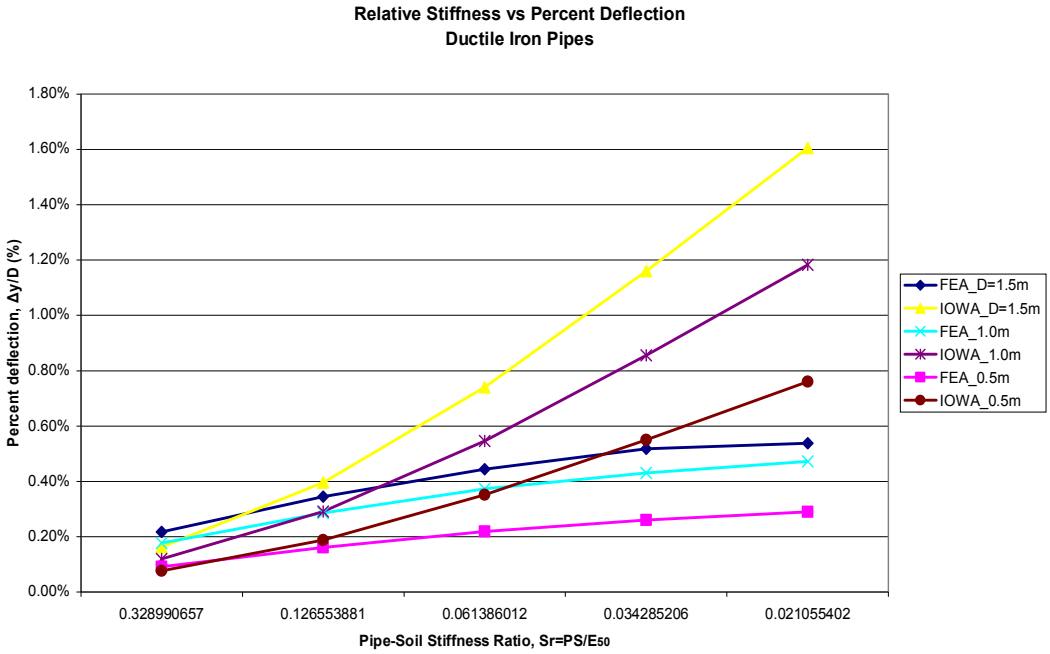

Figure 6.16 Comparison of FEA and Conventional results - Relative Stiffness vs Percent Deflection (Ductile Iron Pipes) _Model 2

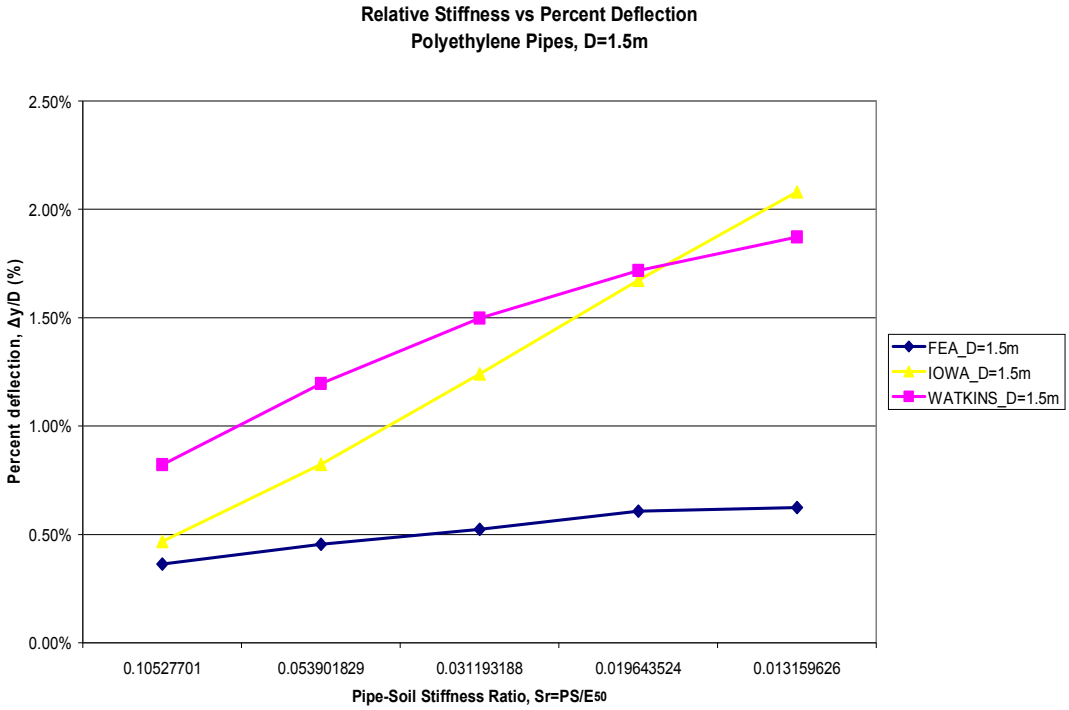

Figure 6.17 Comparison of FEA and Conventional results - Relative Stiffness vs Percent Deflection (Polyethylene Pipes) _Model 2

6.2 *Loads*

6.2.1 Numerical Results and Discussion

As noted before, in order to allow for comparison between the earth load estimates based on the conventional method and the analyses conducted using the FEM, the vertical stress at the pipe crown is used to obtain an estimate of the vertical earth load, by multiplying the stress by the pipe diameter, D.

The numerical results for earth loads on pipes range in the value of 5.142 – 45.401 kN/m for the concrete pipes, 4.359 – 39.236 kN/m for the polyethylene pipes and 4.010 – 42.873 kN/m for the ductile iron pipes (Model 1). These results which are tabulated in Table 6.5 are graphically presented with curves for each diameter and pipe type with respect to the pipe-soil stiffness ratio in Figure 6.19.

The FEA results indicate that, for a given depth of fill, the load transferred to the conduit increases with the increase in pipe wall thickness. The increase in wall thickness leads to a corresponding increase in the pipe-soil stiffness ratio. Therefore, the degree of loads transferred to pipes is higher for a case of higher relative stiffness.

Regarding the effect of pipe diameter at any given pipe-soil stiffness ratio, it is observed that the load transferred to the pipes increases with pipe diameter. This is simply due to the fact that the larger diameter pipes analysed in this study are buried in deeper levels to keep the H/B_d ratio constant. On the other side, when the loads on pipes are checked for a certain diameter, it is observed that the maximum loads are developed on relatively stiffer concrete pipes and the minimum loads are developed on relatively flexible polyethylene pipes. This is attributable to the increasing arching effect due to the higher degree of deflections around conduits with a lower degree of stiffness relative to the surrounding soil. As a result of this increased arching effect, the loads transferred to the pipes are reduced more for more flexible pipes.

When the results are rearranged in a logarithmic plot as in Figure 6.18, indicative trends with respect to the relative stiffness are observed. The various material types used in the study complement each other to form a continuous set of overlapping data, when expressed in terms of pipe-soil stiffness ratio

ranging from 0.5913 to 15.9657. The contribution of the pipe diameter is not limited to the pipe-soil stiffness ratio. Additional elements related to pipe diameter such as trench geometry, result in individual curves for each pipe size analysed. The curves are somewhat parallel, tending to flatten at high values of S_r. Such behaviour is expected given the fact that beyond a given relative stiffness between the pipe and adjacent soil, the load transfer to the pipe reaches its maximum level. The maximum load levels are observed at the minimum pipe deflections which develop at the most rigid pipes.

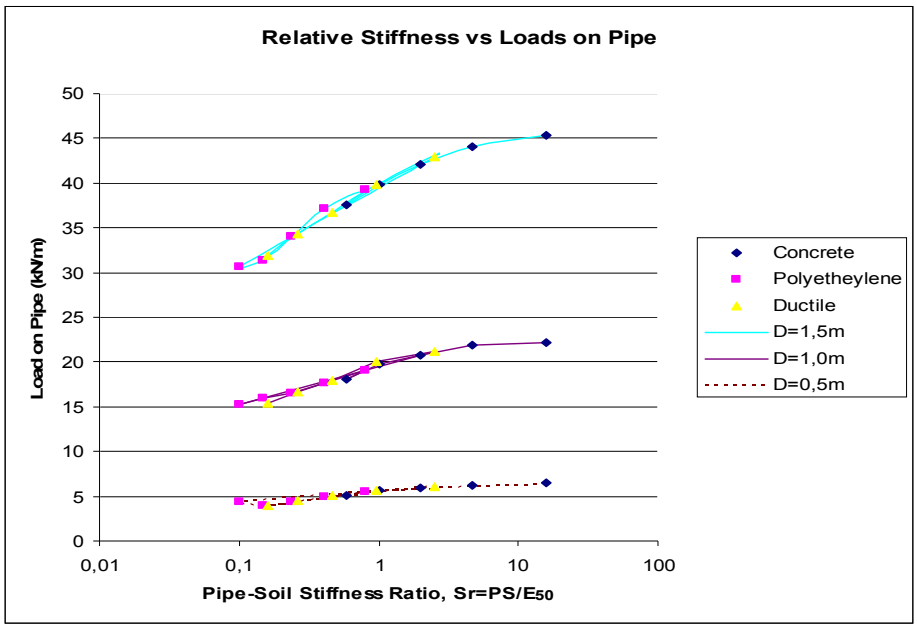

Figure 6.18 Relative Stiffness vs Loads on Pipe_Model 1

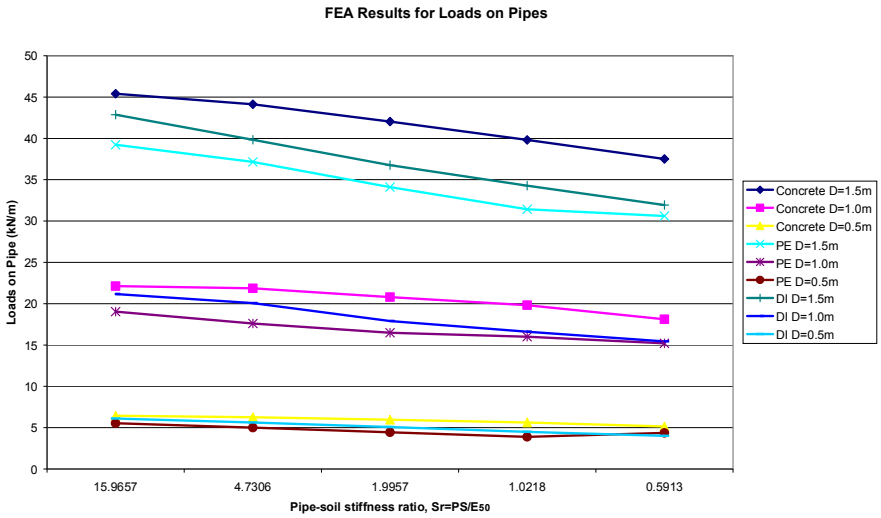

Figure 6.19 FEA Results for Loads on Pipe _Model 1

Table 6.5 FEA and Conventional Results for Loads on Pipes_Model 1

SN	Analysis	Material Type	Diameter D (m)	D/t ratio	Pipe-Soil Stiffness Ratio, Sr	FEA RESULTS	CONVENTIONAL RESULTS		
						Load on Pipe (kN/m)	Prism Load (kN/m)	Load on Rigid Pipe (kN/m)	Load on Flexible Pipe (kN/m)
1	Analysis_C1	Concrete	1.5	10	15.9657	45.401	36.806	50.170	29.724
2	Analysis_C2	Concrete	1.5	15	4.7306	44.123	36.806	50.170	29.724
3	Analysis_C3	Concrete	1.5	20	1.9957	42.041	36.806	50.170	29.724
4	Analysis_C4	Concrete	1.5	25	1.0218	39.819	36.806	50.170	29.724
5	Analysis_C5	Concrete	1.5	30	0.5913	37.514	36.806	50.170	29.724
6	Analysis_C6	Concrete	1.0	10	15.9657	22.120	18.402	27.239	14.601
7	Analysis_C7	Concrete	1.0	15	4.7306	21.858	18.402	27.239	14.601
8	Analysis_C8	Concrete	1.0	20	1.9957	20.796	18.402	27.239	14.601
9	Analysis_C9	Concrete	1.0	25	1.0218	19.826	18.402	27.239	14.601
10	Analysis_C10	Concrete	1.0	30	0.5913	18.121	18.402	27.239	14.601
11	Analysis_C11	Concrete	0.5	10	15.9657	6.435	6.134	11.257	4.693
12	Analysis_C12	Concrete	0.5	15	4.7306	6.268	6.134	11.257	4.693
13	Analysis_C13	Concrete	0.5	20	1.9957	5.961	6.134	11.257	4.693
14	Analysis_C14	Concrete	0.5	25	1.0218	5.619	6.134	11.257	4.693
15	Analysis_C15	Concrete	0.5	30	0.5913	5.142	6.134	11.257	4.693
16	Analysis_PE1	Polyethylene	1.5	10	0.7983	39.236	36.806	50.170	29.724
17	Analysis_PE2	Polyethylene	1.5	12.5	0.4087	37.155	36.806	50.170	29.724
18	Analysis_PE3	Polyethylene	1.5	15	0.2365	34.098	36.806	50.170	29.724
19	Analysis_PE4	Polyethylene	1.5	17.5	0.1490	31.421	36.806	50.170	29.724
20	Analysis_PE5	Polyethylene	1.5	20	0.0998	30.609	36.806	50.170	29.724
21	Analysis_PE6	Polyethylene	1.0	10	0.7983	19.044	18.402	27.239	14.601
22	Analysis_PE7	Polyethylene	1.0	12.5	0.4087	17.605	18.402	27.239	14.601

Table 6.5 (continued)

SN	Analysis	Material Type	Diameter D (m)	D/t ratio	Pipe-Soil Stiffness Ratio, Sr	FEA RESULTS	CONVENTIONAL RESULTS		
						Load on Pipe (kN/m)	Prism Load (kN/m)	Load on Rigid Pipe (kN/m)	Load on Flexible Pipe (kN/m)
23	Analysis_PE8	Polyethylene	1.0	15	0.2365	16.482	18.402	27.239	14.601
24	Analysis_PE9	Polyethylene	1.0	17.5	0.1490	16.006	18.402	27.239	14.601
25	Analysis_PE10	Polyethylene	1.0	20	0.0998	15.210	18.402	27.239	14.601
26	Analysis_PE11	Polyethylene	0.5	10	0.7983	5.531	6.134	11.257	4.693
27	Analysis_PE12	Polyethylene	0.5	12.5	0.4087	4.996	6.134	11.257	4.693
28	Analysis_PE13	Polyethylene	0.5	15	0.2365	4.429	6.134	11.257	4.693
29	Analysis_PE14	Polyethylene	0.5	17.5	0.1490	3.891	6.134	11.257	4.693
30	Analysis_PE15	Polyethylene	0.5	20	0.0998	4.359	6.134	11.257	4.693
31	Analysis_DI1	Ductile Iron	1.5	40	2.4946	42.873	36.806	50.170	29.724
32	Analysis_DI2	Ductile Iron	1.5	55	0.9596	39.830	36.806	50.170	29.724
33	Analysis_DI3	Ductile Iron	1.5	70	0.4655	36.768	36.806	50.170	29.724
34	Analysis_DI4	Ductile Iron	1.5	85	0.2600	34.289	36.806	50.170	29.724
35	Analysis_DI5	Ductile Iron	1.5	100	0.1597	31.935	36.806	50.170	29.724
36	Analysis_DI6	Ductile Iron	1.0	40	2.4946	21.169	18.402	27.239	14.601
37	Analysis_DI7	Ductile Iron	1.0	55	0.9596	20.065	18.402	27.239	14.601
38	Analysis_DI8	Ductile Iron	1.0	70	0.4655	17.901	18.402	27.239	14.601
39	Analysis_DI9	Ductile Iron	1.0	85	0.2600	16.616	18.402	27.239	14.601
40	Analysis_DI10	Ductile Iron	1.0	100	0.1597	15.445	18.402	27.239	14.601
41	Analysis_DI11	Ductile Iron	0.5	40	2.4946	6.098	6.134	11.257	4.693
42	Analysis_DI12	Ductile Iron	0.5	55	0.9596	5.627	6.134	11.257	4.693
43	Analysis_DI13	Ductile Iron	0.5	70	0.4655	5.080	6.134	11.257	4.693
44	Analysis_DI14	Ductile Iron	0.5	85	0.2600	4.491	6.134	11.257	4.693
45	Analysis_DI15	Ductile Iron	0.5	100	0.1597	4.000	6.134	11.257	4.693

In addition to above results and discussion for Model 1, the numerical and conventional results are tabulated in Table 6.6 for Model 2. Again, when the results are rearranged in a logarithmic plot as in Figure 6.20, indicative trends with respect to the relative stiffness are observed. Similarly, different types of pipe materials used in the study complement each other to form a continuous set of overlapping data with the difference that pipe-soil stiffness ratio ranges at a different interval (0.013 to 2.105). The continuous set of data produces three individual curves corresponding to each diameter and the indicative trends presented by these curves are in similar nature to those of Model 1.

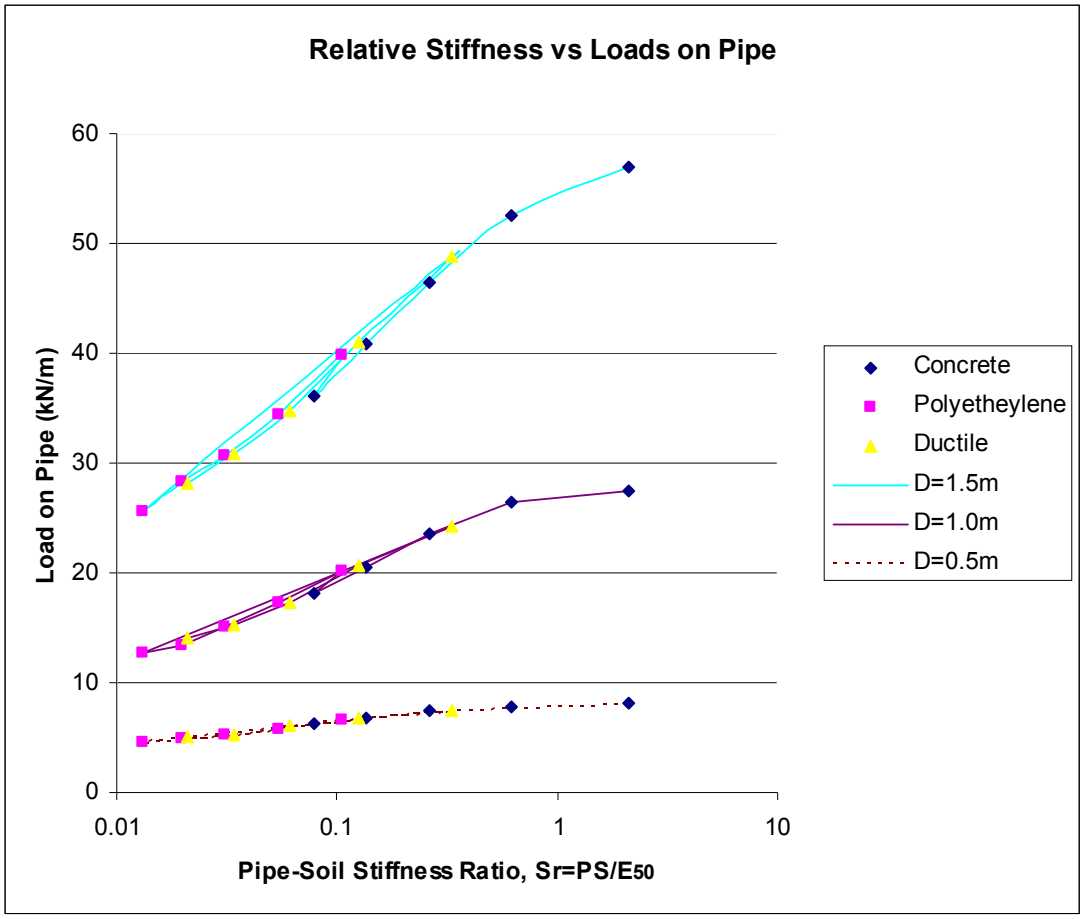

Figure 6.20 Relative Stiffness vs Loads on Pipe_Model 2

Table 6.6 FEA and Conventional Results for Loads on Pipes_Model 2

SN	Analysis	Material Type	Diameter D (m)	D/t ratio	Pipe-Soil Stiffness Ratio, Sr	FEA RESULTS	CONVENTIONAL RESULTS		
						Load on Pipe (kN/m)	Prism Load (kN/m)	Load on Rigid Pipe (kN/m)	Load on Flexible Pipe (kN/m)
1	Analysis_C1	Concrete	1.5	10	2.1055	56.985	48.080	51.766	40.868
2	Analysis_C2	Concrete	1.5	15	0.6239	52.545	48.080	51.766	40.868
3	Analysis_C3	Concrete	1.5	20	0.2632	46.400	48.080	51.766	40.868
4	Analysis_C4	Concrete	1.5	25	0.1348	40.874	48.080	51.766	40.868
5	Analysis_C5	Concrete	1.5	30	0.0780	36.117	48.080	51.766	40.868
6	Analysis_C6	Concrete	1.0	10	2.1055	27.466	23.618	28.105	20.075
7	Analysis_C7	Concrete	1.0	15	0.6239	26.368	23.618	28.105	20.075
8	Analysis_C8	Concrete	1.0	20	0.2632	23.503	23.618	28.105	20.075
9	Analysis_C9	Concrete	1.0	25	0.1348	20.465	23.618	28.105	20.075
10	Analysis_C10	Concrete	1.0	30	0.0780	18.131	23.618	28.105	20.075
11	Analysis_C11	Concrete	0.5	10	2.1055	8.067	7.592	11.615	6.453
12	Analysis_C12	Concrete	0.5	15	0.6239	7.729	7.592	11.615	6.453
13	Analysis_C13	Concrete	0.5	20	0.2632	7.391	7.592	11.615	6.453
14	Analysis_C14	Concrete	0.5	25	0.1348	6.779	7.592	11.615	6.453
15	Analysis_C15	Concrete	0.5	30	0.0780	6.190	7.592	11.615	6.453
16	Analysis_PE1	Polyethylene	1.5	10	0.1053	39.905	48.080	51.766	40.868
17	Analysis_PE2	Polyethylene	1.5	12.5	0.0539	34.388	48.080	51.766	40.868
18	Analysis_PE3	Polyethylene	1.5	15	0.0312	30.623	48.080	51.766	40.868
19	Analysis_PE4	Polyethylene	1.5	17.5	0.0196	28.328	48.080	51.766	40.868
20	Analysis_PE5	Polyethylene	1.5	20	0.0132	25.609	48.080	51.766	40.868
21	Analysis_PE6	Polyethylene	1.0	10	0.1053	20.151	23.618	28.105	20.075
22	Analysis_PE7	Polyethylene	1.0	12.5	0.0539	17.237	23.618	28.105	20.075

Table 6.6 (continued)

SN	Analysis	Material Type	Diameter D (m)	D/t ratio	Pipe-Soil Stiffness Ratio, Sr	FEA RESULTS	CONVENTIONAL RESULTS		
						Load on Pipe (kN/m)	Prism Load (kN/m)	Load on Rigid Pipe (kN/m)	Load on Flexible Pipe (kN/m)
23	Analysis_PE8	Polyethylene	1.0	15	0.0312	15.086	23.618	28.105	20.075
24	Analysis_PE9	Polyethylene	1.0	17.5	0.0196	13.420	23.618	28.105	20.075
25	Analysis_PE10	Polyethylene	1.0	20	0.0132	12.661	23.618	28.105	20.075
26	Analysis_PE11	Polyethylene	0.5	10	0.1053	6.657	7.592	11.615	6.453
27	Analysis_PE12	Polyethylene	0.5	12.5	0.0539	5.797	7.592	11.615	6.453
28	Analysis_PE13	Polyethylene	0.5	15	0.0312	5.242	7.592	11.615	6.453
29	Analysis_PE14	Polyethylene	0.5	17.5	0.0196	4.944	7.592	11.615	6.453
30	Analysis_PE15	Polyethylene	0.5	20	0.0132	4.541	7.592	11.615	6.453
31	Analysis_DI1	Ductile Iron	1.5	40	0.3290	48.896	48.080	51.766	40.868
32	Analysis_DI2	Ductile Iron	1.5	55	0.1266	41.028	48.080	51.766	40.868
33	Analysis_DI3	Ductile Iron	1.5	70	0.0614	34.709	48.080	51.766	40.868
34	Analysis_DI4	Ductile Iron	1.5	85	0.0343	30.858	48.080	51.766	40.868
35	Analysis_DI5	Ductile Iron	1.5	100	0.0211	28.194	48.080	51.766	40.868
36	Analysis_DI6	Ductile Iron	1.0	40	0.3290	24.313	23.618	28.105	20.075
37	Analysis_DI7	Ductile Iron	1.0	55	0.1266	20.651	23.618	28.105	20.075
38	Analysis_DI8	Ductile Iron	1.0	70	0.0614	17.325	23.618	28.105	20.075
39	Analysis_DI9	Ductile Iron	1.0	85	0.0343	15.234	23.618	28.105	20.075
40	Analysis_DI10	Ductile Iron	1.0	100	0.0211	14.135	23.618	28.105	20.075
41	Analysis_DI11	Ductile Iron	0.5	40	0.3290	7.453	7.592	11.615	6.453
42	Analysis_DI12	Ductile Iron	0.5	55	0.1266	6.699	7.592	11.615	6.453
43	Analysis_DI13	Ductile Iron	0.5	70	0.0614	6.128	7.592	11.615	6.453
44	Analysis_DI14	Ductile Iron	0.5	85	0.0343	5.308	7.592	11.615	6.453
45	Analysis_DI15	Ductile Iron	0.5	100	0.0211	5.006	7.592	11.615	6.453

6.2.2 Conventional Results and Discussion

As explained previously, the Marston load theory is based on the concept of a prism of soil in the trench that imposes a load on the pipe. The weight of the soil prism (prism load) is found to be the pipe outside diameter times the height of earth above the pipe times the unit weight of the earth. However, due to the arching effect, the load on a buried pipe is reduced and is not exactly equal to the prism load. As per the Marston's theory, the loads developed on rigid and flexible pipe cases can be determined individually.

Prism Load: $P = \gamma \times H \times D$

Load on Rigid Pipe: $W_d = C_d \times \gamma \times B_d^{\,2}$

Load on Flexible Pipe: $W_c = C_d \times \gamma \times B_d \times B_c$

Parameters used in previously defined above equations (Eq.2.2 and .Eq.2.3) are as follows:

γ : Unit weight (kN/m3); 12.27 kN/m3 (kanto loam); 16.35 kN/m3 (crushed stone) for Model 1.

H : 1.9m (for D=1.5m); 1.4m (for D=1.0m); 0.9m (for D=0.5m)

B_d : 1.9m (for D=1.5m); 1.4m (for D=1.0m); 0.9m (for D=0.5m)

B_c : D=1.5m; D=1.0m; D=0.5m

C_d : 0.85 for H/B_d =1

The conventional results which are tabulated together with the FEA results in Table 6.5 are graphically presented with respect to the pipe-soil stiffness ratio in Figures 6.21, 6.22 and 6.23 for comparison purposes. As an expected result, the conventional methods do not account for the effect of pipe wall thickness (*D/t* ratio) which is related to the pipe stiffness as the earth load results are constant at a given depth. Therefore, regardless of the pipe-soil stiffness ratio, the conventional load estimates for rigid and flexible pipes for a given pipe diameter are individually constant.

When the curves obtained using the finite element methodology are compared to the load predictions based on the conventional method for rigid and flexible pipes respectively, it is concluded that: the values from rigid pipe analyses at any given depth of burial are always greater than those calculated using the FEA and the values from flexible pipe analyses under-predict the load on pipes for certain ranges of pipe-soil stiffness ratio and over-predicts the loads for others. As an example, in Figures 6.24, 6.25 and 6.26 for D=0.5m, the conventional method for flexible pipes result a value of 4.69 kN/m, whereas values from the FEA are consistently lower for polyethylene and ductile iron pipes below the pipe-soil stiffness ratios of approximately 0.30 and 0.33 respectively. For higher stiffness ratios, FEA results for the whole material types are consistently higher than the conventional load estimates for flexible pipes.

As stated above, the conventional rigid conduit analysis appears to always yield conservative results, with the values of loads consistently greater that the values obtained through FEA. Among the three types of materials, the results of Concrete pipes are closer to the load predictions of conventional method for rigid pipes as an expected result.

Ductile Iron pipes represent an intermediate case between Concrete and Polyethylene pipes in terms of the loads transferred to the pipes. This result is expected given the resulting intermediate stiffness.

The suggested vertical load estimates based on the conventional method for flexible pipe are close to those obtained using the FEA for Polyethylene and Ductile Iron pipes.

The limitations of using the conventional approach, which only accounts for the pipe stiffness in terms of either rigid or flexible, are evident in figures presented. When compared with the results obtained using the finite element models, for equal pipe-soil stiffness ratios, it is clear that for the case of rigid pipes, the conventional approach significantly overestimates the transferred earth loads, whereas it produces more reasonable results for flexible conduits. More rigid concrete pipes appear to have loads near or greater than the prism

load for results obtained using the FEA and conventional approach respectively. In contrast, the more flexible Polyethylene pipes appear to redistribute portions of the earth loads to the surrounding soil with the effect of arching.

When the results for a given pipe-soil stiffness ratio are checked for the effect of pipe diameter, it is observed that the FEA results tend to approach to those of conventional flexible pipe analyses in case of smaller diameters. This may be interpreted as the conventional method for flexible pipes predicts the results more in agreement with FEM results in case of small diameters compared to the greater diameter pipes.

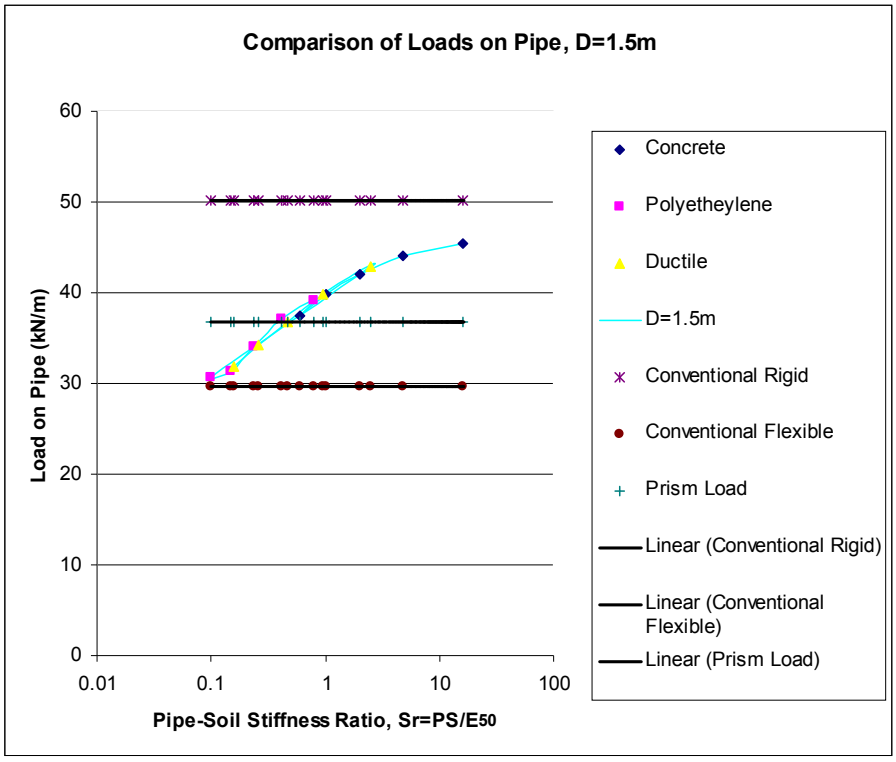

Figure 6.21 Comparison of Loads on Pipe, D=1.5m_Model 1

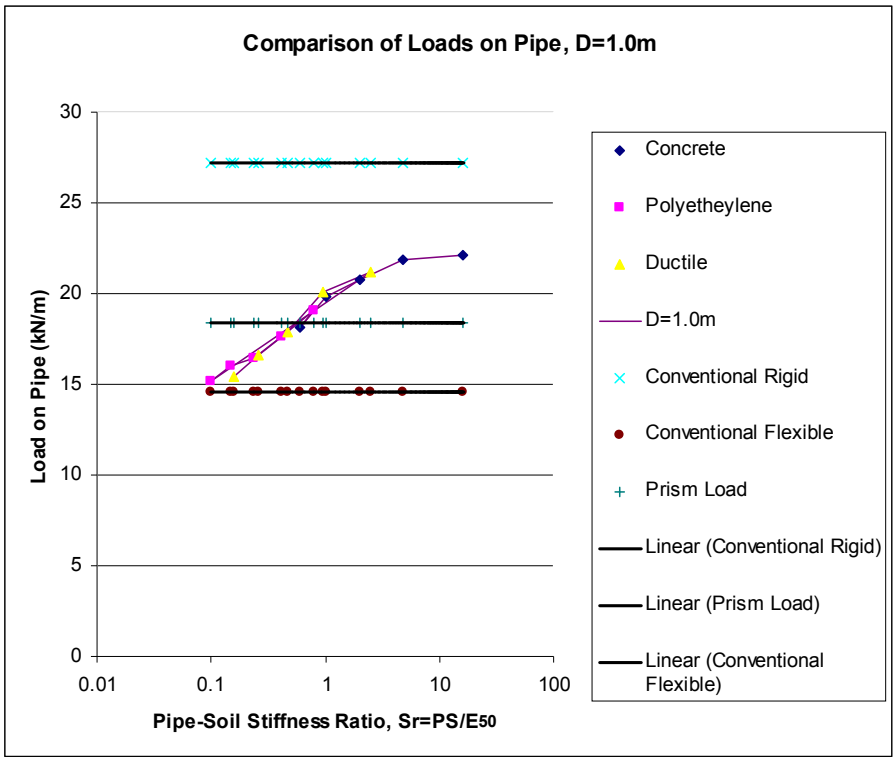

Figure 6.22 Comparison of Loads on Pipes, D=1.0m_Model 1

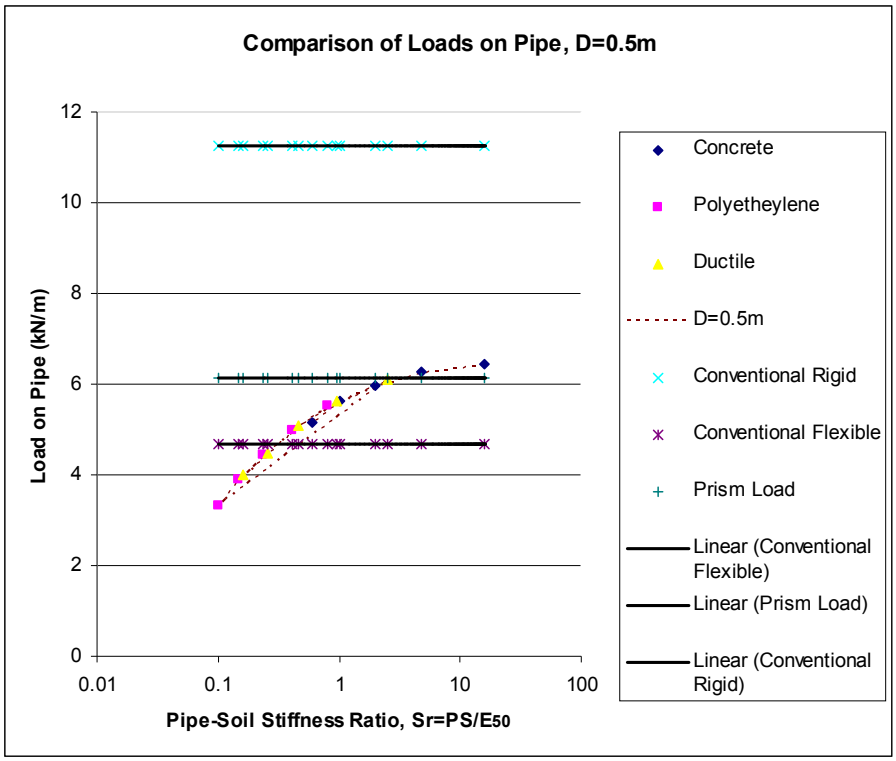

Figure 6.23 Comparison of Loads on Pipes, D=0.5m_Model 1

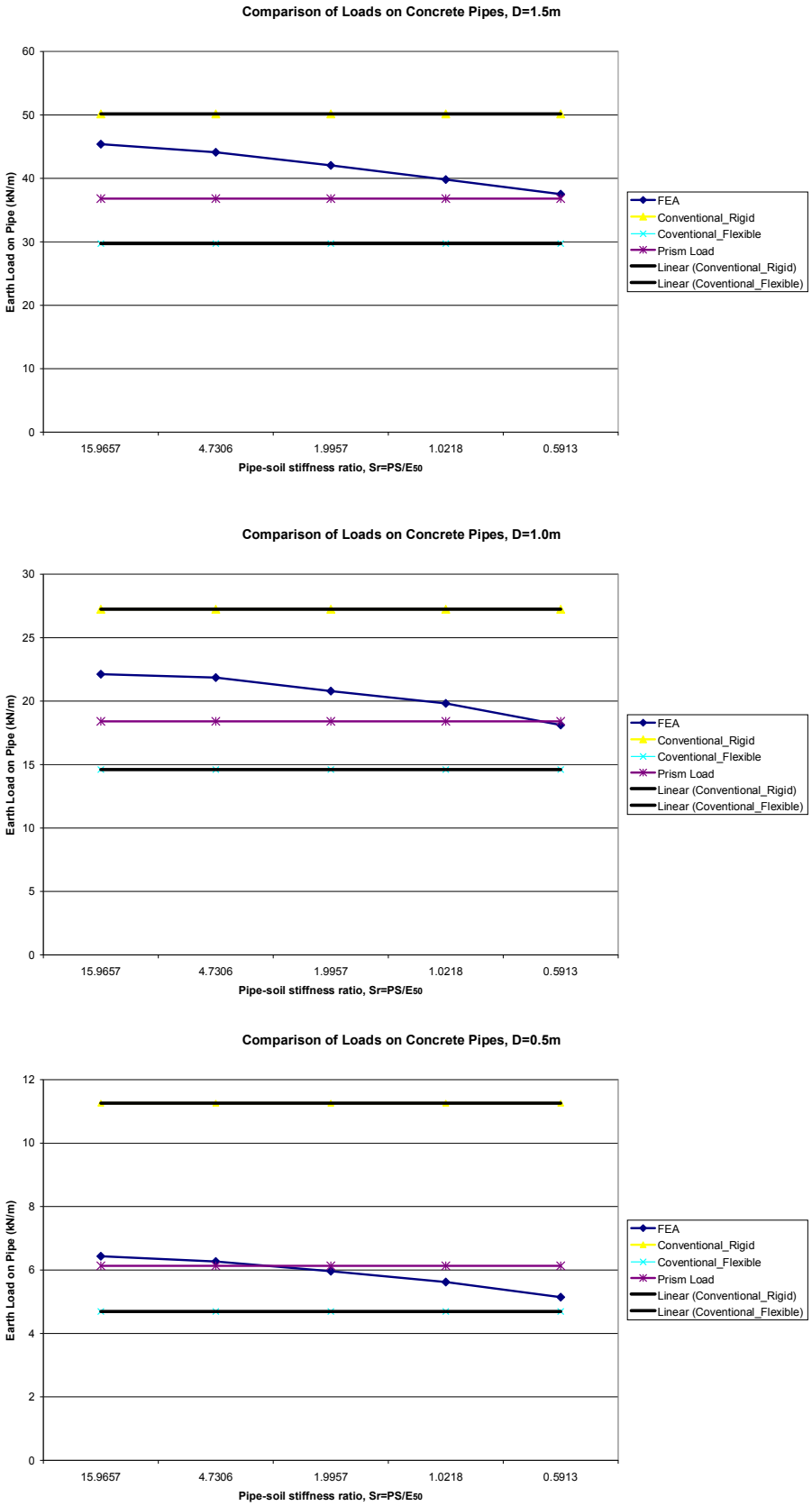

Figure 6.24 Comparison of Loads on Concrete Pipes (D=1.5m, 1.0m, 0.5m respec.) _Model 1

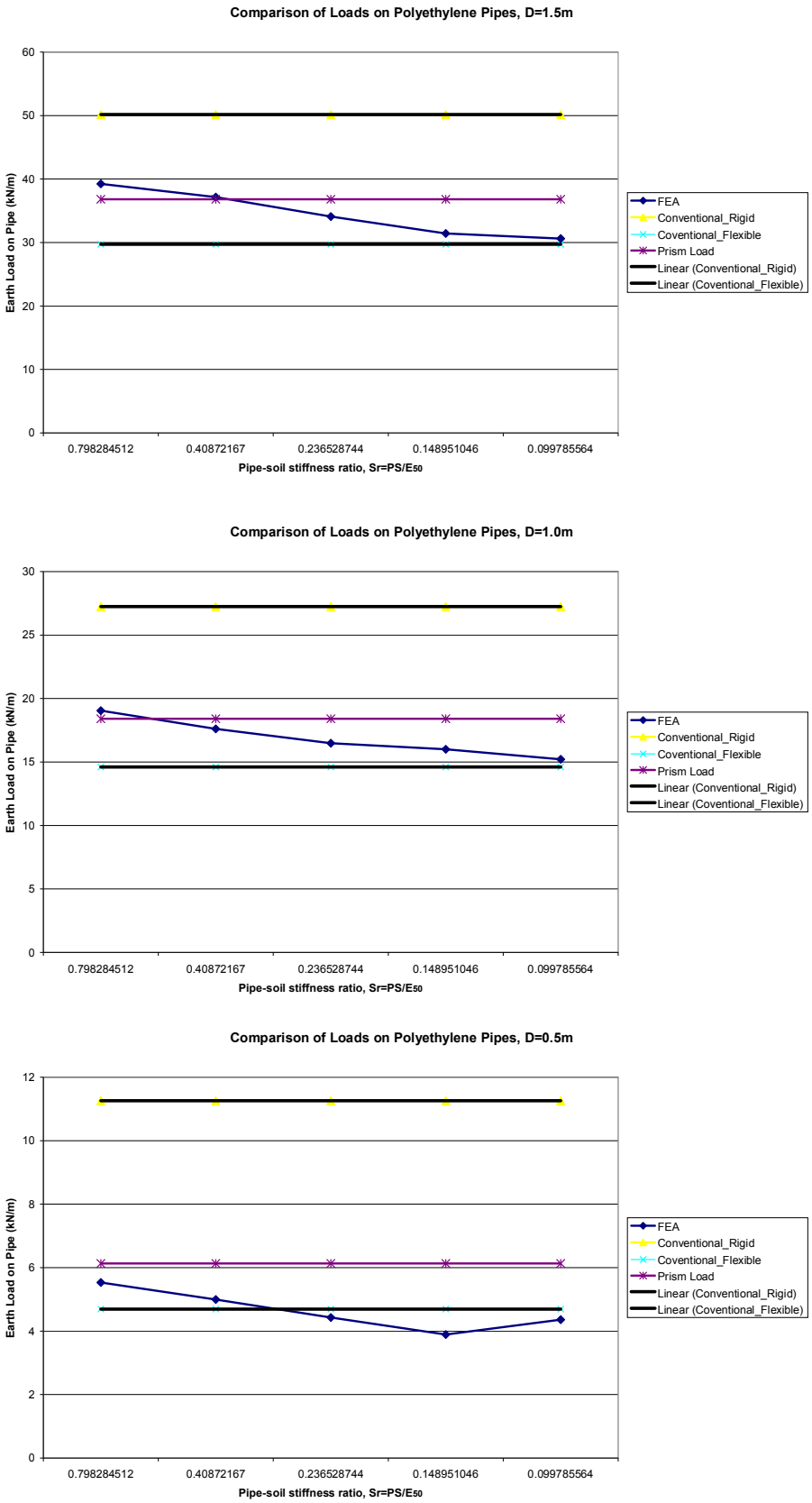

Figure 6.25 Comparison of Loads on PE Pipes (D=1.5m, 1.0m, 0.5m respectively) _Model 1

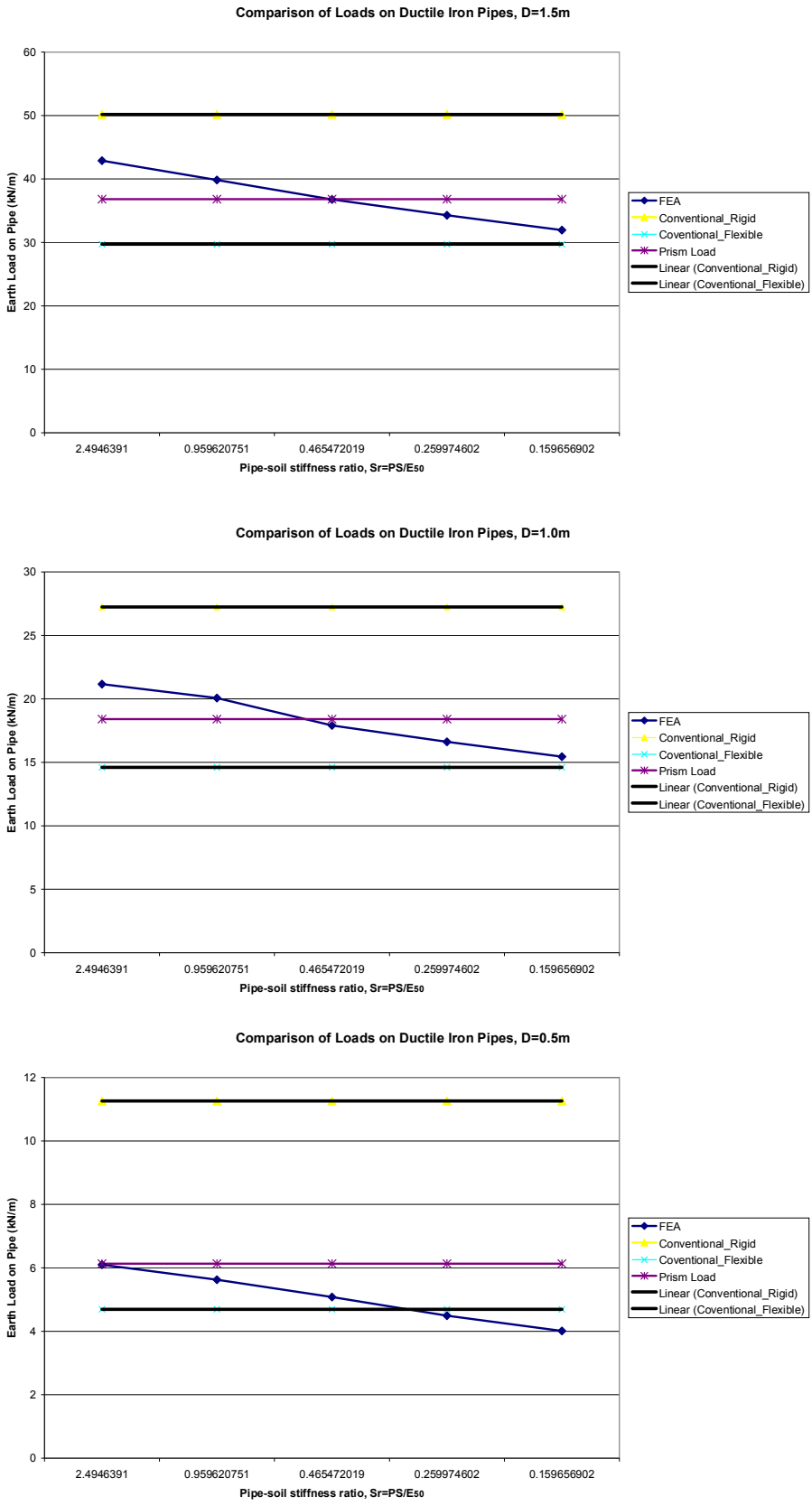

Figure 6.26 Comparison of Loads on DI Pipes (D=1.5m, 1.0m, 0.5m respectively) _Model 1

In addition to Model 1 where the embedment material is crushed stone and the final backfill is kanto loam, the same study is repeated for Model 2 where both the embedment and backfill material is basalt aggregate. Based on the conventional results tabulated at Table 6.6, the above figures demonstrating the change of loads with respect to the pipe-soil stiffness ratio are reproduced and it is observed that the graphical results are mainly similar in nature. (Figures 6.27, 6.28, 6.29). It should be ~~is~~ noted that there are some deviations corresponding to extreme values and such differences are expected considering the range of variation of both the material type for the backfill and the range of pipe-soil stiffness ratio.

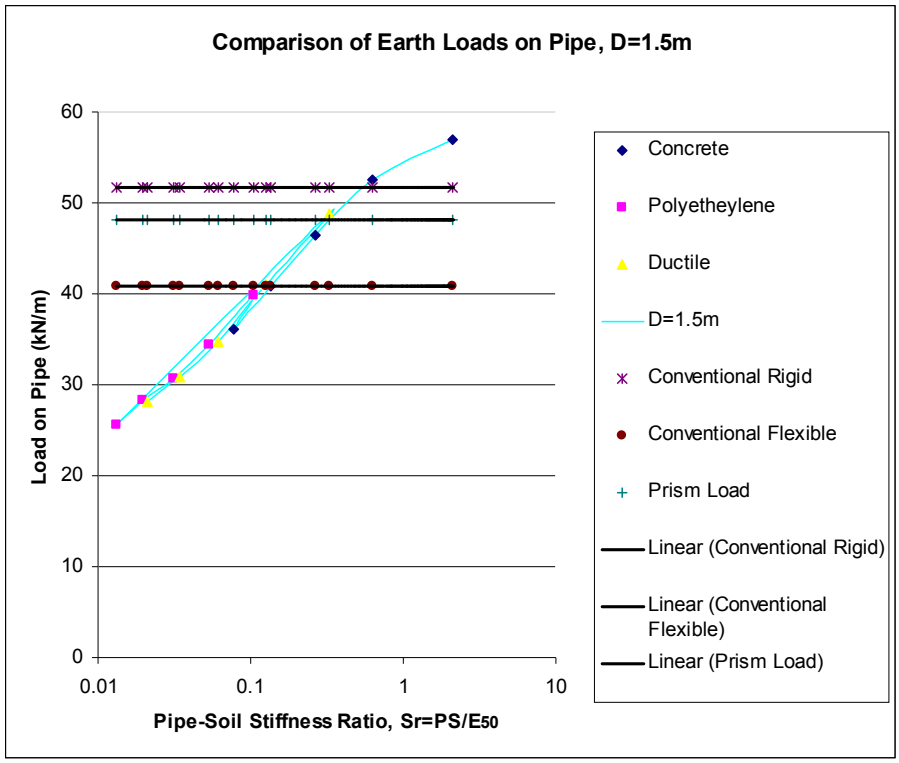

Figure 6.27 Comparison of Loads on Pipes, D=1.5m_Model 2

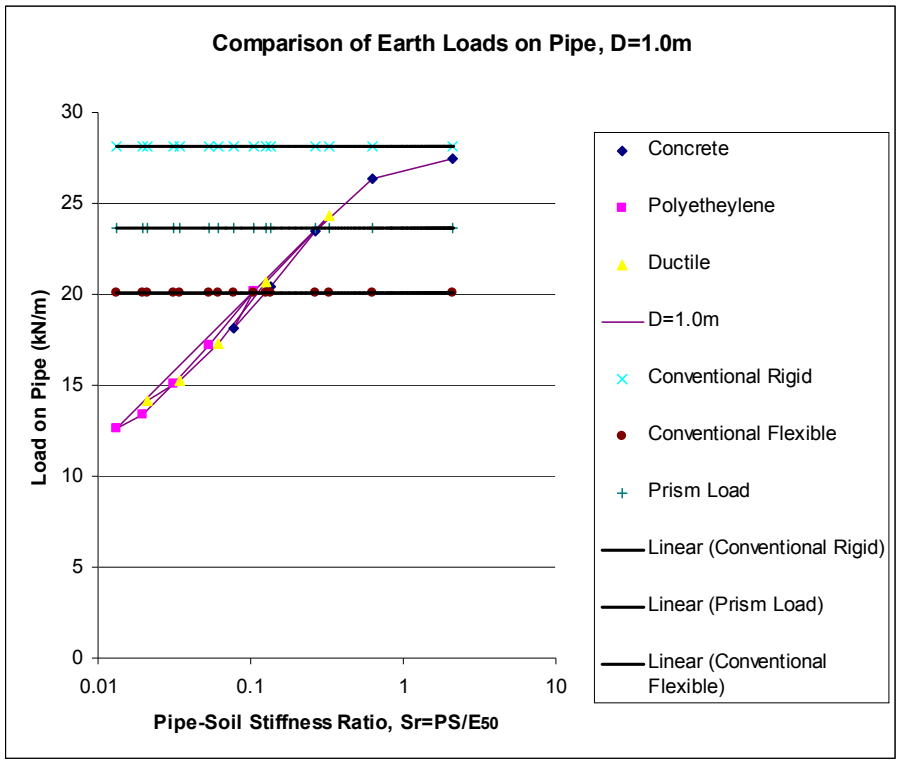

Figure 6.28 Comparison of Loads on Pipes, D=1.0m_Model 2

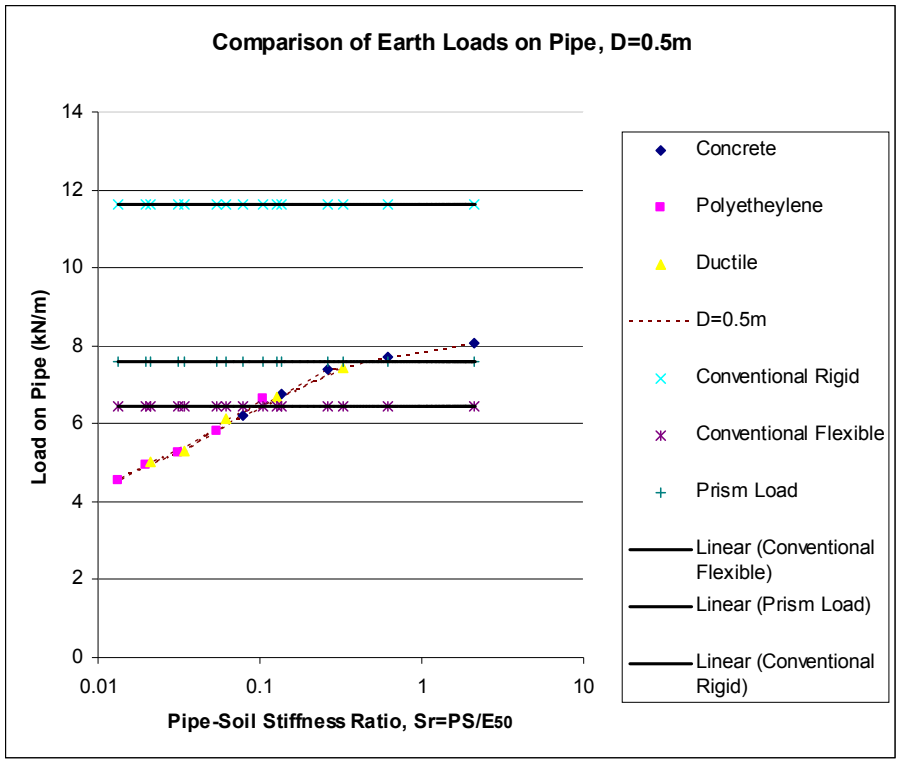

Figure 6.29 Comparison of Loads on Pipes, D=0.5m_Model 2

6.3 *Back-calculated Values of E', Modulus of Soil Reaction*

The horizontal deflections predicted by FEA are used in the back-calculation of modulus of soil reaction values through Iowa formula. If the modified Iowa formula is solved for E' by inserting the values of other parameters, the modulus of soil reaction can be back-calculated from the following equation:

$$dx=DPK/(EI/r^3 + 0.06l\ E')$$

$$E' = \frac{(DPK / dx) - (EI / r^3)}{0.061}$$

The parameters used in the modified Iowa formula are:

- *D*: Deflection lag factor, D=1.0
- *P*: Prism load (γH), 24.54 kPa (D=1.5m); 18.40 kPa (D=1.0m); 12.27 kPA (D=0.5m) for Model 1.
- *K*: 0,1
- d_x: change in horizontal diameter, Δx/D from FEA
- *EI*: As previously tabulated in Tables 5.8 to 5.10 for PE pipe cases.
- r^3: for r = 0.75 m, 0.5m and 0.25m

The representative results of FEA for differing stiffnesses of polyethylene pipe-trench cases yield a range of back-calculated E' values in the same embedment material. The back-calculation results which are tabulated in Table 6.7 are graphically presented and compared to the proposed value of Howard (200 psi ≈1,4 MPa) in Figure 6.30. Howard's proposed value for the current analyses is taken from Table 2.6 for the soil type (coarse grained soils with little or no fines) and compaction degree (dumped, i.e. no compaction) of the embedment material (crushed stone).

As per the numerical results, the back-calculated E' values ranged in an overall interval of 0.1 MPA to 5.42 MPa in the range of pipe-soil stiffness ratio of polyethylene pipes analysed in this study. It was demonstrated in the previous sections that the relative stiffness significantly affects the behaviour of buried flexible pipes both in terms of pipe deflections and the loads transferred to

pipes. The individual curves obtained for each diameter demonstrate some indicative trends of E' values with respect to the pipe-soil stiffness ratio.

As a general trend, the modulus of soil reaction values increase with the decrease in pipe-soil relative stiffness. In other words, as the flexibility of the pipes increase, the capability of the pipe to deflect under load increases which leads to the development of greater passive soil support at the sides of the pipe. The curves are fairly parallel, tending to flatten at low values of S_r; this is expected given the fact that beyond a given relative stiffness between the pipe and adjacent soil, the deflection of the pipe reaches to its maximum level.

When the results are checked for each diameter individually, it is observed that the E' values ranged in the intervals of 2.72 – 5.42 MPa, 0.69-4.37 MPa and 0.1-3.53 MPa for diameters D=1.5m, 1.0m and 0.5m respectively. At a given pipe-soil stiffness ratio, E' values obtained for larger diameters are greater than those obtained for smaller diameters. This can be attributable to the higher degree of deflections for larger diameters (flexibility is more pronounced) which leads to the development of greater resistance from the side fills.

Howard's proposed values are constant for a certain type and compaction degree of embedment material, hence they do not account for the effect of pipe-soil stiffness ratio. When the back-calculated values of E' obtained from FEA results are compared to the proposed value of Howard, it is observed that the E' value is over-estimated by Howard beyond a high degree of relative stiffness and is under-estimated for the rest.

When the analyses were conducted for the case of Model 2 where the embedment and backfill material is composed of basalt aggregate, the back-calculated E' values ranged in an overall interval of 2.020 MPa to 7.498 MPa in the range of pipe-soil stiffness ratio of polyethylene pipes analysed. The back-calculation results which are tabulated in Table 6.8 are graphically presented and compared to the proposed value of Howard (200 psi $\approx$1.4 MPa) in Figure 6.31. When the individual curves produced for each diameter are investigated, they indicate the same trends with those of the crushed stone case.

Table 6.7 Back-calculated E' Values for PE Pipes_Model 1

SN	Analysis	Material Type	Diameter D (m)	D/t ratio	Pipe-Soil Stiffness Ratio, Sr	Percent Deflection, Δx/D (%)	Howard's E' (MPa)	E', Back-calculated
16	Analysis_PE1	Polyethylene	1.5	10	0.7983	0.29%	1.4	2.722
17	Analysis_PE2	Polyethylene	1.5	12.5	0.4087	0.40%	1.4	4.450
18	Analysis_PE3	Polyethylene	1.5	15	0.2365	0.48%	1.4	5.080
19	Analysis_PE4	Polyethylene	1.5	17.5	0.1490	0.55%	1.4	5.294
20	Analysis_PE5	Polyethylene	1.5	20	0.0998	0.59%	1.4	5.419
21	Analysis_PE6	Polyethylene	1.0	10	0.7983	0.26%	1.4	0.692
22	Analysis_PE7	Polyethylene	1.0	12.5	0.4087	0.36%	1.4	2.859
23	Analysis_PE8	Polyethylene	1.0	15	0.2365	0.43%	1.4	3.774
24	Analysis_PE9	Polyethylene	1.0	17.5	0.1490	0.49%	1.4	4.140
25	Analysis_PE10	Polyethylene	1.0	20	0.0998	0.53%	1.4	4.369
26	Analysis_PE11	Polyethylene	0.5	10	0.7983	0.18%	1.4	0.091
27	Analysis_PE12	Polyethylene	0.5	12.5	0.4087	0.26%	1.4	2.204
28	Analysis_PE13	Polyethylene	0.5	15	0.2365	0.32%	1.4	3.015
29	Analysis_PE14	Polyethylene	0.5	17.5	0.1490	0.37%	1.4	3.368
30	Analysis_PE15	Polyethylene	0.5	20	0.0998	0.41%	1.4	3.534

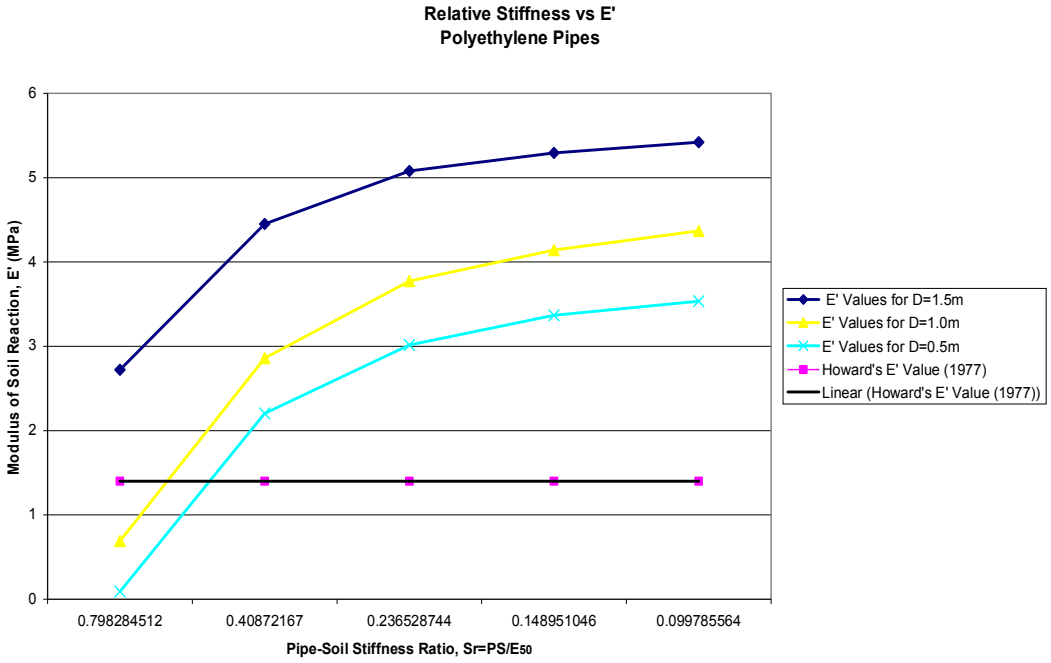

Figure 6.30 Relative Stiffness vs E' Values for Polyethylene Pipes_Model 1

Table 6.8 Back-calculated E' Values for PE Pipes (Updated Model)_Model 2

SN	Analysis	Material Type	Diameter D (m)	D/t ratio	Pipe-Soil Stiffness Ratio, Sr	Percent Deflection, Δx/D (%)	Howard's E' (MPa)	E', Back-calculated
16	Analysis_PE1	Polyethylene	1.5	10	0.1053	0.36%	1.4	3.732
17	Analysis_PE2	Polyethylene	1.5	12.5	0.0539	0.45%	1.4	6.067
18	Analysis_PE3	Polyethylene	1.5	15	0.0312	0.52%	1.4	6.877
19	Analysis_PE4	Polyethylene	1.5	17.5	0.0196	0.61%	1.4	7.188
20	Analysis_PE5	Polyethylene	1.5	20	0.0132	0.62%	1.4	7.498
21	Analysis_PE6	Polyethylene	1.0	10	0.1053	0.30%	1.4	2.020
22	Analysis_PE7	Polyethylene	1.0	12.5	0.0539	0.38%	1.4	4.631
23	Analysis_PE8	Polyethylene	1.0	15	0.0312	0.43%	1.4	5.577
24	Analysis_PE9	Polyethylene	1.0	17.5	0.0196	0.48%	1.4	5.941
25	Analysis_PE10	Polyethylene	1.0	20	0.0132	0.50%	1.4	6.193
26	Analysis_PE11	Polyethylene	0.5	10	0.1053	0.17%	1.4	2.711
27	Analysis_PE12	Polyethylene	0.5	12.5	0.0539	0.22%	1.4	5.518
28	Analysis_PE13	Polyethylene	0.5	15	0.0312	0.26%	1.4	6.122
29	Analysis_PE14	Polyethylene	0.5	17.5	0.0196	0.29%	1.4	6.330
30	Analysis_PE15	Polyethylene	0.5	20	0.0132	0.31%	1.4	6.402

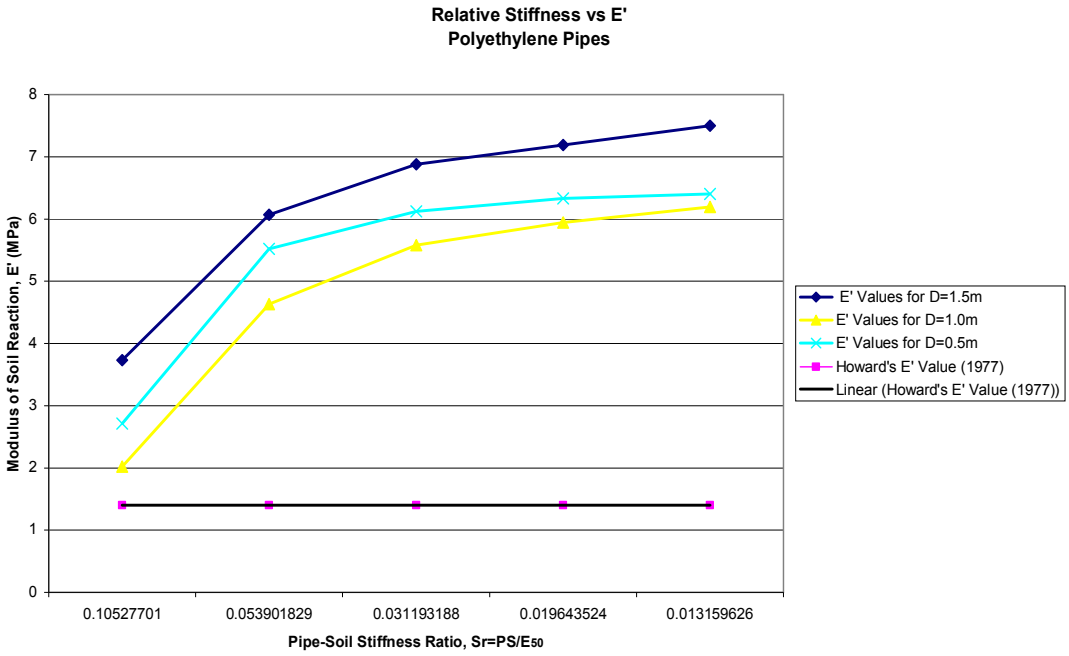

Figure 6.31 Relative Stiffness vs E' Values for PE Pipes_Model 2

In fact, the back-calculation results of E' based on the deformation predictions from FEA is not totally reliable. As noted previously, E' is not a fundamental geotechnical engineering property of the soil. This property can not be measured either in the laboratory or in the field. This is an empirical soil-pipe system parameter, which could be obtained only from back-calculating by knowing the values of other parameters in the modified Iowa equation.

Therefore, the actual site conditions and deformations should be used in the back-calculation process. However, in this study, it was the main aim to present the effect of relative stiffness on the values of E' by way of obtaining some indicative and comparable trends. In this regard, although the figures are not accurate, FEA results indicate comparable trends and results while investigating the relation of E' with the pipe-soil stiffness ratio. The wide range of back-calculated E' values as well as their deviation from the average value proposed in the table of US Bureau of Reclamation clearly pointed out the significance of a number of parameters related to the pipe-soil stiffness ratio. Therefore, as advised by Watkins and Jeyapalan (2004), it is verified that the parameters such as the pipe-soil stiffness ratio as well as the pipe diameter and size should be considered in the selection of E' value which is used as an important design parameter.

CHAPTER 7

SUMMARY AND CONCLUSIONS

In the study presented in this thesis, the effect of pipe-soil relative stiffness on the behaviour of buried flexible pipes was studied considering the effect of pipe size, material, stiffness and interfaces and geometry of the trench installation using the finite element method which allowed to simulate the stages of construction as well as the pipe-soil interaction aspects of the problem. For this purpose, a parametric study was conducted to investigate the effect of different variables on the resulting loads and deformations on the pipes in the same natural ground and backfill conditions. In total, 45 trench pipe-soil cases were analysed with the PLAXIS finite element code at which the soil behaviour was simulated by the Hardening-Soil constitutive model. The finite element results for the deformation of typically flexible Polyethylene pipes were then used to back-calculate the range of E' values for differing pipe-soil relative stiffness. The pipe-soil stiffness ratio, $S_r = PS/E_{50}$ which was defined for the purpose of this study represented the relative stiffness parameter and was used in the comparison and discussion of results.

The literature review identified the most frequently used analytical methods to analyse buried flexible pipes. These methods are the Marston (1913) theory, the Iowa formula by Spangler (1941), the modified Iowa formula by Watkins (1958), the modified Iowa formula by Greenwood and Lang (1990), the elastic solution by Burns and Richard (1964), the elastic solution by Höeg (1968) and the finite element method (FEM). The finite element method is proven to be more reliable because of its capability to consider non-linear soil behaviour, non-homogeneous backfi11 material, stages of construction and pipe-soil

interaction. Further to the presentation of analytical methods, characteristics of buried pipe installations, modelling the behaviour of flexible pipes as well as their performance limits were discussed for a comprehensive review of buried pipe behaviour. In addition, special emphasis was put on the modulus of soil reaction, E' parameter and a detailed review of this design parameter was presented.

Three pipe material types; concrete, polyethylene (PE), and ductile iron (DI) with significantly different moduli of elasticity, E, were analysed in this study. Three conduit diameters, D (0.5, 1.0 and 1.5m), were considered for each material type. The corresponding pipe-wall thicknesses, t, were assigned for each diameter D, such that the diameter to thickness ratio D/t ranged from 10 to 30 (5 cases) for the concrete pipes, 10 to 20 (5 cases) for the PE pipes, and 40 to 100 (5 cases) for ductile iron pipes. The ratio of $H/B_d = 1$ was kept constant in all 45 trench pipe-soil cases (3 Material types x 3 Diameters x 5 Wall Thicknesses) for both Model 1 and Model 2. The pipe-soil stiffness ratio, S_r, was set as the main parameter for which the buried pipe behaviour and results were studied, the loads transferred to the pipes and pipe deflections were predicted and the range of E' values were back-calculated for the given embedment material.

As a remarkable and practical outcome of the finite element analyses performed, different types of pipe materials used in the study complemented each other to form a continuous set of overlapping data, when expressed in terms of pipe-soil stiffness ratio. Such set of data revealed some indicative trends regarding the effect of relative stiffness altered by the pipe material type and pipe size on the resulting loads and deformations. The continuous set of data produced individual curves corresponding to each diameter while studying both the loads and deformations.

In the case of deflection results from FEA, the maximum deflections were observed for the PE pipes, the minimum deflections were recorded for concrete pipes and the deflections for DI pipes which have an intermediate stiffness produced in between results as expected. The curves are somewhat

parallel, however the effect of pipe diameter is less pronounced for relatively stiffer pipes and the pipe deflections converge to a minimum value. On the other side, the slopes of the deflection curves decreasing from more stiff concrete pipes to more flexible PE pipes reveal that that the deflections of the pipes tend to reach a maximum level as the relative stiffness decreases.

The analytical methods used to predict the pipe deflections were the modified Iowa formula by Watkins and Watkins's Soil-Strain theory. It was concluded that the conventional results obtained from Iowa formula were sensitive to the pipe material type and pipe size. The Iowa formula gives results more in line with FEM for relatively stiffer pipes and it yields conservative results for more flexible pipes. It is also observed that the flexibility of pipes is more pronounced for larger diameters. Similar to the case of Iowa formula, the results of Watkins soil-strain theory deviates more from FEM results as the pipe-soil stiffness ratio decreases. If it is compared to the Iowa formula, Watkins's soil strain theory overestimates deflections for relatively high stiffness ratios and underestimates deflections for more flexible pipes.

In the case of load results from FEA, it was observed that the maximum loads were developed on relatively stiffer concrete pipes and the minimum loads were developed on relatively flexible polyethylene pipes. This is because the arching effect is more pronounced and the loads transferred to the pipes are much reduced for more flexible pipes. The load curves presented the fact that beyond a given relative stiffness between the pipe and adjacent soil, the load transfer to the pipe reaches its maximum level.

The limitations of using the conventional approach, which only accounts for the pipe stiffness in terms of either rigid or flexible, were evident. For instance, it does not account for the effect of pipe wall thickness (D/t ratio) which in turn affects the relative stiffness parameter. When compared with the results of FEA, it is clear that for the case of rigid pipes, the conventional approach significantly overestimates the transferred earth loads, whereas it produces more compatible results for flexible conduits. Another observation is that the conventional method for flexible pipes predicts the results more in line with

FEM in case of small diameters compared to the greater diameter pipes.

Further to its impact on the loads and deformations, it was established that the relative stiffness parameter had a significant effect on the modulus of soil reaction, E' value. As per the numerical results, the back-calculated E' values ranged in an overall interval of 0.1 MPa to 5.42 MPa for Model 1 and 2.020 MPa to 7.498 MPa for Model 2 within the relative stiffness range of polyethylene pipe-soil cases analysed in this study. As a general trend, the modulus of soil reaction values increase with the decrease in pipe-soil relative stiffness (where flexibility of the pipes increase). This is because the flexible pipes have an increased deflection capability which leads to the development of greater passive soil support at the sides of the pipe. Additionally, the E' values tend to reach a maximum value at lower degrees of S_r; which is due to the fact that beyond a given relative stiffness between the pipe and adjacent soil, the deflection of the pipe reaches to its maximum level.

When the back-calculated values of E' obtained from FEA results are compared to the proposed value of Howard (as in USBR table), i.e. 1.4 MPa for the current study, it is observed that the E' value is over-estimated by Howard beyond a high degree of relative stiffness and is under-estimated for the rest.

The wide range of back-calculated E' values as well as their deviation from the average value proposed in the table of US Bureau of Reclamation clearly pointed out the significance of a number of parameters related to the pipe-soil stiffness ratio. Therefore, as advised by Watkins and Jeyapalan (2004), it is verified that the parameters such as the pipe-soil stiffness ratio as well as the pipe diameter and size should be considered in the selection of E' value which is used as an important design parameter.

REFERENCES

Allgood, J. F., and Takahashi, H., *Balanced design and finite element analysis of culverts*, Highway Research Record No. 413, 44-56, 1972.

Allgood, J. R., *CANDE: A modern Approach for the Structural Design and Analysis of Buried Culverts*, US Naval Civil Engineering lab, 1976.

American Society of Testing Material (ASTM), *Standard Test Method for External Loading Properties of Plastic Pipe by Parallel-Plate Loading*, ASTM D-2412-93, Vol.08.04, 1995.

ATV-DVWK German Association for Water, Wastewater, and Waste Management, *Richtlinie fur die statische berechnung von entwasserungskanalen und-leitungen,* ATV-A-127, Berlin, 1984.

Bjerrum, L., C. J. Frimann Clausen, and J. M. Duncan, *Earth Pressures on Flexible Structures – A State of the Art Report*, Proceedings, Fifth European Conference on Soil Mechanics and Foundation Engineering, Madrid, Spain, pp. 169-196, 1972.

Bulson, P. S., *Buried structures-static and dynamic strength*, Taylor and Francis Publishers, New York, ISBN 0 412 21560 8, 1985.

Burns, J. Q. and Richard, *Attenuation of Stresses for Buried Cylinders*, Proc. Symp. On Soil-Structure Interaction, Univ. Of Arizona, Tucson, 1964.

Cameron, D. A., *Simulated Vehicular Loading of Rib-Loc Pipes Buried in Non-paved, Backfilled Trenches*, Techsearch Report, School of Civil Engineering, South Australian Institute of Technology, September, 1990.

Chambers, R. F., McGrath, T. J., and Heger, F. J., *Plastic pipe for subsurface drainage of transportation facilities*, National Corporative Highway Research Program, Transportation Research Board Rep. No. 225, 122-140, 1980.

Crabb, G. I. and Carder, D. R., *Loading Tests on Buried Flexible Pipes to Validate a New Design Model*, Transport and Road Research Laboratory, Dept of Transport, Research Report 28, 1985.

Duncan, J. M., Chang, C. Y., *Nonlinear Analysis of Strain and Stress in Soils*, Journal of the Soil Mechanics and Foundations Division, Proceedings of the ASCE, September, pp 1629-1653, 1970.

Greenwood, M. E., Lang, D. C., *Vertical Deflection of Buried Flexible Pipes*, Buried Plastic Pipe Technology, ASTMSTP 1093, Philadelphia, 1990.

Hartley, J. D., and Duncan, J. M., *E' and its variation with depth*, J. Transp. Eng., 113(5), 538-553, 1987.

Heger, F. J., Liepins, A. A., Selig, E. T., *SPIDA: An Analysis and Design System for Buried Concrete Pipe*, Advances in Underground Pipeline Engineering Proc. Of Inter. Conf., ASCE, pp. 143-154, 1985.

Hoeg K, *Stresses Against Underground Structural Cylinders*, Journal of the Soil Mechanics and Foundatiom Division, ASCE, Vol.94, No.SM4, pp 833-858, 1968.

Howard, A. K., *Modulus of Soil Reaction E' Values for Buried Flexible Pipe*, Journal of Geotechnical Eng. Division, ASCE, Vol.103, MGTI, pp 33-43, 1977.

Howard, A. K., *The USBR Equation for Predicting Flexible Pipe Deflection*. Proc. Int. Conf on Advances in Underground Pipeline Engineering. Ed. Jey. K. Jeyapalan. ASCE Pipeline Divn., August, pp 37-54, 1985.

Janson, L-E. and Molin, J., *Design and Installation of Underground Plastic Sewer Pipes*. Proc. Int. Conf on Underground Plastic Pipe, ASCE, ed. J. Schrock, New Orleans, pp 79-88, 1981.

Jaramillo, P. A., *Review of field deflections of plastic pipes under soil loads*, MS thesis, Univ. of Wisconsin, Madison, Wis., 1989.

Jeyapalan, J. K. and Jaramillo, P. A., *New modulus of soil reaction - E' values for buried thermoplastic pipe design*, Proc., ASCE Conf. on Hydraulics of Pipelines, American Society of Civil Engineers, New York, 239-260, 1994.

Jeyapalan, J. K. and Ben Hamida, H., *Comparison of German to Marston Design Method*. ASCE, J. Transportation Engineering, V114, No. 4, pp 420-434, 1988.

Jeyapalan, J. K. and Watkins, R., *Modulus of Soil Reaction Values for Pipeline Design*. Journal of Transportation Engineering, ASCE. V.130, No.l., 2004.

Katona, M. G., *CANDE-1980: Box Culvert and Soil Models*, Report No. FHWA-Rd- 80-172-, Federal Highway Administration, Washington D.C., 1980.
Kellogg, C. G., *Vertical Earth Loads on Buried Engineered Works*, ASCE, J. Geotechnical Engineering, V119, No. 3, March, pp 487-506, 1993.

Kaya, M., *A Study On the Stress-Strain Behaviour of Railroad Ballast Materials By Use of Parallel Gradation Technique*, Ph.D. Thesis, METU, Ankara, 2004.

Kondner, K. L., *A Hyperbolic Stress-Strain Formulation for Sands*, Sec. Pan. Am. ICOSFE Brazil, Vol. 1,pp. 289-324, 1963.

Krizek, R. I., Parmalee, R. A., Kay, J. N., and Elnaggar, H. A., *Structural analysis and design of pipe culverts*, Highway Research Board, Rep. No. 116, National Cooperation Highway Research Program, 155, 1971.

Leonhardt, G., *Die Erdlasten bei Uberschutteten Durchlassen*, Die Bautechunik 56(1), 1979.

Leonhardt, G., *Einflub der Bettungssteifigkeit auf die Tragfahigkeit und die Verformungen von Flexiblen Rohren*, Strasse Bruecke Tunnel, Vol.3, 1972.

Leonhardt, G., *Die belastung von starren rohrleitungen unter dammen*, PhD thesis, Univ. of Hanover, Hanover, Germany, 1973.

McGrath, T. J., Chambers, R. E. and Sharff, P. A., *Recent Trends in Installation Standards for Plastic Pipe, in "Buried Plastic Pipe Technology"*, ASTM, STP 1093, eds. G. S. Buczala and M. J. Cassady, pp 281-293, 1990.

Meyerhof G. G., Baike, L. D., *Strength of steel culvert sheets bearing against compacted sand backfill*, 42nd Annual Meeting, Highway Research Board, Highway Research Record, N0.30, 1963.

Meyerhof, G. G., *Composite design of shallow-buried steel structures*, Proc., 47th Annual Convention of the Canadian Good Roads Association, Halifax, Nova Scotia, Canada, 1966.

Mohri Y. and Kawabata, T., *Behaviour of Buried Large Thin Wall Flexible Pipe-Field Test and Numerical Analysis Considered with Stage of Construction*, Proceedings, Second International Conference, Pipeline division and TCLEE/ASCE, June 25-28, 1995, Bellevue, Washington, 1995.

Molin, J., *Flexible Pipes Buried in Clay*. Proc. Int. Conf. on Underground Plastic Pipe, ASCE, ed. J. Schrock, New Orleans, pp 322-337, 1981.

Moore, I. D., *Structural Design of Profiled Polyethylene Pipe. Part 1 - Deep Burial*, Research Report, University of Western Ontario, Geotechnical Research Centre, GEOT-8-93, March, 1993.

Moser, A.P., Folkman, S., *Buried Pipe Design*, 3rd Edition, Mc Graw-Hill, 2008.

NCHRP, National Cooperative Highway Research Program, *Structural analysis and design of pipe culverts*, Report 116, 1971.

Nielson, F. D., Modulus of soil reaction as determined from triaxial shear test, Highway Research Record No. 185, 80-90, 1967.

PLAXIS 2D-Version 8 User Guide, *PLAXIS Finite Element Code for Soil and Rock Analyses*, *Edited by Brinkgreve, R B. J.*, Delft University of Technology & Plaxis b.v., The Netherlands, A.A. Balkema Publishers, 2002.

Prevost, R. C. and Kienow, K. K., *Basics of Flexible Pipe Structural Design*. ASCE J. of Transportation Eng., V120, No.4, July/August, pp 652-671, 1994.

Rajani, B., Kuraoka, S., *Field Performance of PVC Water Mains Buried in Different Backfills*, Advances in Underground Pipeline Engineering, Second International Conference, Edited by Jeyapalan. J. K. and Jeyapalan, M., pp 138-149, 1995.

Rogers, C. D. F., *The Influence of Surrounding Soil on Flexible Pipe Performance*, Transportation Research Record 1129, 1987, pp 1-11, 1987.

Rogers, C. D. F., Fleming, P. R. and Talby, R., *Use of Visual Methods to Investigate Influence of Installation Procedure on Pipe-Soil Interaction*. Transportation Research Record, 1541, pp 76-85, 1996.

Rogers, C. D. F., Fleming, P. R., Loeppky, M. W. J. and Faragher, E., *Structural Performance of Profile-Wall Drainage Pipe - Stiffness Requirements Contrasted with Results of Laboratory and Field Tests*. Transportation Research Record, 1514, pp 83-92, 1995.

Sargand, S., Masada, T. and Hurd, J. O., *Effect of Rib Spacing on Deformation of Profile Wall Plastic Pipes Buried in Coarse Granular Backfill*, ASTM, Geotechnical Testing Journal, Vol. 19, No. 2, June, pp 217-222, 1996.

Schlick, W.J., *Loads on Pipe in Wide Ditches*, Bulletin 108, Iowa State College, 1932.

Shafer, G. E., *Discussion: Underground conduits - An appraisal of modern research*, Trans. Am. Soc. Civ. Eng., 113, 354-363, 1948.

Sladen, J. A. and Oswell, J. M., *The Induced Trench Method - A Critical Review and Case History*, Canadian Geotechnical J., 25, pp 541-549, 1988.

Szechy, K., *The Art of Tunnelling, 2nd Edition*, Hungarian Academy, Akademiai Kiado, Budapest, 1973.

Spangler, M. G., *The Structural Design of Flexible Pipe Culverts*, The Iowa State College Bulletin, M30, Vol. XL, Iowa Engineering Experimental Station, Iowa State College, 1941.

Spangler, M. G., Discussion: *Rebuilt Wolf Creek culvert behavior*, Highway Research Record No. 262, 10-13, 1969.

Spangler, M.G., Handy, R.L., *Soil Engineering, 4th Edition*, Hamper and Row Publications, New-York, ISBN 0-7002-2533-1, 1982.

Spangler, M.G., Handy, R.L., *Geotechnical Engineering: Soil and Foundation Principles and Practice, 5th Edition*, McGraw-Hill, New-York, ISBN 0-07-148120-6, 2007.

Terzaghi, K., *Theoretical Soil Mechanics*, John Wiley and Sons, New York, pp. 66-76, 1943.

Uni-Bell PVC Pipe Association, *Handbook of PVC Pipe, Third Edition*, Dallas, Texas, 1993.

Valsangkar, A. J. and Britto, A. M., *The Validity of Ring Compression Theory in the Design of Flexible Buried Pipes*, Transport and Road Research Laboratory, TRRL Supplementary Report 440, 1978.

Watkins, R.K., Spangler, M.G., *Some Characteristics of the Modulus of Passive Resistance of Soil: A Study of Similitude*, Highway Research Board. Proceedings of the 37th Annual Meeting, Vol.37, pp 576-583, 1958.

Watkins, R. K., and Nielson, F. D., *Development and use of the modpares device*, Proc. Am. Soc. Civ. Eng., Transportation Research Board, Washington, D.C, 155-178, 1964.

Watkins, R. K., *Structural Mechanics of Buried Pipes*, Utah State University, Dept. of Civil and Environmental Engineering, Logan, Utah, 1988.

Webb, M. C., McGrath, T. J. and Selig, E. T., *Field Tests of Buried Pipe Installation Procedures*, Transportation Research Record, 1541, pp 97-106, 1996.

Wilson, E., *Solid SAP, Static Analysis Program for Three Dimensional Solid Structures*, SESM Report 71-19, Structural Engineering Lab., Univ. Of Cal., Berkeley, Ca., 1971.